Transmission Control Algorithms in Power-Controlled Wireless Ad Hoc Networks

Pouriya Sadeghi

A Thesis

in

The Department

of

Electrical and Computer Engineering

Presented in Partial Fulfillment of the Requirements

for the Degree of Doctor of Philosophy at

Concordia University

Montréal, Québec, Canada

December 2009

Your file Votre référence
ISBN: 978-0-494-67348-5
Our file Notre référence
ISBN: 978-0-494-67348-5

ABSTRACT

Transmission Control Algorithms in Power-Controlled Wireless Ad Hoc Networks

Pouriya Sadeghi, PhD.

Concordia University, 2009

Wireless networks have become an indispensable component of almost any communication systems. In particular, there has been a growing interest in wireless ad hoc networks, where no centralized management is required and therefore, they can be set up and become operational in almost no time. Due to the shared nature of the wireless channels and the existence of high co-channel interference in wireless ad hoc networks, the role of the transmission control algorithms such as power control and admission control schemes becomes extremely important. Power control algorithms manage the power allocation process and admission control algorithms grant network access to a new link while protecting the transmission quality of other links. Because of the distributed nature of ad hoc networks, the transmission control algorithms have to be also distributed and should not rely on any information to be provided at the network level.

In this work, new transmission control algorithms for power-controlled ad hoc networks are investigated where each algorithm is designed to achieve a specific performance objective. In particular, an autonomous power control algorithm is proposed to achieve the maximum uniform signal-to-interference-plus-noise ratio (SIR) of the network. Moreover, an asynchronous power control with active link protection is introduced which allows the links to update their powers asynchronously and at the same time, guarantees the target SIR of the existing links when a new link enters the network. Furthermore, a novel distributed admission control algorithm is proposed which can be used as an add-on module to most of the asynchronous power control algorithms and delivers an ideal admission decision. Finally, the feasible SIR region is investigated which can be considered as the upper bound for the achievable rates of any transmission control algorithm.

ACKNOWLEDGEMENTS

The completion of this thesis would not have been possible without the advice, guidance and support of my supervisor, Prof. M. Reza Soleymani to which I am forever grateful.

I would like to thank Prof. Shahrokh Valaee, Prof. Yousef Shayan, Prof. Walaa Hamouda and Prof. Rajamohan Ganesan, members of my Ph.D. committee, for their valuable feedback and suggestions.

I am forever indebted to my mother, Mahin, my sister, Naghmeh and my brother, Ali, for their unflagging love and support throughout my life. My deepest gratitude goes to my wife Neda for her unconditional love, understanding and patience. In addition to her emotional support throughout my studies, during the last months of my research, she graciously went through my thesis and provided me feedback when I needed it the most. Without her help, none of this would have been possible.

TABLE OF CONTENTS

LIST OF FIGURES

LIST OF TABLES

LIST OF IMPORTANT SYMBOLS

$\mathcal{A}$	Set of all parameters representing a specific network configuration
η_i	Thermal and background noise of link i (single-hop)
η_{ij}	Thermal and background noise of link i in path j (multi-hop)
G_{ij}	Channel gain from link j to link i (single-hop)
$G_{ij,kl}$	Channel gain from link k in path l to link i in path j (multi-hop)
γ_i	SIR of link i (single-hop)
γ_{ij}	SIR of link i in path j (multi-hop)
γ_{Un}	Uniform link SIR
$\gamma_{Un}^{\max}$	Maximum uniform link SIR
$I_i(k)$	Total interference received at link i at kth iteration
$In(i,k)$	Total interference received at link 1 after power update of link i at kth iteration
Γ_j	Path SIR of path j
Γ_{Un}	Uniform path SIR
$\Gamma_{Un}^{\max}$	Maximum uniform path SIR
$M_i(k)$	SIR metric of link i at kth iteration (single-hop)
$M_{ij}(k)$	SIR metric of link i in path j at kth iteration (multi-hop)
$M_{\min}(k)$	Minimum SIR metric of all link at kth iteration
P_i	Power element of link i (single-hop)
P_{ij}	Power element of link i in path j (multi-hop)

P_{ij}^{L}	Minimal power element of link i in path j
$P^{\max}$	Maximum power
ρ_f	Maximum modulus (Perron-Frobenius) eigenvalue
Q_i	QoS of link i (single-hop)
Q_{ij}	QoS of link i in path j (multi-hop)
T_i	Power updating period of link i
$\mathcal{X}(\mathbf{\Gamma})$	Set of all power vectors generating path SIR vector $\mathbf{\Gamma}$

LIST OF ABBREVIATIONS

ACD	Adaptive Critic Design
ALP	Active Link Protection
FDMA	Frequency Division Multiple Access
FDO	Forced Drop-Out
PCMA	Power-Controlled Multiple Access
OFDMA	Orthogonal Frequency Division Multiple Access
QoS	Quality of Service
S&S	Soft and Safe algorithms
SER	Symbol Error Ratio
SIR	Signal-to-Interference-plus-Noise Ratio
TDMA	Time Division Multiple Access
TES	Trial-and-Error Search algorithm

Chapter 1

Introduction

An overview of the thesis is presented in this chapter. The concept of wireless ad hoc networks including a brief literature review of the related transmission control algorithms is presented in Section 1.1. In Section 1.2, the research objectives of this thesis are discussed. The original contributions of this work are listed in Section 1.3. Finally, an outline of the upcoming chapters is presented in Section 1.4.

1.1 Wireless Ad Hoc Networks

Due to the tremendous popularity of wireless networks in recent years, there is an enormous demand to increase the transmission quality of the wireless links and to decrease the power consumption of portable/mobile terminals. These improvements are feasible by using advanced transmission control methods such as power control techniques, admission control algorithms, etc.

Most of the wireless networks are based on the centralized structure where all users are communicating with a central base station [1, 2]. The base station has the real-time knowledge of all users in the network and therefore, it can control the admission process and the power allocation of each user. However, there is a growing interest in the wireless networks which do not have any centralized control unit and therefore, can be setup and become operational in almost no time. This network model is referred to as the wireless ad hoc network and in its basic form, is defined as a collection of the radio links each

consisting of a transmitting node and a receiving node.

Due to the absence of a central control unit in ad hoc networks, there are two major differences between ad hoc networks and centralized networks. First, in ad hoc networks no channelization of the resources such as the ones employed in centralized networks, e.g., FDMA and TDMA in cellular networks, can be used and as a result, one or more wireless channels are shared among all links. Although all links are communicating independently, they affect the transmission qualities of each others through the shared wireless channel, where the transmitting power of one link is considered as the interference signal at the receivers of other links. These interfering signals can decrease the transmission rates of the individual links and consequently, they can reduce the throughput of the whole network. This transmission scheme is sometimes referred to as the power-controlled multiple access (PCMA) [3].

The second major difference between ad hoc networks and centralized networks is the way that the transmission control algorithms operate in these networks. These transmission control algorithms are responsible for achieving or maintaining a predefined quality of service (QoS) for each link. Due to the distributed nature of ad hoc networks, the transmission control algorithms have to be distributed as well, i.e., they should only rely on the available information at the link level, rather than any signaling provided at the network level. For example, one of the local information available to each link is the signal-to-interference-plus-noise ratio (SIR) measurement, which is used extensively by the transmission control algorithms.

It is important to note that due to the layered architecture of wireless networks, the QoS has different definitions at different layers. At the physical layer, the QoS usually translates into the minimum required SIR, whereas at the network layer the QoS may refer to the end-to-end transmission delay, the required bandwidth, the call blocking and dropping probabilities, etc. [4, 5, 6]. Because of these different definitions of the QoS at the physical and network layers, their QoS-related algorithms, such as admission control algorithms, refer to two different concepts. In this work, we only address the transmission control algorithms at the physical layer where the QoS parameters refer to the minimum SIR requirements in a shared wireless interference channel.

In this thesis, we mainly focus on the transmission control algorithms in the power-controlled wireless ad hoc networks where the maximum powers of the links are limited. Due to the shared nature of the wireless channels and the existence of the high co-channel interference in wireless ad hoc networks, the role of the transmission control algorithms such as power control and admission control schemes, becomes extremely crucial. The common element of these algorithms is that they all control the quality of the transmission through power elements and SIR measurements in a distributed manner. Depending on the objective of each of these algorithms, they improve different transmission qualities of the network. In the following, some of these transmission control objectives and performance upper bounds are described and the related works are briefly reviewed.

Maximum Uniform SIR

One of the parameters representing the overall throughput of the network is the maximum uniform SIR, which is the maximum achievable SIR when the SIR values of all links are the same. This value describes the maximum QoS that all links can support at the same time. When there is no constraint on the transmitting power, the problem of finding the maximum uniform SIR is identified as an eigenvalue problem, and given the full knowledge of the network parameters, it can be solved by using the theory of non-negative matrices [7, 8]. In practice, the mobile terminals have a limited battery power and therefore, their maximum transmitting power is constrained. In such power-constrained networks, the maximum uniform SIR and its corresponding power vector can be calculated if the full knowledge of the network, such as the channel gain matrix, is known [9, 10]. However, in most of the practical applications the full knowledge of network parameters is not available. In [11] and similarly in [12], a more practical approach is presented in which a central unit effectively searches for the maximum uniform SIR. This power control method does not require the full knowledge of the network parameters, however, it requires a central control unit to implement a state-machine process tracing and coordinating the candidate uniform rates in order to find the maximum one.

Power Control Algorithm

Power control algorithms manage the power allocation process in a wireless network where the participating links share an interference channel. A power control mechanism not only helps the links to acquire their QoS, but also minimizes the power consumption resulting in a longer battery life of the mobile terminals [13, 14, 15].

Most of the existing power control algorithms address centralized wireless networks where the central unit has the real-time knowledge of all users in the network and controls the transmission power of each user [1, 2]. As mentioned earlier, due to the absence of a centralized management in ad hoc networks, a power control algorithm has to be distributed at the link level. This means that each link determines its transmitting power exclusively based on the only available local information at its receiving node, i.e., the SIR measurements, and no or very limited signaling provided at the network level. The pioneer work on the distributed power control for wireless networks was done by Foschini and Miljanic [16] and Mitra [17] independently, in 1993. They propose a distributed asynchronous power control algorithm which converges to the minimal power elements required for a set of QoS values. This algorithm provides the groundwork for distributed power control algorithms such as the ones presented in [18, 19, 20, 14, 21].

The algorithm proposed by Foschini and Miljanic does not guarantee the QoS of the existing links, while a new link enters the network [22, 23]. To solve this issue, in [19] Bambos *et al.* propose a modified version of this algorithm with the active link protection (ALP) capability. One of the requirements of the aforementioned algorithm is that all links have to synchronously update their powers at the same time [18].

Distributed Admission Control Algorithm

When a new link enters the network, the power elements and the SIR values of the existing links may be widely affected and therefore, some links might experience power outage and/or service interruption. To avoid such scenarios, an admission control algorithm should be emplaced to grant network access to a new user while protecting QoS of the existing users from any degradation.

When the full knowledge of the network is available, the admissibility of the new link can be examined by the feasibility criteria developed based on the theory of non-negative matrices [24, 25]. In the literature, various admission control algorithms have been proposed based on the mentioned robust feasibility criteria. For example, in [26], Bambos and Pottie examine a preliminary version of this approach where the channel gain matrix is calculated by using pilot signals. A more distributed and comprehensive pilot-based method is investigated in [14] where Andersin *et al.* present an interactive method providing both the admission control and active link protection. Due to the use of pilot signals these algorithms are not distributed and therefore, not applicable to ad hoc networks.

In [27], Xiao *et al.* propose an error free distributed admission control algorithm, however, this algorithm has a slow convergence and is not applicable to the power control algorithms with ALP. In [19], Bambos *et al.* propose two admission control algorithms based on the SIR convergence of the new link. These two admission control algorithms are fully distributed, however, their performances are not ideal and they require some threshold values to be optimized for each network realization.

Feasible SIR Region

In order to design better transmission control algorithms, it is of a great importance to identify the upper bound for the achievable rates of these algorithms. In theory, this upper limit is described by the general capacity region of wireless ad hoc networks, which is yet unknown. However, there are several researches addressing capacity-related regions of wireless networks for some special cases and scenarios. For example, in [28], Gupta and Kumar present a method evaluating the capacity of the wireless networks by allowing the number of nodes to go to infinity. In [29], Toumpis and Goldsmith define the capacity of a network under a given transmission protocol as the convex hull (time sharing) of all basic rate matrices. Also, the capacity-related properties of wireless networks are studied in the context of the power allocation [17, 16].

Note that in almost all these works, the interference received from other links is

modeled as the additive noise. Therefore, the calculated regions are considered as the collection of the feasible SIR vectors rather than the capacity region itself. In addition, no matter which transmission control algorithm the network uses, at any given instant (snapshot) the network is dealing with only one power vector. In this case, the upper bound for the achievable rates of any transmission control algorithm can be described by the feasible SIR region, which is defined as the set of all achievable SIR vectors generated by a single power vector. For example, an ideal power control can only achieve a rate vector within the feasible SIR region and an ideal admission control should reject any new link which results in a rate vector outside of this region. It is important to note that in this definition of the feasible SIR region, no time domain scheduling (time sharing) is considered.

1.2 Research Objective

The main objective of this work is to develop new distributed transmission control algorithms in order to achieve and/or maintain the QoS of the links in a power-controlled ad hoc network where the transmission powers are limited. These new algorithms provide a better performance and/or a faster convergence than the existing ones.

This objective is achieved by improving the existing algorithms and introducing new concepts and parameters. In particular, in this thesis the following aspects of the power-controlled ad hoc networks are investigated in detail.

1. Maximum Uniform SIR:

   Most of the algorithms for achieving the maximum uniform SIR of wireless networks require having either the full knowledge of the network or a base station to coordinate a trial-and-error state-machine process. Both of these requirements are not feasible in wireless ad hoc networks. Therefore, it is very useful to have a maximum uniform SIR achieving algorithm which does not rely on the full knowledge of the network or on the existence of a central management.

2. Power Control Algorithm with ALP:

   The power control algorithm with the ALP property, introduced in [19], requires

updating the power elements synchronously. Attaining such a requirement in an ad hoc network, where there is no central unit to impose the synchronous power updating, is very difficult. It is useful to investigate the possibility of modifying this algorithm in order to relax the synchronous power updating requirement and at the same time, keep the ALP property.

3. Admission Control Algorithm:

   A distributed admission control relies on the local measurements such as the SIR values. It is interesting to investigate whether the admission process can be further improved and optimized by using the detailed knowledge of the processing steps of the power control algorithms. Moreover, as mentioned earlier, the use of the feasibility criteria results in an ideal admission decision at the expense of requiring the full knowledge of the network. It is of a great importance to investigate the possibility of applying the feasibility criteria to the ad hoc networks where the full knowledge of the network is not available.

4. Feasible SIR Region:

   Most of the research in this field study the feasible SIR region for single-hop communications. It is important to develop a theoretical framework to study the feasible SIR region for both the single-hop and multi-hop scenarios where a single channel or multiple channels are available to the network. The feasible SIR region of ad hoc networks provides a valuable insight into the general capacity region of ad hoc networks and helps us to design better transmission schemes for them.

1.3 Contributions

First, we design a new power control algorithm which converges to the maximum uniform rate of a power-constrained ad hoc network. The proposed algorithm requires only one phase of power convergence and less information to be broadcast from the links compared to other algorithms. Most importantly, the proposed algorithm is autonomous in the sense that it does not require a central unit to perform any state-machine process. The design

and the performance of this algorithm are investigated for both the single-hop and multi-hop communications with the possibilities of having a single channel or multiple channels available to the network.

Next, we try to fill the gap between the *asynchronous* power control algorithm proposed by Foschini and Miljanic [16] and the *synchronous* power control algorithm with the ALP property proposed by Bambos *et al.* [19]. We introduce some modifications to the algorithm proposed by Bambos *et al.* and develop a generalized algorithm which not only is asynchronous, but also provides the active link protection property.

Later, we propose a new admission control by taking full advantage of the power control scheme and the feasibility criteria. We show that in the admission control process, the full knowledge of the network is not required to set up the feasibility criteria. In fact, a normalization process is presented where the unknown parameters are normalized without affecting the admissibility property of the network. The proposed admission control algorithm has a fast convergence and results in an ideal admission decision. In addition, it is completely distributed, does not require any optimization and is compatible with the power control algorithms with the ALP property.

Finally, the feasible SIR region for both the single-hop and multi-hop communications power-constrained ad hoc networks is studied. In particular, the properties of the power vectors generating the border of the feasible SIR region are investigated for both scenarios where either a single channel or multiple channels are available. Moreover, simple algorithms are proposed to generate the border of the feasible SIR region for each case.

The contributions of this work lead to a number of publications in the peer-reviewed journals and referred conferences. In the following the list of publications resulting from this thesis is presented:

P1 P. Sadeghi and M. R. Soleymani, "Capacity of single hop ad hoc networks," in *Proc. Canadian Workshop on Inform. Theory CWIT 2005*, Montréal, Canada, Jun. 2005.

P2 P. Sadeghi and M. R. Soleymani, "Snapshot capacity of multi hop ad hoc networks," in *Proc. IEEE ICC*, Istanbul, Turkey, Jun. 2006.

P3 P. Sadeghi and M. R. Soleymani, "Asynchronous power control with active link protection algorithms for wireless ad hoc networks," in *Proc. IEEE VTC Fall 2006*, Montréal, Canada, Sept. 2006.

P4 P. Sadeghi and M. R. Soleymani, "A novel admission control for asynchronous active link protected ad hoc networks," in *Proc. IEEE GLOBECOM*, San Francisco, CA, Dec. 2006.

P5 P. Sadeghi and M. R. Soleymani, "A distributed admission control for asynchronous power-controlled ad hoc networks," *IEEE/ACM Trans. on Networking*, Under revision.

P6 P. Sadeghi and M. R. Soleymani, "An autonomous power control for achieving the maximum uniform SIR in wireless networks," *IEEE Commun. Lett.*, Accepted for publication.

1.4 Thesis Organization and Notation

This thesis is organized as follows.

A framework of single-hop and multi-hop ad hoc networks is presented in Chapter 2, describing the overall system model and defining some commonly used parameters in this thesis.

The maximum uniform SIR for both the single-hop and multi-hop wireless ad hoc networks is investigated in Chapter 3. In particular, the properties of the power vector corresponding to the maximum uniform SIR of the network are studied in detail and based on those properties, an autonomous power control algorithm is proposed to achieve this maximum uniform SIR.

Chapter 4 studies the distributed power control in ad hoc networks. In this chapter, an asynchronous power control algorithm is proposed which provides the active link protection for the existing active links when a new link enters the network.

In Chapter 5, the problem of distributed admission control in ad hoc networks is considered. In particular, a new admission control algorithm is proposed for the general

case of the asynchronous power control algorithm and as a special case, its application is investigated for the asynchronous power control algorithm proposed in Chapter 4. This admission control algorithm is fully distributed and has a fast convergence with an ideal admission decision.

Chapter 6 investigates the feasible SIR region for both the single-hop and multi-hop wireless ad hoc networks. The basic conditions of the power vectors to producing rate vectors on the border of the feasible SIR region are investigated, and based on those conditions, some algorithms are proposed to generate the border of the feasible SIR region. In addition, the convexity of the feasible SIR region for single-channel single-hop networks is investigated.

Finally, Chapter 7 concludes this thesis and presents some ideas for the future work.

Notation: Matrices and vectors are written using uppercase bold letters. $\mathbf{I}_M$ denotes the $M \times M$ identity matrix. We use A_{ij} to refer to the (i, j) entry of matrix $\mathbf{A}$, and use B_i to refer to the (i) entry of vector $\mathbf{B}$. The operator $\lceil . \rceil$ denotes the ceiling function mapping a real number to the next largest integer.

Chapter 2

Framework of Ad Hoc Networks

The mathematical tools that are mostly used to model wireless networks are mainly based on the Graph Theory [30]. In these models, the wireless network is considered as a graph with its users as the nodes and its connections as the graph edges. The channel is modeled as a gain matrix with its elements corresponding to the power gain values between the transmitting and the receiving nodes.

In the literature, two major models are introduced for ad hoc networks; the *nodal model* and the *link model*. The nodal model or the physical model was first introduced by Gupta and Kumar [28], and later on, completed by Toumpis and Goldsmith [29]. The basic component of this model is a node. In general, this model has the highest flexibility and is capable of modeling the transmission or the reception to or from any nodes in the network. Consequently, the complexity of this model increases exponentially with the number of the users. In most scenarios, in order to limit the complexity growth, it is assumed that each node is either silent, i.e., no transmission at all, or sending with its maximum available power. This assumption makes the nodal model inapplicable to the networks where the users can control the level of their transmitting powers.

The most popular model for wireless networks, especially wireless ad hoc networks, is the link model [16, 20, 31, 19]. The basic component of this model is the radio link consisting of one transmitting node and one receiving node. The transmission pairs and the radio channels are pre-assigned and therefore, the only variable parameters are the value of power elements. The quality of the transmission is usually measured by its symbol error

ratio (SER). However, since there is a monotonically increasing relationship between the signal-to-interference-plus-noise ratio (SIR) and the SER, achieving a certain SER is equal to achieving its equivalent SIR. Therefore, in the link model the quality of the communication for each link is measured by its SIR. This model is widely used in the context of the wireless network capacity, power control, admission control, etc. Therefore, in this thesis, we consider the link model. It is important to note that the link model is mainly designed for the single-hop communications. However, in this work the multi-hop model is considered as well.

The rest of this chapter is organized as follows. First, the framework of the link model for the single-hop wireless networks is introduced in Section 2.1. Then, in Section 2.2 this model is extended to the multi-hop networks.

2.1 Single-Hop Networks

We consider the wireless ad hoc network as a collection of N radio links [19]. Each link consists of one transmitting node and one receiving node as depicted in Figure 2.1. Moreover, each link communicates over a pre-assigned generic channel (a specific frequency or time slot [14]) labeled as C_i where $1 \leq i \leq M$. All the M channels are orthogonal, i.e., links from different channels do not interfere and as a result, only co-channel interference is considered. In practice, one of the methods to detect the signal in the presence of the co-channel interference is the spread spectrum technique.

No broadcasting or multiple accessing is allowed, i.e., each node can transmit to or receive from only one node. However, a node may transmit and receive at the same time over two separate channels. Therefore, each node can be a part of up to two links; the receiving node of one link and the transmitting node of another link (this setup is widely used in the multi-hop case).

For the sake of simplicity and without any loss of generality, for the single-hop networks we assume all links transmit over the same channel, i.e., $M = 1$, unless otherwise stated.

The wireless channel is described by the gain matrix $\mathbf{G} = [G_{ij}]$ where G_{ij} represents

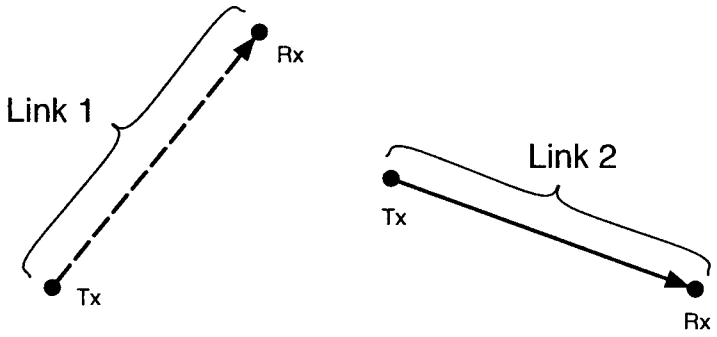

Figure 2.1: An example network of two links and four nodes; each link consists of one node as the transmitter and another node as the receiver.

the channel gain (in fact channel loss) from the transmitting node of the link j to the receiving node of the link i, modeling large-scale propagation effects, i.e., the path loss and the shadowing effects [32]. Variations due to small-scale propagation effects are usually assumed to be averaged out in the context of the SIR-based power-controlled systems [33]. In this work, the channel gain is considered as a static parameter in the observation period, following the same modeling used in the literature [16, 19, 27, 14]. This assumption corresponds to the practical scenario where the convergence of the power control and admission control schemes is much faster than the channel variability [20].

Each link i transmits with any positive power $P_i \leq P_i^{\max}$ where $P_i^{\max}$ denotes the maximum transmitting power due to the transmitter's hardware and/or power limitations. Without any loss of generality, we assume that the power constraints of all links are the same and equal to $P^{\max}$. The set of the transmitting powers of all links is denoted by power vector $\mathbf{P} = [P_i]$.

The transmission quality of the link i is defined by its SIR as

$$\gamma_i = \frac{G_{ii}P_i}{\sum_{j \neq i} G_{ij}P_j + \eta_i} \tag{2.1}$$

where η_i jointly models the thermal and background noise powers as a single source of the noise. The set of SIR of all links is represented by the SIR vector $\boldsymbol{\gamma} = [\gamma_i]$. Note that in this work, the *SIR* and the *rate* refer to the same concept and are used interchangeably.

Definition 2.1 *The uniform link SIR γ_{Un} is defined as an achievable link SIR value supported by all links, i.e.,*

$$\forall i : \gamma_i = \gamma_{Un}.$$

The maximum achievable uniform link SIR of the network is referred to as the *maximum uniform link SIR* and is denoted by $\gamma_{Un}^{\max}$.

The QoS requirement of the network is defined as a set of the minimum required SIR values, denoted by $\mathbf{Q} = [Q_i]$, which has to be maintained by all links, i.e.,

$$\forall i : \gamma_i \geq Q_i.$$

The QoS requirements are set by the higher layers of the network.

Definition 2.2 *The feasible link SIR region is defined as the set of all achievable link SIR vectors generated by a single power vector.*

Moreover, we represent a network by its set of parameters $\mathcal{A}$ consisting of all Q_i, G_{ij} and η_i values, i.e.,

$$\mathcal{A} = \{\forall i, j : Q_i, G_{ij}, \eta_i\}.$$

2.1.1 Feasibility and Admissibility Criteria

The feasibility of achieving a set of QoS requirements by a non-negative power vector depends on the network configuration and parameters. Although, the existence of such a power vector for a general case remains as an open problem, for the case of power-unconstrained single-hop single-channel wireless networks there exists a well-known theoretical solution based on the theory of non-negative matrices [16, 24, 25]. In the following, this solution is briefly reviewed. It is important to note that this method requires the full knowledge of network parameters such as the network gain matrix, the receiver noise powers and the QoS requirements of all links which may not be available at each link in practical applications.

The QoS requirements can be represented in the matrix form of

$$(\mathbf{I}_N - \mathbf{F})\mathbf{P} \geq \mathbf{u}\ ,\ \mathbf{P} > 0 \tag{2.2}$$

where

$$\mathbf{u} = (\frac{Q_1\eta_1}{G_{11}}, \frac{Q_2\eta_2}{G_{22}}, ..., \frac{Q_i\eta_i}{G_{ii}}, ..., \frac{Q_N\eta_N}{G_{NN}})^T$$

is a column vector containing the noise powers scaled by the channel gains and the QoS requirements. The entries of matrix $\mathbf{F}$ are given by

$$F_{ij=}\begin{cases} 0, & \text{if } i = j \\ \frac{Q_iG_{ij}}{G_{ii}} & \text{if } i \neq j \end{cases} \tag{2.3}$$

with $i, j \in \{1, 2, \cdots, N\}$. Since, the matrix $\mathbf{F}$ has non-negative elements and disjoint networks are not considered, $\mathbf{F}$ is irreducible as well.

Let ρ_f be the *maximum modulus eigenvalue* (Perron-Frobenius eigenvalue) of the matrix $\mathbf{F}$, i.e.,

$$\forall i : \rho_f = \max_i(|\lambda_i|)$$

where λ_i denote eigenvalues of $\mathbf{F}$. By the Perron-Frobenius theorem [25, 19], ρ_f of such a non-negative and irreducible matrix is a positive real value.

Moreover, considering the standard matrix theory and the Perron-Frobenius theorem [24], the following statements are equivalent:

1. $\rho_f < 1$.

2. There exists a power vector $\mathbf{P} > 0$ such that $(\mathbf{I}_N - \mathbf{F})\mathbf{P} \geq \mathbf{u}$.

If such a solution exists, then

$$\mathbf{P}^* = (\mathbf{I}_N - \mathbf{F})^{-1}\mathbf{u} \tag{2.4}$$

where $\mathbf{P}^*$ is the Pareto-optimal solution of (2.2), i.e., if $\mathbf{P}$ is a non-negative solution of (2.2), then $\mathbf{P} \geq \mathbf{P}^*$ component-wise [17]. This property implies that $\mathbf{P}^*$ has the minimum total power among all solutions of (2.2). Therefore, if the SIR constraints of all users are

simultaneously feasible, i.e., $\rho_f < 1$, then the best choice for the power allocation is $\mathbf{P}^*$ due to its minimum total power property.

The condition of the Perron-Frobenius eigenvalue can be used as a test for admissibility of a new link into a wireless network; when a new link enters a wireless network and starts transmitting, it generates extra interference on other links and changes the gain matrix and the topology of the network. By constructing the matrix $\mathbf{F}$ of this new network, if its Perron-Frobenius eigenvalue is less than 1, then there exists a power vector solution for which all links including the new one achieve their target QoS values. Therefore, the new link is considered *admissible* and is admitted in the network. However, if the Perron-Frobenius eigenvalue is equal to or greater than 1, then the QoS of all links are not feasible at the same time. This implies that upon the entrance of this new link there is at least one link (either the new link or one of the existing links) which cannot maintain its target QoS. In this case, the new link is considered *inadmissible* and it has to drop out and become silent.

2.2 Multi-Hop Networks

In this section, we extend the single-hop model of Section 2.1 to the multi-hop networks.

In the single-hop communications, an original source node and a final destination node communicate directly and are modeled as one radio link. For the multi-hop communications, the concept of the routing path is introduced in which the original source node and final destination node communicate via some intermediate nodes. However, all connections are still modeled as radio links.

The concept of the multi-hop routing in our model can be further clarified by a simple example. Figure 2.2 depicts a routing path consisting of 4 nodes. In this figure, the original source node a communicates with the final destination node d via the intermediate nodes b and c. The link 1 is modeled as the transmitter of the node a and the receiver of the node b, the link 2 is modeled as the transmitter of the node b and the receiver of the node c and finally, the link 3 is modeled as the transmitter of the node c and the receiver of the node d. It is important to note that the nodes b and c are transmitting and receiving at the same

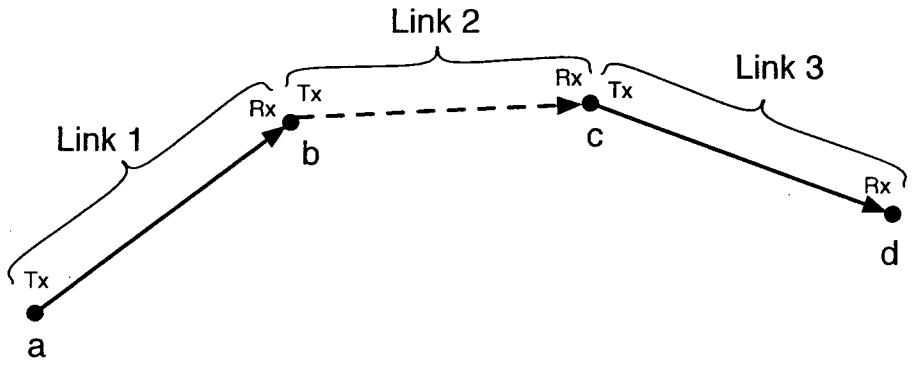

Figure 2.2: An example multi-hop network with 3 links.

time and as explained in Section 2.1, in practice such a simultaneous communication at one node is only possible on two separate channels. We consider a multi-hop wireless network with N links, M channels and L routing paths, and without any loss of generality, assume that each path has an equal number of links, i.e., $\frac{N}{L}$.

Although, both single-hop and multi-hop network models are based on the basic link model, there are two major differences between these two models; a different link indexing and the introduction of the path SIR. In the following, each of these differences is explained in detail.

In the single-hop model each link is addressed by a single index i where $1 \leq i \leq N$, e.g., P_i refers to the transmit power of the link i. In the multi-hop case each link is addressed by a 2-tuple ij where j is the index of the routing path and i represents the ith link in that path. By integrating this indexing method with the single-hop model, the multi-hop parameters are defined as follows. P_{ij} is the transmit power of the link i in routing path j. The set of the transmit powers in all routing paths is denoted by $\mathbf{P} = [P_{ij}]$. Similar to the single-hop model, the transmit powers are constrained to $P^{\max}$. The wireless channel is represented by $\mathbf{G} = [G_{ij,kl}]$ where $G_{ij,kl}$ refers to the power gain from the link k of the path l to the link i of the path j. The transmission quality of the link i in the path j is measured by its SIR as

$$\gamma_{ij} = \frac{G_{ij,ij}P_{ij}}{\sum_{kl \neq ij} G_{ij,kl}P_{kl} + \eta_{ij}}$$

where η_{ij} models the thermal and background noise at the receiver of the link i in the path j. The set of SIRs of all links in all paths is represented by the link SIR matrix $\boldsymbol{\gamma} = [\gamma_{ij}]$.

In order to maintain a continuous transmission in each routing path from its original source node to its final destination node, a certain level of transmission quality has to be supported by all participating links in that path. Obviously, this transmission quality is dominated by the minimum SIR of all links in that path. Based on this fact the following definition is presented.

Definition 2.3 *The path SIR of a routing path j is defined as the minimum SIR of all links in that path, i.e.,*

$$\Gamma_j = \min_i(\gamma_{ij}).$$

The set of path SIR values is represented by the path SIR vector $\boldsymbol{\Gamma} = [\Gamma_j]$.

Definition 2.4 *The uniform path SIR Γ_{Un} is defined as an achievable path SIR value supported by all paths, i.e.,*

$$\forall j : \Gamma_j = \Gamma_{Un}.$$

The maximum achievable uniform path SIR of the network is referred to as the *maximum uniform path SIR* and is denoted by $\Gamma_{Un}^{\max}$.

Definition 2.5 *The feasible path SIR region is defined as the set of all achievable path SIR vectors generated by a single power vector.*

Chapter 3

Maximum Uniform SIR

This chapter presents a new power control algorithm to achieve the maximum uniform SIR of wireless ad hoc networks. Previous works in this area have focused on using a central control unit to either coordinate the target SIR values or collect the full information of the network. However, in ad hoc networks such a centralized management is not plausible. In this chapter, first we introduce a new measurement parameter and then, based on that parameter, propose an autonomous power control algorithm to achieve the maximum uniform SIR. This algorithm does not require the full knowledge of the network or a central unit to coordinate the target SIR values.

3.1 Introduction

One of the parameters representing the overall throughput of the network is the maximum uniform link SIR (rate) of the network, which is the maximum achievable SIR when the SIR values of all links are the same, as defined in Chapter 2. Consequently, it is of a great importance to have a transmission control algorithm which can achieve the maximum uniform SIR of the network. Note that having a uniform SIR for all links guarantees a fair resource allocation (fairness) among all links. Theoretically, when there is no limit on the dynamic range of the transmitting powers, the problem of finding the maximum uniform link SIR is identified as an eigenvalue problem and given the full knowledge of the network parameters, it can be solved by using the theory of non-negative matrices [34, 7, 8, 18]. However,

in the real world applications, the mobile terminals are limited in battery power and have maximum constraints on their transmitting powers. In the literature, two approaches are proposed to find the maximum uniform rate of such power-constrained networks. In the first approach, this problem is formulated as an optimization problem and by relaxing some conditions, it is transformed into a convex problem solvable by the standard optimization methods [9, 10]. However, this optimization requires the full knowledge of the network, which may not be available in most wireless networks, and therefore, it may not be used in practice. In the second approach, a simple trial-and-error method is used where almost every value of the uniform rate has to be tested in order to find the maximum one [11, 12]. This method does not require the full knowledge of the network parameters, however, it requires a central control unit to implement a state-machine process tracing and coordinating the candidate uniform rates in order to find the maximum one.

In this chapter, we study the maximum uniform SIR in wireless ad hoc networks by investigating the necessary and sufficient conditions of its corresponding power vector. Based on these conditions, an iterative power control algorithm is developed which converges to the maximum uniform rate. The proposed algorithm requires only one parameter to be broadcast. This single parameter provides the required information for both finding the maximum uniform rate and complying with the maximum power constraints. Consequently, our algorithm requires less information to be broadcast from the links compared to other algorithms. Moreover, in contrast to the algorithm presented in [11], the proposed algorithm requires only one power convergence phase and most importantly, it is autonomous in the sense that it does not require a central unit to perform any state-machine process.

The rest of this chapter is organized as follows. In Section 3.2, the related works in the literature are briefly reviewed. In Section 3.3, we introduce the main concept of the proposed algorithm and investigate its convergence issues for single-hop wireless ad hoc networks where both scenarios of having a single channel and multiple channels are considered. Finally, in Section 3.4, the findings and the proposed algorithm are extended to multi-hop ad hoc networks.

Note that, as explained in Chapter 2, the concept of the maximum uniform SIR for

single-hop networks refers to the maximum uniform link SIR, whereas for multi-hop networks it refers to the maximum path SIR. The notion of the link or path in these definitions is omitted when they can be easily deduced from the context.

3.2 Related Work

Most of the research in this area assumes that the transmitting power can be adjusted without any limitations. However, in practice the transmitting power of a terminal has a maximum constraint and cannot be greater than a certain value, i.e., $\forall i : P_i \leq P^{\max}$. Therefore, in this review we examine the power-unconstrained and power-constrained networks separately. Note that this review considers the single-hop network model described in Section 2.1, where all links communicate over a single shared wireless channel.

3.2.1 Power-Unconstrained Networks

The maximum uniform link SIR of the power-unconstrained networks can be modeled as an eigenvalue problem [7, 8, 35]. This eigenvalue problem can be solved by using the theory of non-negative matrices as follows [16, 24, 25]. Recalling from Section 2.1.1, the power vector requirement for a set of QoS values for an N-link network is expressed by (2.2), i.e.,

$$(\mathbf{I}_N - \mathbf{F})\mathbf{P} \geq \mathbf{u} \ , \ \mathbf{P} > 0. \tag{3.1}$$

In order to achieve a uniform rate, all links require to maintain an equal SIR of γ_{Un}. Considering this requirement, (3.1) can be rewritten as

$$(\mathbf{I}_N - \gamma_{\mathbf{Un}}\mathbf{F}')\mathbf{P} \geq \mathbf{u}' \ , \ \mathbf{P} > 0 \tag{3.2}$$

where

$$\mathbf{u}' = (\frac{\gamma_{Un}\eta_1}{G_{11}}, \frac{\gamma_{Un}\eta_2}{G_{22}}, ..., \frac{\gamma_{Un}\eta_i}{G_{ii}}, ..., \frac{\gamma_{Un}\eta_N}{G_{NN}})^T$$

is a column vector of the noise powers scaled by the channel gains and the target SIR. Also,

the matrix $\mathbf{F}'$ is defined by its entries as

$$F'_{ij=}\begin{cases} 0, & \text{if } i=j \\ \frac{G_{ij}}{G_{ii}} & \text{if } i\neq j \end{cases}$$

with $i,j \in \{1,2,\cdots,N\}$. Note that $\mathbf{F}'$ has the same properties as those of $\mathbf{F}$.

The inequality (3.2) has a non-negative solution, if and only if the maximum modulus eigenvalue, i.e., the Perron-Frobenius eigenvalue, of the matrix $(\gamma_{\mathbf{Un}}\mathbf{F}')$ is less than 1. Let ρ'_f be the Perron-Frobenius eigenvalue of $\mathbf{F}'$. Therefore, there exists a non-negative power vector solution for (3.2), if $(\gamma_{Un}\rho'_f) < 1$. As a result, the maximum possible value of the uniform SIR is equal to $\gamma_{Un}^{\max} = 1/\rho'_f$. Moreover, any achievable uniform SIR γ_{Un}, for which $\gamma_{Un} \leq \gamma_{Un}^{\max}$, is generated by a power vector equal to

$$\mathbf{P} = (\mathbf{I}_N - \gamma_{\mathbf{Un}}\mathbf{F}')^{-1}\mathbf{u}'. \tag{3.3}$$

The optimum power vector in the above equation can be also calculated in a distributed format as

$$P_i(k+1) = \frac{\gamma_{Un}}{\gamma_i(k)}P_i(k) \tag{3.4}$$

where $P_i(k)$ and $\gamma_i(k)$ denote the power and SIR of the link i at the kth iteration, respectively [16, 35, 36].

Note that in this method, the maximum uniform rate only depends on the Perron-Frobenius eigenvalue and the power limits have not been considered in the eigenvalue calculations. Therefore, it is not possible to directly apply this method to power-constrained networks.

3.2.2 Power-Constrained Networks

In the literature, two different approaches are proposed to find the maximum uniform rate of the power-constrained networks; rearranging the problem as an optimization problem and using a trial-and-error search method.

Rearranging as an Optimization Problem

In [9, 10], the problem of finding the maximum uniform rate is considered as a constrained optimization problem where the equal rate of the links is maximized based on the power elements, given by

$$\max_{\mathbf{P}} \ \gamma_{Un}$$

$$\text{subject to} \qquad \forall i : \ \gamma_{Un} = \frac{G_{ii}P_i}{\eta_i + \sum_{j \neq i} G_{ij}P_j} \ .$$

$$\forall i : 0 \leq P_i \leq P^{\max}$$

where further transformation is also required to convert this problem into a convex optimization. Note that this optimization requires a central unit to provide the full knowledge of the network parameters such as the channel gain parameters $\forall i, j : G_{ij}$. However, as mentioned earlier, in most wireless networks, and specifically in wireless ad hoc networks, this full information is not available at any link and therefore, it is not practical to apply this technique.

Using a Trial-and-Error Search

In [11], Grandhi and Zander present a practical approach in which a central unit effectively searches for the maximum uniform link SIR. A similar approach is also considered in [12]. In this method, first the central unit starts with a small SIR and commands all links to target this SIR value. Then, all links update their powers targeting that SIR, based on the distributed power equation of (3.4). When all power elements converge, each link informs the central unit of its power level and if no link has achieved the maximum power limit, the central unit increases the target SIR by a small amount. This procedure is repeated until one of the links reaches its maximum power. We refer to this algorithm as the *Trial-and-Error Search (TES)* algorithm.

Although this is a simple algorithm, it has certain drawbacks. In order to have an accurate maximum uniform rate, the step-size of the candidate γ_{Un} has to be small, which

consequently results in a slow convergence of each step. Also, since at each step all power elements have to converge prior to increasing the SIR target, the speed of the overall convergence of the algorithm is slow as well. Moreover, there are two pieces of information per iteration required to be communicated between the central unit and each link; the transmission power and target SIR γ_{Un}. But, most importantly, in this algorithm the central control unit has to perform a state-machine process in order to trace the target SIR values and decide and coordinate the new target SIR at each step. Therefore, it is not possible to implement this process in a distributed format.

3.3 Single-Hop Ad Hoc Networks

In this section, we consider the single-hop network model, as described in Section 2.1. In the following, the main concept of the proposed algorithm is initially introduced for the ad hoc networks communicating over only one shared channel; first, the necessary and sufficient conditions for the power vector to achieve the maximum uniform SIR are investigated in Section 3.3.1. Next, in Section 3.3.2, based on those aforementioned conditions the main algorithm is proposed and its convergence is evaluated. Finally, in Section 3.3.3, the proposed algorithm is extended to the case of having multiple channels available to the network.

3.3.1 Conditions for Achieving the Maximum Uniform SIR

The SIR values of all links can be directly calculated by having the set of power elements. Therefore, in order to calculate the maximum uniform link SIR of the network, it is sufficient to find its achieving power vector. In order to accomplish this, in this section the necessary and sufficient conditions of the power vector achieving the maximum uniform link SIR are investigated for a single-channel single-hop ad hoc network.

We start with the general problem of maximizing the minimum link SIR in a power-constrained network and as the first step, we show that this problem is equivalent to the problem of maximizing the uniform link SIR. The following theorem shows that if a power vector achieves the maximum of the minimum link SIR, then all of its link SIR values have

to be the same and equal to the maximum uniform link SIR.

Theorem 3.1 *If the link SIR vector $\boldsymbol{\gamma} = [\gamma_i]$ corresponding to the power vector $\mathbf{P} = [P_i]$ has the maximum $\min_i(\gamma_i)$ in all achievable SIR vectors, then*

a) All links have the same SIR

b) This equal SIR value is the maximum uniform link SIR of the network ($\gamma_{Un}^{\max}$), i.e.,

$$\forall i : \gamma_i = \gamma_{Un}^{\max}.$$

Proof:

a) Using a counter example, assume $\exists k : \min_i(\gamma_i) < \gamma_k$. Build $\hat{\mathbf{P}} = [\hat{P}_i]$ with power elements $\forall i \neq k : \hat{P}_i = P_i$ and set $\hat{P}_k$ corresponding to $\hat{\gamma}_k$ where $\min_i(\gamma_i) < \hat{\gamma}_k < \gamma_k$. Obviously, $\hat{P}_k < P_k$. Since, $\hat{P}_k$ is less than P_k and other power elements of $\hat{\mathbf{P}}$ are equal to those of $\mathbf{P}$, in a network using $\hat{\mathbf{P}}$ the interference at the receiver of any link except link k is less than that of in a network based on $\mathbf{P}$ and consequently, $\forall i \neq k : \gamma_i < \hat{\gamma}_i$. Therefore, considering the fact that $\min_i(\gamma_i) < \hat{\gamma}_k$, we have

$$\min_i(\gamma_i) < \min_i(\hat{\gamma}_i)$$

which is in contradiction with the assumption of maximum $\min_i(\gamma_i)$ property of $\mathbf{P}$.

b) From part (a), the SIR values of all the links produced by the power vector $\mathbf{P}$ are the same and let them be equal to $\gamma_{Un}^{\max}$. Now, by a counter example, assume that there exists another power vector $\hat{\mathbf{P}} = [\hat{P}_i]$ with the link SIR vector $\hat{\boldsymbol{\gamma}} = [\hat{\gamma}_i]$ which has a uniform SIR of $\hat{\gamma}_{Un}$ greater than $\gamma_{Un}^{\max}$. Consequently,

$$\gamma_{Un}^{\max} < \hat{\gamma}_{Un} \Rightarrow \forall i : \gamma_i < \hat{\gamma}_i \Rightarrow \min_i(\gamma_i) < \min_i(\hat{\gamma}_i)$$

which is again in contradiction with the assumption of maximum $\min_i(\gamma_i)$ property of $\mathbf{P}$. □

Note that a concept similar to Theorem 3.1 is also studied in [37]. The following lemmas are used later in this section to prove the necessary and sufficient conditions of the

power vector corresponding to the maximum uniform SIR.

Lemma 3.2 (A greater link SIR vector has a greater power vector) *For any link SIR vector* $\gamma = [\gamma_i]$ *with the power vector* $\mathbf{P} = [P_i]$ *and any link SIR vector* $\hat{\gamma} = [\hat{\gamma}_i]$ *with the power vector* $\hat{\mathbf{P}} = [\hat{P}_i]$, *if* $\hat{\gamma}$ *is element-wise equal to or greater than* γ, *then* $\hat{\mathbf{P}}$ *is also element-wise equal to or greater than* $\mathbf{P}$, *i.e.,*

$$\forall i \; : \; \gamma_i \leq \hat{\gamma}_i \Rightarrow \forall i \; : \; P_i \leq \hat{P}_i. \tag{3.5}$$

Proof: Set $\forall i \; : \; b_i = \frac{P_i}{\hat{P}_i}$ for all links and assume $\exists k \; : \; b_k = \max_i(b_i)$. As a counter example, assume that there exists at least one link that $P_i > \hat{P}_i$, or equivalently $b_i > 1$, which guarantees that $b_k > 1$. According to the assumption, for the link k we have

$$\gamma_k \leq \hat{\gamma}_k$$

$$\frac{G_{kk}P_k}{\sum_{j\neq k} G_{kj}P_j + \eta_k} \leq \frac{G_{kk}\hat{P}_k}{\sum_{j\neq k} G_{kj}\hat{P}_j + \eta_k}.$$

By substituting P_i with $b_i \times \hat{P}_i$, the above inequality can be further simplified to

$$\eta_k(b_k - 1) + \sum_{j\neq k} G_{kj}(b_k\hat{P}_j - b_j\hat{P}_j) \leq 0. \tag{3.6}$$

Since $\eta_k \, (b_k - 1) > 0$, to satisfy the above inequality at least one of the components of the summation in (3.6) has to be negative, i.e.,

$$\exists l : G_{kl}\hat{P}_l \, (b_k - b_l) < 0 \Longrightarrow b_k < b_l$$

which is impossible, since $b_k = \max_i(b_i)$. □

Lemma 3.3 *For any link SIR vector* $\gamma = [\gamma_i]$ *with the power vector* $\mathbf{P} = [P_i]$ *and any link SIR vector* $\hat{\gamma} = [\hat{\gamma}_i]$ *with the power vector* $\hat{\mathbf{P}} = [\hat{P}_i]$, *if* $\hat{\gamma}$ *is element-wise equal to or greater than* γ *and there exists at least one link for which* $\gamma_k < \hat{\gamma}_k$, *then* $\hat{\mathbf{P}}$ *is element-wise*

greater than $\mathbf{P}$*, i.e.,*

$$\forall i \,:\, \gamma_i \leq \hat{\gamma}_i \; and \; \exists k \,:\, \gamma_k < \hat{\gamma}_k \Rightarrow \forall i \,:\, P_i < \hat{P}_i.$$

Proof: Since $\forall i \,:\, \gamma_i \leq \hat{\gamma}_i$, according to Lemma 3.2

$$\forall i \,:\, P_i \leq \hat{P}_i \tag{3.7}$$

therefore

$$1 \leq \frac{\sum_{j \neq k} G_{kj} \hat{P}_j + \eta_k}{\sum_{j \neq k} G_{kj} P_j + \eta_k}. \tag{3.8}$$

By rewriting $\gamma_k < \hat{\gamma}_k$, we have $\frac{G_{kk} P_k}{\sum_{j \neq k} G_{kj} P_j + \eta_k} < \frac{G_{kk} \hat{P}_k}{\sum_{j \neq k} G_{kj} \hat{P}_j + \eta_k}$ or equivalently

$$\frac{\sum_{j \neq k} G_{kj} \hat{P}_j + \eta_k}{\sum_{j \neq k} G_{kj} P_j + \eta_k} < \frac{\hat{P}_k}{P_k}. \tag{3.9}$$

Comparing (3.9) to (3.8) shows that $1 < \frac{\hat{P}_k}{P_k}$ or $P_k < \hat{P}_k$. Now, by combining this inequality with (3.7), for any $i \neq k$ we have

$$1 < \frac{\sum_{j \neq i} G_{ij} \hat{P}_j + \eta_i}{\sum_{j \neq i} G_{ij} P_j + \eta_i}. \tag{3.10}$$

Furthermore, by rewriting $\forall i : \gamma_i \leq \hat{\gamma}_i$, it can be verified that

$$\frac{\sum_{j \neq i} G_{ij} \hat{P}_j + \eta_i}{\sum_{j \neq i} G_{ij} P_j + \eta_i} \leq \frac{\hat{P}_i}{P_i} \tag{3.11}$$

and by comparing (3.10) and (3.11), it can be seen that $\forall i \neq k : P_i < \hat{P}_i$. □

The following statement is a direct corollary of Lemma 3.3;

Corollary 3.4 *For any link SIR vector* $\boldsymbol{\gamma} = [\gamma_i]$ *with the power vector* $\mathbf{P} = [P_i]$ *and any link SIR vector* $\hat{\boldsymbol{\gamma}} = [\hat{\gamma}_i]$ *with the power vector* $\hat{\mathbf{P}} = [\hat{P}_i]$*, if* $\hat{\boldsymbol{\gamma}}$ *is element-wise greater than* $\boldsymbol{\gamma}$*, then* $\hat{\mathbf{P}}$ *is also element-wise greater than* $\mathbf{P}$*, i.e.,*

$$\forall i \,:\, \gamma_i < \hat{\gamma}_i \Rightarrow \forall i \,:\, P_i < \hat{P}_i. \tag{3.12}$$

Before discussing the conditions of the maximum uniform SIR, one of the important questions in this context is that whether it is possible to have two power vectors producing the same link SIR vector or not. The following lemma addresses this issue and shows that there is a one-to-one relationship between a power vector and its link SIR vector.

Lemma 3.5 *Each link SIR vector* $\gamma = [\gamma_i]$ *is produced by only one power vector* $\mathbf{P} = [P_i]$.

Proof: By a counter example, assume that there is another power vector $\hat{\mathbf{P}} = [\hat{P}_i]$ with $\hat{\gamma} = [\hat{\gamma}_i]$ where these two link SIR vectors are the same, i.e., $\hat{\gamma} = \gamma$. Now, according to Lemma 3.2, we have

$$\forall i \; : \; \gamma_i \leq \hat{\gamma}_i \Rightarrow \forall i \; : \; P_i \leq \hat{P}_i$$

and

$$\forall i \; : \; \hat{\gamma}_i \leq \gamma_i \Rightarrow \forall i \; : \; \hat{P}_i \leq P_i$$

which is impossible, unless $\forall i \; : \; P_i = \hat{P}_i$. □

Now, using the above lemmas and theorem, we can state and prove the necessary and sufficient conditions for the power vector corresponding to the maximum uniform link SIR in single-hop wireless networks;

Theorem 3.6 *The power vector* $\mathbf{P} = [P_i]$ *has the maximum uniform link SIR, i.e.,* $\gamma_{Un} = \gamma_{Un}^{\max}$, *if and only if:*

1. The SIR of every link is equal to γ_{Un}.

2. At least the power of one link is equal to its maximum value, i.e., $\exists l : P_l = P^{\max}$.

Proof:

a) *if* part: We show that if the power vector $\mathbf{P} = [P_i]$ has the above conditions, then it has the maximum uniform link SIR.

Let $\hat{\mathbf{P}} = [\hat{P}_i]$ be the power vector corresponding to the uniform SIR of $\hat{\gamma}_{Un}$, i.e., $\forall i : \hat{\gamma}_i = \hat{\gamma}_{Un}$. Considering a counter example, assume that $\gamma_{Un} < \hat{\gamma}_{Un}$. Since $\forall i : \gamma_i < \hat{\gamma}_i$, from Corollary 3.4

$$\forall i \; : \; P_i < \hat{P}_i$$

which is in contradiction with the assumption, since $P_l = P^{\max}$ and $\hat{P}_l$ cannot be greater than the maximum power. Therefore $\gamma_{Un} = \gamma_{Un}^{\max}$ and no other uniform SIR can be greater than γ_{Un}.

b) *only if* part:

Assuming that $\mathbf{P} = [P_i]$ has the maximum uniform rate $\gamma_{Un}^{\max}$, we need to prove those two conditions. The first condition is derived by the definition of the uniform SIR. For the second condition, by a counter example, we show that if there is no link in $\mathbf{P} = [P_i]$ equal to $P^{\max}$, then there exists another power vector with a minimum SIR greater than $\gamma_{Un}^{\max}$. Therefore, $\gamma_{Un}^{\max}$ cannot be the maximum uniform rate of the network.

Theorem 3.1 states that the condition of maximizing the minimum link SIR is equivalent to the condition of maximizing the uniform link SIR. Therefore, $\mathbf{P} = [P_i]$ also satisfies the maximum of the minimum SIR condition. Assuming $\forall i : P_i < P^{\max}$, for each link i set $a_i = \frac{P^{\max}}{P_i}$ and let $a_k = \min_i(a_i)$. Obviously, $a_k > 1$. Now build a new power vector $\hat{\mathbf{P}} = [\hat{P}_i]$ by setting $\hat{P}_i = a_k \times P_i$. Clearly, $\hat{P}_k = P^{\max}$ and $\forall i \neq k : \hat{P}_i \leq P^{\max}$. By substituting $\hat{P}_i$ with $a_k \times P_i$ in (2.1), we have

$$\forall i : \ \hat{\gamma}_i = \frac{G_{ii}\hat{P}_i}{\sum_{j \neq i} G_{ij}\hat{P}_j + \eta_i} = \frac{G_{ii}P_i}{\sum_{j \neq i} G_{ij}P_j + \frac{\eta_i}{a_k}}$$

and since $a_k > 1$,

$$\forall i : \ \frac{G_{ii}P_i}{\sum_{j \neq i} G_{ij}P_j + \frac{\eta_i}{a_k}} > \frac{G_{ii}P_i}{\sum_{j \neq i} G_{ij}P_j + \eta_i}.$$

Therefore, $\forall i : \hat{\gamma}_i > \gamma_i$. Consequently, $\min_i(\hat{\gamma}_i) > \min_i(\gamma_i)$ which is in contradiction with the assumption of the maximum $\min_i(\gamma_i)$ property of $\mathbf{P}$. □

3.3.2 Autonomous Power Control Algorithm

In this section, first an autonomous power control algorithm is introduced to achieve the maximum uniform link SIR and its corresponding power vector. Next, the proposed algorithm is briefly compared to the TES algorithm. Later, the properties and convergence issues of the proposed algorithm are investigated. Finally, some numerical results are presented.

Any power control algorithm achieving the maximum uniform SIR requires some periodically broadcast feedback from the links due to the power constraints, requirement of equal SIRs, etc. Therefore, there is no algorithm that updates the power elements in a fully distributed manner and at the same time, achieves the maximum uniform rate. In our proposed method, we show that all the information required to find the maximum uniform rate and to comply with the power constraints is extracted from only one parameter per link, whereas the TES algorithm requires two (see Section 3.2.2).

The new parameter is referred to as the *SIR Metric* of the link i at the kth iteration and is defined as

$$M_i(k) \triangleq \gamma_i(k) \times \frac{P^{\max}}{P_i(k)}. \tag{3.13}$$

This value can be considered as the maximum possible SIR of the link i at the kth iteration, which can be achieved by maximizing its power while other power elements remain the same. Moreover, let

$$M_{\min}(k) \triangleq \min_i(M_i(k)) = \tilde{\gamma}(k) \times \frac{P^{\max}}{\tilde{P}(k)} \tag{3.14}$$

where $\tilde{\gamma}(k)$ and $\tilde{P}(k)$ are the parameters of the link corresponding to this minimum SIR metric, i.e., $M_{\min}(k)$.

The proposed power control algorithm is as follows; the power of each link i at the kth iteration, i.e., $P_i(k)$, is updated as

$$\forall i: \; P_i(k) = P_i(k-1) \times \frac{M_{\min}(k-1)}{\gamma_i(k-1)}. \tag{3.15}$$

As shown in the next section, the updated power elements always comply with the maximum power limits and by iteratively performing this power control algorithm, the conditions of Theorem 3.6 are satisfied and therefore, the maximum uniform link SIR is achieved.

The most important characteristic of the proposed algorithm is that it is autonomous in the sense that, contrary to the TES algorithm, the central unit (if any) does not require to perform any kind of state-machine process. Even in the scenarios where a new link enters

the network or an existing link leaves the network, no extra processing is required and the proposed algorithm adjusts the maximum uniform link SIR and the power levels automatically. Moreover, there is only one phase of power convergence needed, whereas the TES algorithm requires several phases of power convergence as mentioned earlier (note that the overall convergence speeds of these algorithms depend also on the number of iterations per power convergence phase, and depending on the network realization and target SIRs, one might be faster than the other one or vice versa). From the practical point of view, the SIR metrics can be either transmitted from each link to a central unit and then the minimum value is broadcast in the network, or all links can directly broadcast their SIR metrics throughout the network and then each link operates based on the minimum one.

3.3.2.1 Properties and Propositions

The main properties of the proposed power control algorithm are investigated in this section.

The following proposition shows that given the necessary and sufficient conditions of Theorem 3.6, the proposed power control algorithm, introduced in (3.15), does not change the power elements and therefore, those conditions provide a stable point for the proposed algorithm;

Proposition 3.7 *The set of conditions stated in Theorem 3.6, is a stable point for the proposed algorithm, i.e., if* $\forall i : \gamma_i(k) = \gamma_{Un}$ *and* $\exists l : P_l(k) = P^{\max}$, *then*

$$\forall i : P_i(k+1) = P_i(k).$$

Proof: By the assumption, $M_l(k) = \gamma_l(k) \times \frac{P^{\max}}{P_l(k)} = \gamma_{Un}$ and since $M_i(k) = \gamma_{Un} \times \frac{P^{\max}}{P_i(k)} \geq \gamma_{Un}$, we have $M_{\min}(k) = \gamma_{Un}$. As a result, the power control algorithm (3.15) can be rewritten as

$$\forall i, k : \; P_i(k+1) = P_i(k) \times \frac{M_{\min}(k)}{\gamma_i(k)} = P_i(k) \times \frac{\gamma_{Un}}{\gamma_{Un}} = P_i(k)$$

which completes the proof. □

The following proposition shows that the proposed power control algorithm does not violate the power constraints of the links in the network;

Proposition 3.8 *By using the power control algorithm (3.15), the updated power of each link is always equal to or less than its maximum limit, i.e.,* $\forall k, i : P_i(k) \leq P^{\max}$.

Proof: Considering the fact that $M_{\min}(k) \leq \gamma_i(k) \times \frac{P^{\max}}{P_i(k)}$ and (3.15), we have $P_i(k+1) \leq P_i(k) \times \frac{P^{\max}}{P_i(k)} = P^{\max}$. □

The following proposition shows that, at any given time, there is at least one link transmitting with its maximum power;

Proposition 3.9 *By using the power control algorithm (3.15), in each iteration there is at least one link transmitting with its maximum power, i.e.,* $\exists j : P_j(k) = P^{\max}$.

Proof: It is straightforward to show that the updated power of the link corresponding to $M_{\min}(k-1)$ is always equal to its maximum value at the kth iteration. □

The following two propositions show that the minimum SIR metric, in the proposed algorithm, is bounded by $\gamma_{\min}(k)$ and $\gamma_{\max}(k)$. These propositions are used later to prove the convergence of that algorithm.

Proposition 3.10 *By using the power control algorithm (3.15), the minimum SIR metric is always equal to or greater than the minimum SIR, i.e.,*

$$\forall k: \ M_{\min}(k) \geq \gamma_{\min}(k) \tag{3.16}$$

with equality only if $\tilde{\gamma}(k) = \gamma_{\min}(k)$ *and* $\tilde{P}(k) = P^{\max}$.

Proof: By the definition of $M_{\min}(k)$ and $\gamma_{\min}(k)$, the proof is apparent. □

Proposition 3.11 *By using the power control algorithm (3.15), we have*

1. *The minimum SIR metric is always equal to or less than the maximum SIR, i.e.,*

$$\forall k: \ M_{\min}(k) \leq \gamma_{\max}(k). \tag{3.17}$$

2. *If* $\tilde{\gamma}(k) = \gamma_{\max}(k)$, *then* $\tilde{P}(k) = P^{\max}$.

Proof: According to Proposition 3.9, $\exists l : P_l(k) = P^{\max}$. Therefore, by the definition of $M_{\min}(k)$, it can be shown that $M_{\min}(k) \leq \gamma_l(k)$ and since $\forall i : \gamma_i(k) \leq \gamma_{\max}(k)$, the proof of part (1) is complete. The statement of part (2) is a direct result of (3.17). □

3.3.2.2 Algorithm Convergence

In order to show that the proposed algorithm converges to the maximum uniform link SIR, we study the evolutions of the minimum SIR and maximum SIR of the network in the following two theorems.

Theorem 3.12 *The minimum SIR of the network strictly increases in each iteration until the necessary and sufficient conditions of the maximum uniform link SIR are met and afterwards, the minimum SIR becomes constant, i.e.,*

$$\forall k : \ \gamma_{\min}(k+1) \geq \gamma_{\min}(k) \tag{3.18}$$

with equality only if $\forall i : \gamma_i(k) = \gamma_{\min}(k)$ *and* $\exists j : P_j(k) = P^{\max}$.

Proof: In order to prove (3.18), it is sufficient to show that $\forall i, k : \gamma_i(k+1) \geq \gamma_{\min}(k)$. By rewriting $\gamma_i(k+1)$, we have

$$\begin{aligned}
\forall i, k : \ \gamma_i(k+1) &= \frac{G_{ii}P_i(k+1)}{\eta_i + \sum_{j \neq i} G_{ij}P_j(k+1)} \\
&= \frac{M_{\min}(k) \times G_{ii}\frac{P_i(k)}{\gamma_i(k)}}{\eta_i + M_{\min}(k) \times \sum_{j \neq i} G_{ij}\frac{P_j(k)}{\gamma_j(k)}} \\
&= \frac{1}{\gamma_i(k)} \times \frac{G_{ii}P_i(k)}{\frac{\eta_i}{M_{\min}(k)} + \sum_{j \neq i} G_{ij}\frac{P_j(k)}{\gamma_j(k)}} \\
&\geq \frac{1}{\gamma_i(k)} \times \frac{G_{ii}P_i(k)}{\frac{\eta_i}{\gamma_{\min}(k)} + \sum_{j \neq i} G_{ij}\frac{P_j(k)}{\gamma_{\min}(k)}}
\end{aligned} \tag{3.19}$$

The last inequality in (3.19) is based on the fact that $\forall i, k : \gamma_i(k) \geq \gamma_{\min}(k)$ and Proposition 3.10. It can also be verified that the equality is achieved only if $\forall i : \gamma_i(k) = \gamma_{\min}(k)$ and

$\tilde{P}(k) = P^{\max}$. By the definition of $\gamma_i(k)$, this inequality can be rewritten as

$$\forall i, k: \ \gamma_i(k+1) \geq \frac{\gamma_{\min}(k)}{\gamma_i(k)} \times \gamma_i(k) = \gamma_{\min}(k).$$

Finally, according to Proposition 3.7, once the necessary and sufficient conditions are met, i.e., in this case $\forall i \ : \ \gamma_i(k) = \gamma_{\min}(k)$ and $\tilde{P}(k) = P^{\max}$, the power elements remain unchanged and therefore, the minimum SIR becomes constant. □

Theorem 3.13 *The maximum SIR of the network strictly decreases in each iteration until the necessary and sufficient conditions of the maximum uniform link SIR are met and afterwards, the maximum SIR becomes constant, i.e.,*

$$\forall k: \ \gamma_{\max}(k+1) \leq \gamma_{\max}(k) \tag{3.20}$$

with equality only if $\forall i : \gamma_i(k) = \gamma_{\max}(k)$ *and* $\exists j : P_j(k) = P^{\max}$.

Proof: In order to prove (3.20), it is sufficient to show that $\forall i, k : \gamma_i(k+1) \leq \gamma_{\max}(k)$. Recalling from (3.19)

$$\forall i, k : \gamma_i(k+1) = \frac{1}{\gamma_i(k)} \times \frac{G_{ii}P_i(k)}{\frac{\eta_i}{M_{\min}(k)} + \sum_{j \neq i} G_{ij} \frac{P_j(k)}{\gamma_j(k)}}. \tag{3.21}$$

Considering the fact that $\forall i : \gamma_i(k) \leq \gamma_{\max}(k)$ and Proposition 3.11, the following inequality is resulted

$$\forall i, k : \gamma_i(k+1) \leq \frac{1}{\gamma_i(k)} \times \frac{G_{ii}P_i(k)}{\frac{\eta_i}{\gamma_{\max}(k)} + \sum_{j \neq i} G_{ij} \frac{P_j(k)}{\gamma_{\max}(k)}} \tag{3.22}$$

where the equality is achieved only if $\forall i \ : \ \gamma_i(k) = \gamma_{\max}(k)$ and $\tilde{P}(k) = P^{\max}$. By the definition of $\gamma_i(k)$, this inequality can be rewritten as

$$\forall i, k : \gamma(k+1) \leq \frac{\gamma_{\max}(k)}{\gamma_i(k)} \times \gamma_i(k) = \gamma_{\max}(k). \tag{3.23}$$

Finally, according to Proposition 3.7, once the necessary and sufficient conditions are met, i.e., in this case $\forall i \ : \ \gamma_i(k) = \gamma_{\max}(k)$ and $\tilde{P}(k) = P^{\max}$, the power elements remain

unchanged and therefore, the maximum SIR becomes constant. □

Now, we can prove that the iterative power control algorithm in (3.15) converges to the maximum uniform link SIR of the network. According to Theorems 3.12 and 3.13, by performing each iteration the maximum SIR of the network is strictly decreased whereas the minimum SIR is strictly increased, until the necessary and sufficient conditions of Theorem 3.6 are met. Therefore, in each iteration the difference of the maximum SIR the minimum SIR becomes smaller and smaller until these two values become equal and constant. This implies that the necessary and sufficient conditions are met, and the resulted equal rate is indeed the maximum uniform rate of the network.

3.3.2.3 Numerical Results

In this section, the numerical results for two example networks are presented. In the following, first the simulation setup is described and then, the properties of the minimum and maximum SIR values per iteration, the necessary and sufficient conditions of the maximum uniform link SIR and the convergence of the proposed power control algorithm are investigated.

Consider an N-link wireless network according to the single-hop model described in Section 2.1. The transmitter of each link is placed at random with a uniform distribution in a square area of 200×200 m^2. The receiver of each link is placed at a random distance from its transmitter according to the Gaussian distribution with a mean of 10 m and a standard deviation of 2 m. Also, the angle of each receiver compared to its transmitter is distributed uniformly in the range of $[0, 2\pi)$ given a reference direction. Note that given this setup, an extremely rare event of having a negative distance between a transmitter and its receiver implies an additional π radian rotation of the original angle of those two nodes. The channel gain models large-scale propagation effects, i.e., the path loss and the shadowing effects [32]. Variations due to small-scale propagation effects are usually assumed to be averaged out in the context of SIR-based power control [33]. The channel gain between the transmitter of the link j and the receiver of the link i, is modeled as

$$G_{ij} = K_o \frac{a_{ij}}{r_{ij}^4} \tag{3.24}$$

where r_{ij} represents the distance between these two nodes, a_{ij} models the power attenuation due to the shadowing and K_o is a unitless constant depending on other parameters such as antenna characteristics, reference distance, etc. [32]. All a_{ij} variables are assumed to be independent and log-normally distributed with a mean of 0 dB and a standard deviation of 8 dB [38, 39]. For all links, the maximum transmitting power P^{max} is equal to 1 W, the thermal noise power η is set to 10^{-12} W and K_o is set to 0.0142 (corresponding to $f_c = 2$ GHz and a reference distance of 10 m). The initial powers of all links are set to 0.1 W.

In the following, we consider two network realizations randomly generated according to the aforementioned network configuration. In these example networks, it is assumed that $N = 6$, i.e., the total number of the links in the network is equal to 6. The SIR evolutions of these two example networks are illustrated in Figure 3.1. In both graphs, the minimum SIR value of each iteration is represented by a dashed line whereas the maximum SIR value is represented by a solid line. As shown, at each iteration the minimum SIR increases whereas the maximum SIR decreases until the maximum SIR and minimum SIR become the same, or in other words, all SIR values become equal. This observation confirms the theoretical findings of Theorems 3.12 and 3.13. Moreover, it is verified that at each iteration there is at least one link transmitting with its maximum power. As a result, the SIR values corresponding to the convergence points of these examples, i.e., 23 dB in Figure 3.1.a in 18.5 dB for Figure 3.1.b, are indeed the maximum uniform link SIR of these example networks.

3.3.3 Multi-Channel Communications

In the previous sections, it was assumed that there is only one wireless channel shared among the links. In this section, we show that all the results and the algorithms can be extended to the multi-channel communications scenario where there is more than one channel available to the network and each link is pre-assigned to communicate over one of these channels. Clearly, each channel contains at least one link.

In Section 3.3.1, the maximum uniform link SIR of the single-channel networks was studied. We started with the general problem of maximizing the minimum link SIR and

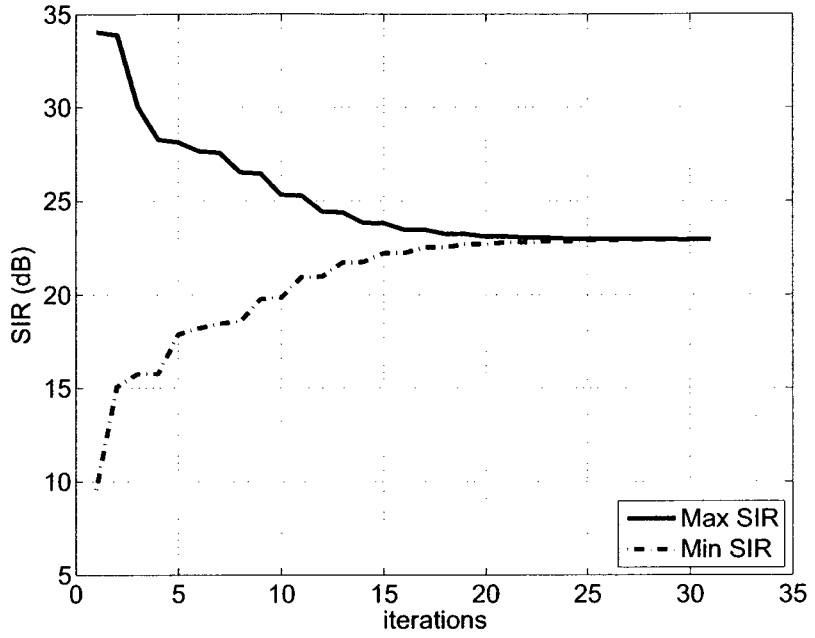

a)

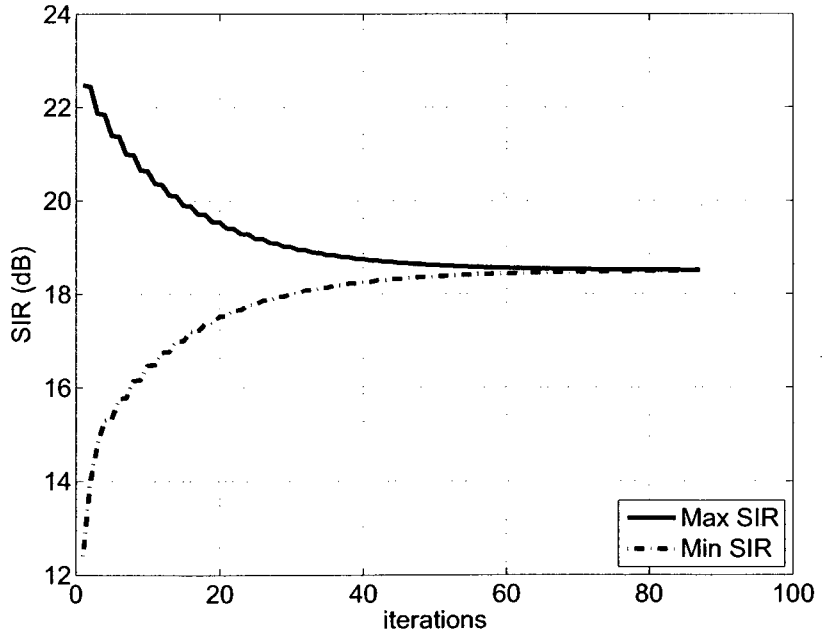

b)

Figure 3.1: Min/Max link SIR evolutions of two example networks resulting in the maximum uniform link SIR of : a) 23 dB, b) 18.5 dB.

in Theorem 3.1 we showed that, for single-channel networks, this problem is equivalent to the problem of maximizing the uniform SIR. The rationale behind Theorem 3.1 is that since only one channel is shared among all links and the power of each link is considered as an interference signal at other receivers, having the SIR of even one link greater than the minimum link SIR (i.e., having that link transmitting with a power more than the minimum requirement), increases the interference level at other links and subsequently, decreases the overall minimum SIR of the network. Therefore, in order to achieve the maximum of minimum link SIR, all links must maintain the same SIR as $\gamma_{Un}^{\max}$.

In the multi-channel communications scenario, all channels are independent and the transmission powers in one channel have no effect on the SIR of the links in other channels. In other words, only the co-channel interference is considered. Because of this interference isolation between subchannels, the findings of the previous sections regarding the single-channel communications are not directly applicable to this case. However, those findings can be applied to each subchannel and its corresponding links. That is, the maximum of the minimum link SIR of each subchannel is equal to that subchannel's maximum uniform link SIR. Apparently, the maximum of the minimum link SIR of the network is equal to the smallest value of all subchannels' maximum of the minimum link SIRs. In contrary to the single-channel case where all links need to have the same SIR to achieve the maximum of the minimum link SIR, in multi-channel communications the links in the subchannels other than the one with this smallest value may maintain any SIR equal to or greater than this value. As a result, there is an infinite number of feasible link SIR vectors resulting in the maximum of the minimum link SIR of the network.

One algorithm to generate the maximum uniform link SIR is to use the maximum uniform SIR algorithm of Section 3.3.2 for the single-channel communications on each subchannel and then, find the smallest value as the overall maximum uniform link SIR. A further processing step can be taken to minimize the overall power consumption of the network, i.e., reducing the uniform SIR of other subchannels to be equal to that of the subchannel with the smallest value. Clearly in this case, the link SIR vector and its corresponding power vector are unique. Moreover, the resulted power vector is the minimum power vector, i.e., it has the minimum total power among all vectors generating the same

overall maximum uniform link SIR in the network (minimal power vector concept is investigated in more detail later in this chapter). However, note that this approach requires a base station to track the activities of all subchannels, receive the maximum uniform SIR of each subchannel and command all links to target the minimum of the maximum uniform values. As a result, this method is not practical in wireless ad hoc networks where such a central management unit does not exist.

A more practical approach, and in fact a simpler algorithm, to find the maximum uniform link SIR is to use exactly the same algorithm as the one proposed for the maximum uniform link SIR of the single-channel networks in Section 3.3.2. The only conceptual difference is that no matter which subchannel each link belongs to, the minimum SIR metric $M_{\min}(k)$ is set to the minimum SIR metric $M_i(k)$ of all links in all subchannels. This guarantees that the SIR values of all links converge to the same value which is indeed the maximum uniform link SIR of the network. In this case, the resulted power vector has the minimum total power among all power vectors achieving such a maximum uniform rate.

3.4 Multi-Hop Ad Hoc Networks

The single-hop ad hoc networks were considered in the previous section. In particular, the properties of the maximum uniform link SIR were examined and a novel autonomous power control algorithm was proposed to achieve that SIR. In this section, those concepts are investigated for multi-hop wireless ad hoc networks and the proposed algorithms are extended to the networks based on the multi-hop network model presented in Section 2.2.

In multi-hop ad hoc networks, each pair of the original source and final destination nodes is communicating via a routing path. Since the routing path selection is considered as a separate research topic, this thesis studies neither the routing path selection nor the link allocation. Instead, we assume proactive (predefined) routing path scenarios where the information about the routing path selection and the link allocation is already provided by other layers/sub-layers of the network [40].

In this section, we initially consider the single-channel networks. In Section 3.4.1, the path SIR vectors are studied and the concept of the minimal power vector is introduced.

The necessary and sufficient conditions for the minimal power vector to achieve the maximum uniform path SIR are investigated in Section 3.4.2. The main algorithm is described in Section 3.4.3, where its convergence and performance are also evaluated. Finally, in Section 3.4.4, the proposed algorithm is extended to the case of having multiple channels available to the network.

3.4.1 Minimal Power Vector

As explained in Chapter 2, the principal component of an ad hoc network is the radio link where its quality of transmission is measured by its link SIR. Moreover, as mentioned earlier, in single-hop networks the transmission quality of the whole network is also determined by these link SIR values. However, in multi-hop communications there are two different quantities representing the quality of the transmission: the link SIR and the path SIR. In the following, each of these concepts is explained in detail.

As in single-hop networks, the link SIR of multi-hop networks is an indication of the quality of the transmission of the principal components of the network, i.e., the links. In fact, a multi-hop ad hoc network can be considered as a single-hop network at the link level. The most important consequence of this compatibility is that all theorems and findings of the link SIR for single-hop networks are directly applicable to the link SIR of multi-hop networks. In particular, in this section Lemmas 3.2 and 3.5 are used frequently which state that the greater element-wise link SIR vector has the greater element-wise power vector and each link SIR vector is produced by only one power vector. However, the overall transmission quality of multi-hop ad hoc networks is measured by the path SIR rather than the link SIR (see Chapter 2 for more detail). The concept of the path SIR can be further clarified by an example. Figure 3.2 shows an example network with two routing paths each consisting of two links where the solid lines represent the routing paths and the dashed lines represent the interference signals from other links. According to Definition 2.3, the path SIRs are expressed as

$$\Gamma_1 = \min(\gamma_{1,1}, \gamma_{2,1})$$

$$\Gamma_2 = \min(\gamma_{1,2}, \gamma_{2,2})$$

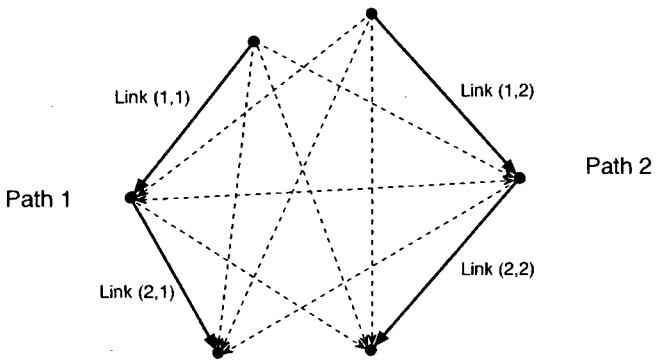

Figure 3.2: An example network with 2 paths and 4 links.

where the path SIR of each routing path is determined by the smallest link SIR of that path. This value is not affected by the link SIR of other links of that path or the position of the link with the minimum SIR. Therefore, there may exist several link SIR vectors (clearly produced by different power vectors) resulting in the same path SIR vector. We refer to the set of all power vectors producing the same path SIR $\mathbf{\Gamma} = [\Gamma_j]$ as $\mathcal{X}(\mathbf{\Gamma})$. These different quality merits of transmission result in one of the main differences of the single-hop and multi-hop ad hoc networks in the context of the overall transmission quality. In multi-hop networks, each path SIR can be generated by infinite number of power vectors, whereas in single-hop networks, each link SIR corresponds to only one power vector (see Lemma 3.5).

We show that there exists a power vector $\mathbf{P}^L = [P_{ij}^L] : \mathbf{P}^L \in \mathcal{X}(\mathbf{\Gamma})$ for which all link SIR values in each routing path are the same and equal to the path SIR of that path. For example, for the network in Figure 3.2, the link SIRs corresponding to $\mathbf{P}^L = [P_{ij}^L]$ has the following properties

$$\Gamma_1 = \min(\gamma_{1,1}, \gamma_{2,1}) = \gamma_{1,1} = \gamma_{2,1}$$

$$\Gamma_2 = \min(\gamma_{1,2}, \gamma_{2,2}) = \gamma_{1,2} = \gamma_{2,2}$$

Furthermore, we prove that this power vector $\mathbf{P}^L = [P_{ij}^L]$ is unique and it is the *minimal*

power vector of the path SIR vector $\mathbf{\Gamma} = [\Gamma_j]$ in the sense that

$$\forall \hat{\mathbf{P}} \in \mathcal{X}(\mathbf{\Gamma}), \forall i,j : P_{ij}^L \leq \hat{P}_{ij}.$$

Theorem 3.14 (Existence of $\mathbf{P}^L$ with equal link SIRs in each path) *For each achievable path SIR vector* $\mathbf{\Gamma} = [\Gamma_j]$, *there exists a power vector* $\mathbf{P}^L = [P_{ij}^L]$ *in* $\mathcal{X}(\mathbf{\Gamma})$ *with the link SIR vector* $\boldsymbol{\gamma}^L = [\gamma_{ij}^L]$, *for which each link SIR* γ_{ij}^L *is equal to its corresponding path SIR* Γ_j, *i.e.,*

$$\forall i,j : \gamma_{ij} = \Gamma_j.$$

Proof: We provide a constructive proof for this theorem. Since the path SIR vector $\mathbf{\Gamma} = [\Gamma_j]$ is achievable, there exists at least one power vector $\mathbf{P} = [P_{ij}]$ with the link SIR vector $\boldsymbol{\gamma} = [\gamma_{ij}]$ in $\mathcal{X}(\mathbf{\Gamma})$.

Considering $\mathbf{P} = [P_{ij}]$, if all link SIR values are equal to their corresponding routing paths, the proof is complete. Otherwise, there exists at least one link SIR γ_{rt} higher than the SIR of its corresponding routing path, i.e., Γ_t. Clearly, reducing P_{rt} results in a smaller value of γ_{rt}. Assuming that $\hat{P}_{rt}$ is the new value of P_{rt} for which $\hat{\gamma}_{rt} = \Gamma_t$, a new power vector $\hat{\mathbf{P}} = [\hat{P}_{ij}]$ is constructed by using $\hat{P}_{rt}$ for the link rt and setting

$$\forall ij \neq rt : \hat{P}_{ij} = P_{ij}.$$

Considering the fact that the interference in the whole network is reduced due to $\hat{P}_{rt} < P_{rt}$, we have $\forall i : \Gamma_j \leq \hat{\Gamma}_j$. This procedure can be repeated and the power elements of $\hat{\mathbf{P}} = [\hat{P}_{ij}]$ can be decreased iteratively until there is no link with a link SIR higher than its original path SIR in $\mathbf{\Gamma} = [\Gamma_j]$. In this case, the resulted power vector is indeed $\mathbf{P}^L = [P_{ij}^L]$ of $\mathbf{\Gamma} = [\Gamma_j]$. □

Now we show that the power vector $\mathbf{P}^L = [P_{ij}^L]$ has the power minimality property.

Theorem 3.15 (Minimal power vector) *For any path SIR vector* $\mathbf{\Gamma} = [\Gamma_j]$, *the power vector* $\mathbf{P}^L = [P_{ij}^L] \in \mathcal{X}(\mathbf{\Gamma})$, *with the link SIR vector* $\boldsymbol{\gamma}^L = [\gamma_{ij}^L]$, *has power elements equal to or*

smaller than those of all other power vectors in $\mathcal{X}(\mathbf{\Gamma})$, i.e.,

$$\forall \mathbf{P} \in \mathcal{X}(\mathbf{\Gamma}), \forall i,j : P_{ij}^{L} \leq P_{ij}.$$

Proof: By the definition, each power vector $\mathbf{P} = [P_{ij}] \in \mathcal{X}(\mathbf{\Gamma})$, with the link SIR vector $\boldsymbol{\gamma} = [\gamma_{ij}]$, has its link SIR elements equal to or greater than their corresponding path SIR. Moreover, the link SIR elements of $\boldsymbol{\gamma}^{L}$ are exactly equal to their path SIR values. Therefore,

$$\forall i,j : \gamma_{ij}^{L} \leq \gamma_{ij}.$$

Consequently, according to Lemma 3.2 which states that the greater link SIR vector has the greater power elements, for these two link SIR vectors and their corresponding power vectors we have

$$\forall i,j : P_{ij}^{L} \leq P_{ij}.$$

This proves the power minimality property of $\mathbf{P}^{L} = [P_{ij}^{L}]$. □

The minimal power vector concept provides us important information about the power allocation in ad hoc networks. That is, in order to achieve a specific path SIR vector, the minimal power vector is the minimum power requirement. In other words, since each element of the minimal power vector has the minimum power value, the summation of these power elements determines the minimum total power required by the network. Moreover, the concept of the minimal power vector extremely facilitates the study of multi-hop networks. In fact, in this work, the path SIR vectors are identified and analyzed by their minimal power vectors.

3.4.2 Conditions for Achieving the Maximum Uniform SIR

In this section, the necessary and sufficient conditions of the minimal power vector generating the maximum uniform path SIR of a single-channel multi-hop network are investigated.

The single-channel multi-hop networks are similar to the single-channel single-hop networks, in the sense that both are using a common shared channel among all links. The use of this shared channel lets us extend some of the results of the single-channel single-hop

communications directly to the single-channel multi-hop networks. For example, it can be shown that the problem of maximizing the minimum path SIR of the network is equivalent to the problem of finding the maximum uniform path SIR.

Theorem 3.16 *If the path SIR vector* $\mathbf{\Gamma} = [\Gamma_j]$ *with the minimal power vector* $\mathbf{P}^L = [P_{ij}^L]$, *has the maximum* $\min_j(\Gamma_j)$ *in all achievable path SIR vectors, then*

a) All paths and links have the same SIR.

b) This equal path SIR is the maximum uniform path SIR of the network ($\Gamma_{Un}^{\max}$), *i.e.,*

$$\forall j : \Gamma_j = \Gamma_{Un}^{\max}.$$

Proof: Assume $\boldsymbol{\gamma}^{\boldsymbol{L}} = [\gamma_{ij}^L]$ is the link SIR vector of $\mathbf{P}^L = [P_{ij}^L]$. Considering the fact that $\forall ij : \gamma_{i,j}^L = \Gamma_j$, the rest of the proof is similar to that of Theorem 3.1. □

Now, we extend Lemmas 3.2 and 3.3 to the multi-hop case.

Lemma 3.17 (A greater path SIR vector has a greater minimal power vector) *For any path SIR vector* $\mathbf{\Gamma} = [\Gamma_j]$ *with the minimal power vector* $\mathbf{P}^L = [P_{ij}^L]$ *and any path SIR vector* $\hat{\mathbf{\Gamma}} = [\hat{\Gamma}_j]$ *with the minimal power vector* $\hat{\mathbf{P}}^L = [\hat{P}_{ij}^L]$, *if* $\hat{\mathbf{\Gamma}}$ *is element-wise greater than or equal to* $\mathbf{\Gamma}$, *then* $\hat{\mathbf{P}}^{\mathbf{L}}$ *is also element-wise greater than or equal to* $\mathbf{P}^{\mathbf{L}}$, *i.e.,*

$$\forall i : \Gamma_i \leq \hat{\Gamma}_i \Rightarrow \forall i, j : P_{ij} \leq \hat{P}_{ij}.$$

Proof: Since we are using the minimal power vectors, the assumption of $\forall j : \Gamma_j \leq \hat{\Gamma}_j$ is equivalent to $\forall i, j : \gamma_{ij} \leq \hat{\gamma}_{ij}$. The rest of the proof is similar to that of Lemma 3.2. □

Lemma 3.18 *For any path SIR vector* $\mathbf{\Gamma} = [\Gamma_j]$ *with the minimal power vector* $\mathbf{P}^L = [P_{ij}^L]$ *and any path SIR vector* $\hat{\mathbf{\Gamma}} = [\hat{\Gamma}_j]$ *with the minimal power vector* $\hat{\mathbf{P}}^L = [\hat{P}_{ij}^L]$, *if* $\hat{\mathbf{\Gamma}}$ *is element-wise greater than or equal to* $\mathbf{\Gamma}$ *and there exists at least one path* k *for which* $\Gamma_k < \hat{\Gamma}_k$, *then* $\hat{\mathbf{P}}$ *is element-wise greater than* $\mathbf{P}$, *i.e.,*

$$\forall j : \Gamma_j \leq \hat{\Gamma}_j \text{ and } \exists k : \Gamma_k < \hat{\Gamma}_k \Rightarrow \forall i, j : P_{ij}^L < \hat{P}_{ij}^L.$$

Proof: Using the minimal power vectors, the assumption of $\forall i : \Gamma_i \leq \hat{\Gamma}_i$ is equivalent to $\forall i,j : \gamma_{ij} \leq \hat{\gamma}_{ij}$. Consider the link (rk) in the path k. Since $\Gamma_k < \hat{\Gamma}_k$, then $\gamma_{rk} < \hat{\gamma}_{rk}$. Now, by applying Lemma 3.3 to all SIR links of this network, we have $\forall i,j : P_{ij}^L < \hat{P}_{ij}^L$ which completes the proof. □

The following corollary can be directly derived from Lemma 3.18:

Corollary 3.19 *For any path SIR vector* $\mathbf{\Gamma} = [\Gamma_j]$ *with the minimal power vector* $\mathbf{P}^L = [P_{ij}^L]$ *and any path SIR vector* $\hat{\mathbf{\Gamma}} = [\hat{\Gamma}_j]$ *with the minimal power vector* $\hat{\mathbf{P}}^L = [\hat{P}_{ij}^L]$, *if* $\hat{\mathbf{\Gamma}}$ *is element-wise greater than* $\mathbf{\Gamma}$, *then* $\hat{\mathbf{P}}^{\mathbf{L}}$ *is also element-wise greater than* $\mathbf{P}^{\mathbf{L}}$, *i.e.,*

$$\forall j : \Gamma_j < \hat{\Gamma}_j \Rightarrow \forall i,j : P_{ij} < \hat{P}_{ij}.$$

In the following, first a theorem regarding the maximum power element is stated and then, the necessary and sufficient conditions of the minimal power vector generating the maximum uniform path SIR of a single-channel multi-hop network are presented.

Theorem 3.20 *In a single-channel multi-hop network, the minimal power vector* $\mathbf{P}^L = [P_{ij}^L]$, *corresponding to the maximum uniform path SIR* $\Gamma_{Un}^{\max}$, *has at least one link transmitting with its maximum power, i.e.,* $P^{\max}$.

Proof: If there is no power element equal to the maximum value, then by applying the power scaling method described in the proof of part (b) of Theorem 3.6, i.e., setting $a = \min(\frac{P^{\max}}{P_{ij}})$ and building $\hat{P}_{ij} = a \times P_{ij}$, a new power vector $\hat{\mathbf{P}} = [\hat{P}_{ij}]$ with the link SIR vector $\hat{\boldsymbol{\gamma}} = [\hat{\gamma}_{ij}]$ is resulted where $\hat{\boldsymbol{\gamma}}$ is element-wise greater than $\boldsymbol{\gamma}$, and since $\forall i,j : \gamma_{ij} = \Gamma_{Un}^{\max}$, we have

$$\forall i,j : \Gamma_{Un}^{\max} < \hat{\gamma}_{ij}. \tag{3.25}$$

Consequently, the minimum path SIR of $\hat{\mathbf{\Gamma}}$ is higher than $\Gamma_{Un}^{\max}$, which is in contradiction to the definition of maximum uniform path SIR. □

Theorem 3.21 (The condition of the minimal power vector of the maximum uniform path SIR) *The uniform path SIR* Γ_{Un}, *with the minimal power vector* $\mathbf{P}^L = [P_{ij}^L]$, *is the maximum uniform path SIR of the network, i.e.,* $\Gamma_{Un} = \Gamma_{Un}^{\max}$, *if and only if its minimal power vector has at least one link transmitting with its maximum power, i.e.,* $P^{\max}$.

Proof: Let $\boldsymbol{\gamma^L} = [\gamma_{ij}^L]$ be the link SIR vector of $\mathbf{P}^L = [P_{ij}^L]$. We prove this theorem in two parts:

a) *if* part: We show that if $\mathbf{P}^L$ has a maximum power element, i.e., $\exists r, t : P_{rt} = P^{\max}$, then Γ_{Un} has to be the maximum uniform path SIR.

As a counter example, assume that Γ_{Un} is not the maximum uniform path SIR, i.e., there exists another uniform path SIR $\hat{\Gamma}_{Un}$ with the minimal power vector $\hat{\mathbf{P}}^{\mathbf{L}} = [\hat{P}_{ij}^L]$ for which $\Gamma_{Un} < \hat{\Gamma}_{Un}$. Let $\hat{\boldsymbol{\gamma}}^{\boldsymbol{L}} = [\hat{\gamma}_{ij}^L]$ be the link SIR vector corresponding to $\hat{\mathbf{P}}^{\mathbf{L}} = [\hat{P}_{ij}^L]$. Therefore, $\forall j : \Gamma_j < \hat{\Gamma}_j$ and according to Corollary 3.19

$$\forall i, j : P_{ij}^L < \hat{P}_{ij}^L \tag{3.26}$$

which is impossible, since $P_{rt}^L = P^{\max}$ and $\hat{P}_{rt}^L$ cannot be greater than the maximum value.

b) *only if* part: The proof of this part is given by Theorem 3.20. □

3.4.3 Autonomous Power Control Algorithm

The necessary and sufficient conditions to achieve the maximum uniform path SIR of a multi-hop network are provided by Theorem 3.21. These conditions can be used to develop an autonomous power control algorithm to achieve the maximum uniform path SIR and its corresponding minimal power vector. In the following, it is shown that the problem of finding such a minimal power vector is equivalent to the problem of finding a power vector corresponding to the maximum uniform link SIR of the network, when the network is considered in the single-hop mode.

From the definition of the uniform path SIR, all path SIR values have to be equal, i.e., $\forall j : \Gamma_j = \Gamma_{Un}$, and furthermore, by the definition of the minimal power vector, all link SIR values have to be the same as their corresponding path SIR, i.e., $\forall i, j : \gamma_{ij}^L = \Gamma_j$. As a result, all link SIRs of the minimal power vector of the maximum uniform path SIR are the same, i.e.,

$$\forall i, j : \gamma_{ij}^L = \Gamma_{Un}^{\max}.$$

Moreover, according to Theorem 3.21, at least one power element has to be maximum. By comparing these requirements with those of single-hop single-channel networks provided by Theorem 3.6, it is straightforward to verify that the problem of finding the minimal power vector of the maximum uniform path SIR of a single-channel multi-hop network is equivalent to the problem of finding the power vector that maximizes the equal link SIR or in other words, the power vector that achieves the maximum uniform link SIR of the network.

In Section 3.3.2, a novel autonomous iterative algorithm to achieve the maximum uniform link SIR was developed for single-channel single-hop networks. That algorithm can be used for the multi-hop case with modifying its notations according to the multi-hop communications model. For the multi-hop case, the SIR metric of the link (ij) at the kth iteration is defined as

$$M_{ij}(k) \triangleq \gamma_{ij}(k) \times \frac{P^{\max}}{P_{ij}(k)}. \tag{3.27}$$

The minimum SIR metric of the network at the kth iteration is calculated as

$$M_{\min}(k) \triangleq \min_{ij}(M_{ij}(k)) = \tilde{\gamma}(k) \times \frac{P^{\max}}{\tilde{P}(k)} \tag{3.28}$$

where $\tilde{\gamma}(k)$ and $\tilde{P}(k)$ are the parameters of the link corresponding to this minimum SIR metric, i.e., $M_{\min}(k)$.

Considering these definitions, the proposed power control algorithm updates the power of each link (ij) at the kth iteration, i.e., $P_{ij}(k)$, as

$$\forall i,j:\ P_{ij}(k) = P_{ij}(k-1) \times \frac{M_{\min}(k-1)}{\gamma_{ij}(k-1)}. \tag{3.29}$$

3.4.3.1 Numerical Results

In this section, the numerical results for two example networks are presented. First, the simulation setup is described and then, the properties of the minimum and maximum path SIR values per iteration, the necessary and sufficient conditions of the maximum uniform path SIR and the convergence of the proposed power control algorithm are investigated.

Consider an N-link wireless network with L routing paths according to the multi-hop model described in Section 2.2. The original transmitter of each routing path is placed at random with a uniform distribution in a square area of 200×200 m^2. The receiver of each link is placed at a random distance from its transmitter according to the Gaussian distribution with a mean of 10 m and a standard deviation of 2 m. Also, the angle of each receiver compared to its transmitter is distributed uniformly in the range of $[0, 2\pi)$ given a reference direction where an extremely rare event of having a negative distance between a transmitter and its receiver implies an additional π radian rotation of the original angle of those two nodes. Note that each intermediate node, i.e., the node which is neither the original source nor the final destination of a routing path, consists of one receiver and one transmitter where the channel gain between these two modules is set to zero. The channel gains, maximum transmitting powers, thermal noise and other parameters are the same as those of the simulation configuration considered in Section 3.3.2.3.

In the following, we consider two network realizations randomly generated according to the aforementioned network configuration. In these example networks, it is assumed that $N = 10$ and $L = 5$, i.e., there are 5 routing paths in the network each consisting of 2 links.

The SIR evolutions of these two example networks are illustrated in Figure 3.3. In both graphs, the minimum path SIR value of each iteration is represented by a dashed line whereas the maximum path SIR value is represented by a solid line. As shown, at each iteration the minimum path SIR increases, however, the maximum path SIR fluctuates before converging to the minimum value. This interesting observation can be justified as follows. The minimum path SIR is indeed the same as the minimum link SIR of the network and according to Section 3.3, this value monotonically increases until the conditions of the maximum uniform link SIR are met. On the other hand, the maximum path SIR of the network is not necessarily equal to the maximum link SIR (represented by a dotted line in Figure 3.3). Therefore, the monotonically decreasing property of the maximum link SIR does not automatically apply to the maximum path SIR. However, the maximum link SIR can be considered as an upper limit for the maximum path SIR. Therefore, due to the fact that the maximum link SIR converges to the minimum one (according to the single-hop maximum uniform link SIR achieving algorithm), the maximum path SIR has to converge

to the minimum path SIR as well. This confirms the convergence of the algorithm.

In Figure 3.3, it is verified that at each iteration there is at least one link transmitting with its maximum power. As a result, the SIR values corresponding to the convergence points of these examples, i.e., 16.8 dB in Figure 3.3.a and 11.3 dB in Figure 3.3.b, are indeed the maximum uniform path SIRs of those example networks.

3.4.4 Multi-Channel Communications

In the previous section, single-channel multi-hop ad hoc networks were studied providing a valuable insight into multi-hop networks. However, using a transceiver for the intermediate routing nodes to send and receive simultaneously on the same channel has some implementation difficulties due to non-ideal isolation of the transmitting and receiving signals and the near-far effect of the antennas. There exist a few limited expensive methods to achieve some reasonable signal isolation such as the ones used in continuous-wave radar system [41, 42, 43]. However, the considerable high cost of these methods are not justified in the commercial wireless products and therefore, it is recommended to use two separate channels to receive and transmit on the same antenna in order to overcome the near-far interference problem. As a result, in this section, the maximum uniform path SIR of the multi-channel multi-hop networks is investigated.

The problem of finding the maximum path SIR in multi-channel multi-hop networks can be modeled as the problem of finding the maximum uniform path SIR in single-channel multi-hop networks considering the multi-channel requirements as of those presented for multi-channel single-hop networks. That is, to use exactly the same algorithm as the one for the maximum uniform path SIR of the single-channel multi-hop networks in Section 3.3.2 with the conceptual difference that no matter which subchannel each link belongs to, the minimum SIR metric $M_{\min}(k)$ is set to the minimum SIR metric $M_{ij}(k)$ of all links in all subchannels. This guarantees that the SIRs of all links converge to the same value which is indeed the maximum uniform path SIR of the network and the resulted power vector has the minimum total power among all power vectors achieving that maximum uniform rate.

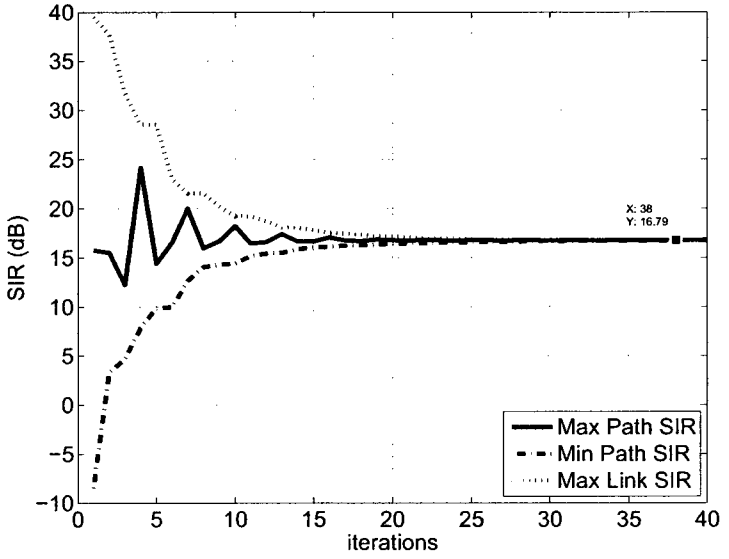

(a)

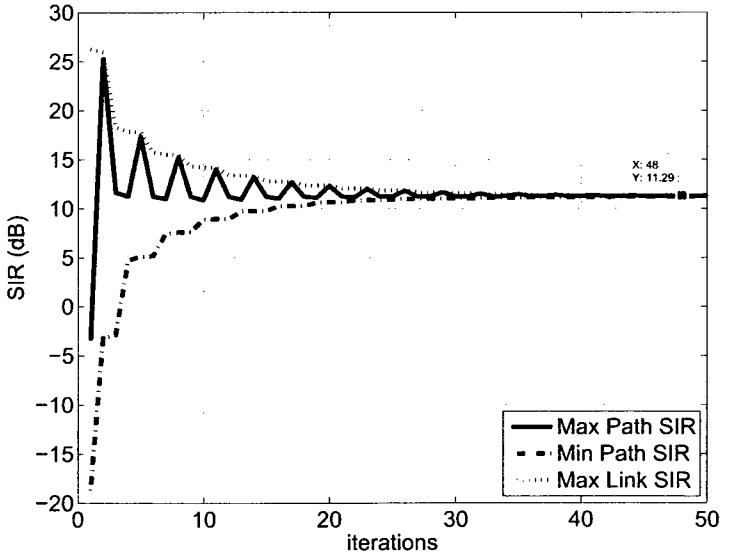

(b)

Figure 3.3: Min/Max SIR evolutions of two multi-hop example networks of Figure 3.2, converging to the maximum uniform path SIR of: a) 16.8 dB, b) 11.3 dB.

3.5 Conclusion

The maximum uniform SIR refers to the maximum achievable SIR value in a power-constrained wireless network, where the SIR values of all links (or paths) are the same. In this chapter, a new power control algorithm was proposed which converges to the maximum uniform SIR of wireless ad hoc networks. The proposed algorithm requires only one phase of power convergence and less information to be broadcast from the links compared to other algorithms. Most importantly, this algorithm is autonomous in the sense that it does not require a central unit to perform any state-machine process coordinating the candidate SIR values. The design of the proposed algorithm was investigated for both single-hop and multi-hop communications with both possibilities of having a single channel or multiple channels available to the network. Moreover, the convergence and the performance of the proposed algorithm were evaluated through some computer simulations.

Chapter 4

Semi-Asynchronous Power Control with Active Link Protection

This chapter presents a new semi-asynchronous power control algorithm with active link protection for wireless ad hoc networks. Previous works in this area have focused on either asynchronous power control algorithms with no protection or synchronous power control algorithms with active link protection. Here, we fill the gap between these two approaches and propose a generalized semi-asynchronous power control algorithm with active link protection.

4.1 Introduction

Power control algorithms manage the power allocation process in a wireless network where the participating links share an interference channel. A power control mechanism not only helps the links to acquire their QoS, but also minimizes the power consumption resulting in a longer battery life of the mobile terminals [13]. Such a minimum power allocation method reduces the interference levels on all links in the network, yielding a higher overall network capacity/throughput [14, 15].

Most of the existing power control algorithms address centralized wireless networks where all users are communicating with a central base station [1, 2]. The base station has the real-time knowledge of all users in the network and therefore, it can control the

transmission and the power of each user. However, in this work we consider wireless ad hoc networks which do not have any centralized control unit. In this chapter, we consider the single-hop ad hoc networks communicating over a single channel as described in Section 2.1. Due to the absence of a centralized management in ad hoc networks, a power control algorithm has to be distributed at the link level. This means that each link determines its transmitting power exclusively based on the only available local information at its receiving node, i.e., the SIR measurements, and no or very limited signaling provided at the network level.

The pioneer work on the distributed power control for wireless networks was done by Foschini and Miljanic [16] and Mitra [17] independently, in 1993. They propose a distributed asynchronous power control algorithm which converges to the minimal power elements for a set of user-defined QoS values in an ad hoc network. This algorithm provides the groundwork for various distributed power control algorithms such as those in [19, 20, 14, 21]. In fact, almost all distributed power control algorithms can be considered as variants of this algorithm. In [18], Yates unifies most of the distributed power control algorithms under a framework referred to as the *standard power control algorithm.*

Although the algorithm proposed by Foschini and Miljanic converges geometrically fast, it does not guarantee the QoS of the existing links while a new link tries to achieve its QoS. For example, when a new link enters a stable ad hoc network, the SIR of some of the existing links may fluctuate and go below their required QoS resulting in the service interruption of those links [22, 23]. To solve this issue, in [19], Bambos *et al.* propose a modified version of the power control algorithm proposed by Foschini and Miljanic with the active link protection (ALP) capability. This algorithm guarantees that once a link becomes active, i.e., it reaches its QoS value, it remains active for the rest of the process. In this algorithm, the active link protection is provided at the expense of operating at a higher than required QoS and also requiring all links to update theirs powers at the same time, i.e., synchronized power updating. Note that the latter in ad hoc networks where there is no central unit to impose the synchronous power updating, is not practical.

In this chapter, we try to fill the gap between the *asynchronous* power control proposed by Foschini-Miljanic [16] and the *synchronous* power control algorithm proposed by

Bambos *et al.* [19]. We develop a generalized algorithm which not only is asynchronous (updating in a round-robin fashion), but also provides the active link protection property. The proposed algorithm is indeed a modified version of the algorithm proposed by Bambos *et al.* and includes that algorithm as a special case. We show that the proposed algorithm can also provide the users with some information about the network structure such as the total number of the links in the network.

The rest of this chapter is organized as follows; in Section 4.2, the distributed power control algorithm proposed by Foschini and Miljanic [16] as well as the algorithm proposed by Bambos *et al.* [19] are briefly reviewed. In Section 4.3, the proposed semi-asynchronous power control algorithm with active link protection is introduced and its key features are discussed. Section 4.4 investigates the power-updating timing issues of the proposed algorithm in theory and for real world applications. Computer simulations and numerical results are presented in Section 4.5. Finally, Section 4.6 concludes this chapter.

4.2 Review of Power Control Algorithms

The core idea of the power control algorithm proposed by Foschini and Miljanic [16] is based on the theory of non-negative matrices and the feasibility criteria of Section 2.1.1. This algorithm is described by the following iterative equation

$$\mathbf{P}(k+1) = \mathbf{F}\mathbf{P}(k) + \mathbf{u} \tag{4.1}$$

where k refers to the power iteration index (see Section 2.1, for the definition of $\mathbf{P}, \mathbf{F}, \mathbf{u}$ and other parameters). If the set of QoS requirements $\mathbf{Q} = [Q_i]$ is feasible, i.e., $\rho_f < 1$, then the above equation converges to the Pareto-optimal power solution ($\mathbf{P}^*$), and diverges to infinity otherwise. We refer to this algorithm as the *Foschini-Miljanic* power control algorithm. In [19], the distributed version of (4.1) with the same convergence properties is presented as

$$P_i(k+1) = \frac{Q_i}{\gamma_i(k)} P_i(k). \tag{4.2}$$

It is shown that (4.2) is a distributed algorithm at the link level where the link i can update its power solely based on the measurements at its receiving node and some information from its transmitter. Under this scheme, if γ_i is lower than Q_i, then P_i is increased and if γ_i is higher than Q_i, then P_i is decreased. Moreover, it is shown that the power control algorithm (4.2) converges for totally asynchronous power updates, i.e., each link has different rate of power updates [11].

In a feasible ad hoc network based on (4.2), when a new link enters the network and starts transmitting, the interference levels of the existing links in the network are increased. Consequently, some of the initially active links, i.e., the links with $\gamma_i(k) \geq Q_i$, may become inactive and their SIR values may go below their QoS, i.e., $\gamma_i(k) < Q_i$. In this case, these links experience some service interruption which is not acceptable for most of the wireless network applications. In order to avoid such scenarios, in [19], Bambos *et al.* propose an interesting extension of (4.2) providing the active link protection property. We refer to this algorithm as the *Bambos* algorithm. This algorithm is developed based on two key concepts of a) the gradual power-up of the new links, and b) an extra QoS margin protecting the SIR of the active links. In particular, the power increase per iteration of each new link is limited resulting in a limited interference increase on the active links, and at the same time each active link maintains an extra QoS margin protecting it from unpredicted interference increase caused by entering the new links into the network. This algorithm is as follows; let $\mathcal{L}$ be the set of all links in the network. The link $i \in \mathcal{L}$ at the time k is considered active, if $\gamma_i(k) \geq Q_i$ and inactive if $\gamma_i(k) < Q_i$. Let $\mathcal{A}_k$ and $\mathcal{B}_k$ be the sets of all active and inactive links at the time k, respectively, and $\delta = 1 + \epsilon > 1$ be a control parameter related to the extra QoS margin. The Bambos algorithm updates all power elements at each iteration $k+1$ as follows

$$P_i(k+1) = \begin{cases} \frac{\delta Q_i}{\gamma_i(k)} P_i(k) & \text{if } i \in \mathcal{A}_k \\ \delta P_i(k) & \text{if } i \in \mathcal{B}_k \end{cases}$$

or equivalently

$$P_i(k+1) = \begin{cases} \frac{\delta Q_i}{G_{ii}} I_i(k) & \text{if } i \in \mathcal{A}_k \\ \delta P_i(k) & \text{if } i \in \mathcal{B}_k \end{cases} \tag{4.3}$$

where

$$I_i(k) = \sum_{j \in \mathcal{L}-\{i\}} G_{ij} P_j(k) + \eta_i$$

and $P_i(0) > 0$ denotes the initial transmitting power of the link i.

Under this scheme, the active link i updates its power aiming for an enhanced target δQ_i and each inactive link increases its power by the factor of δ. The Bambos algorithm has the following important properties:

1. Once a link becomes active it remains active.

2. If the QoS of all links are feasible, then eventually all links become active in finite time.

3. If the QoS of some of the links in $\mathcal{B}_k$ are infeasible, then all power elements of the network go to infinity geometrically fast.

In [35], Yates studies the Bambos power control algorithm in the asynchronous mode and mentions that although the Bambos algorithm still converges to the optimal solution corresponding to the increased QoS, it does not provide the active link protection property anymore. We can conclude that in Bambos power control algorithm, the active link protection property is achieved at the expense of first, operating at a QoS higher than the minimum requirement and secondly, a synchronization arrangement to have all powers updated at the same exact time at each iteration.

4.3 Semi-Asynchronous Power Control Algorithm with ALP

As we mentioned in Section 4.2, the Bambos algorithm described by (4.3) provides the active link protection property by operating at a higher than required SIR, i.e., $\delta \mathbf{Q}$, and using a network-wide synchronization signal synchronizing all power updates. In this section, we propose some modifications to relax the synchronization requirement and introduce a generalized semi-asynchronous power control algorithm with active link protection for which the Bambos algorithm can be considered as a special case. The proposed algorithm is asynchronous in the sense that each link can update its power at an arbitrary time, however, the

links adjust their powers in a round robin fashion [11] (note that it is not fully asynchronous as the Foschini-Miljanic algorithm). This algorithm also provides some information about the network structure which can be used for channel access algorithms.

Power updating equation (4.3) is based on the fact that each active link is assigned an extra QoS margin and between two consecutive power updates of this link, its SIR degradation is less than that extra margin. The limited SIR decrease is a direct result of having a limited interference increase received from other links. This is due to the fact that within two consecutive power update of any link, other links in the network can update their powers only once and in addition to that, the possible power increases of those links are limited to a certain percentage. We extend this concept to a semi-asynchronous case by assuming that between two consecutive power updates of the link $i \in \{1, \cdots, N\}$ other links have to be updated *at most* once. In the following, we investigate this power updating arrangement and examine that to what extent the synchronous power updating requirement can be relaxed.

Assuming that the power of each link i is updated in a fixed interval (T_i), the following lemma can be stated;

Lemma 4.1 (Equal power update intervals) *If between two consecutive power updates of any link the powers of other links are updated at most once, then the power update intervals of all links have to be the same as T_o, i.e.,*

$$\forall i \in \{1, \cdots, N\}: \quad T_i = T_o.$$

Proof **:** As a counter example, it is shown that if there exist at least two links with different power updating periods, i.e., $\exists i, j : T_i > T_j$ where $T_i = T_j + T_d$, then there is a power update interval of the link i in which the link j is updated twice.

Let $k = \left\lceil \frac{T_j}{T_d} \right\rceil$, then

$$kT_d \geq T_j. \tag{4.4}$$

By the assumption

$$kT_i = k(T_j + T_d). \tag{4.5}$$

By substituting kT_d from (4.4) in (4.5) we have

$$kT_i \geq (kT_j + T_j = (k+1)T_j).$$

As a result, in this fixed time period of kT_i the number of T_j intervals is one more than the number of T_i intervals. Therefore, according to pigeonhole principle [44], there exists a period of T_i which contains two time intervals of T_j. In other words, there exists a power updating period of the link i in which the link j is updated twice. □

This lemma helps us to establish the power updating arrangement required for developing a semi-asynchronous power control algorithm. Note that a direct result of having equal power updating period for all links is that these links have to update their powers in a round robin fashion.

In the following, first the semi-asynchronous power control algorithm with active link protection is introduced and then, the features of this algorithm are discussed in detail.

In a wireless ad hoc network consisting of N links where each link i updates its power starting at an arbitrary moment in a fixed interval of T_o, the semi-asynchronous power control algorithm with active link protection is defined as follows

$$P_i(k+1) = \begin{cases} \frac{\delta Q_i}{\gamma_i(k)} P_i(k) & \text{if } i \in \mathcal{C}_k \\ \min(\delta P_i(k), \frac{\delta Q_i}{\gamma_i(k)} P_i(k)) & \text{if } i \in \mathcal{D}_k \end{cases} \tag{4.6}$$

or equivalently

$$P_i(k+1) = \begin{cases} \frac{\delta Q_i}{G_{ii}} I_i(k) & \text{if } i \in \mathcal{C}_k \\ \min(\delta P_i(k), \frac{\delta Q_i}{G_{ii}} I_i(k)) & \text{if } i \in \mathcal{D}_k \end{cases} \tag{4.7}$$

where $\mathcal{C}_k$ and $\mathcal{D}_k$ denote the active and inactive sets of the links, respectively. These two sets are slightly different from $\mathcal{A}_k$ and $\mathcal{B}_k$ in (4.3). When the link $i \in \mathcal{C}_k$ updates its power, it has to maintain a SIR value higher than Q_i until its next power update during which other links are powering up; this is feasible only when the link i achieves its full extra QoS margin. In other words, the link i is considered active when at the time of its power update it has $\gamma_i(k) = \delta Q_i$ or equivalently $P_i(k) = \frac{\delta Q_i}{G_{ii}} I_i(k-1)$. Similarly, the link i is

considered inactive, if at the time of its power update $\gamma_i(k) < \delta Q_i$. Note that $\gamma_i(k)$ and $I_i(k)$ are calculated prior to the power update of the link i at the kth iteration based on the most recent values of the power elements.

An undesirable situation occurs when an inactive link i has a SIR value right before its power update at the kth iteration, i.e., $\gamma_i(k-\epsilon)$, as

$$Q_i \leq \gamma_i(k-\epsilon) < \delta Q_i. \tag{4.8}$$

Considering the new definitions of the active and inactive links, if the Bambos algorithm (4.3) was used, the updated power would be

$$P_i(k+1) = \delta P_i(k)$$

and the SIR of that link right after this update, i.e., $\gamma_i(k+\epsilon)$, would become

$$\gamma_i(k+\epsilon) = \frac{P_i(k+1)G_{ii}}{I_i(k)} = \frac{\delta P_i(k)G_{ii}}{I_i(k)} = \delta\gamma_i(k-\epsilon) \tag{4.9}$$

assuming that the interference during the power update stays the same. By comparing (4.8) and (4.9), we would have

$$\delta Q_i \leq \gamma_i(k+\epsilon)$$

and the link i would become active. However, in this case this SIR value would be more than the required extra QoS margin or in other words, the value of $P_i(k+1)$ would become higher than the required one. This higher power level would cause a higher interference on other links and subsequently, higher power updates for all links which might have resulted in an unstable network or even, might have prevented the iterative power updating process to converge. In order to prevent the SIR and power overshoots, in the proposed power control algorithm (4.7), the updated power of the inactive link i is calculated as $\min(\delta P_i(k), \frac{\delta Q_i}{G_{ii}} I_i(k))$ and the link i is considered active only when this minimum is equal to $\frac{\delta Q_i}{G_{ii}} I_i(k)$.

The proposed algorithm is indeed a modified version of the Bambos algorithm and

preserves most of the properties of that algorithm. By comparing these two algorithms, it can be verified that a) the proposed algorithm relaxes the synchronization requirement in the Bambos algorithm, and b) the proposed algorithm prevents inactive links to excessively increase their SIR and power values. It is important to note that this power control algorithm is asynchronous, in the sense that the links are not obliged to update their power elements at the same moment. However, they still have to update their powers in a round robin fashion which can be considered as a restricted asynchronous mode compared to that of the Foschini-Miljanic algorithm [11]. For this reason the proposed algorithm is referred to as the semi-distributed algorithm.

4.4 Power-Updating Timing

In theory, each link can start the transmission process at any given time as long as the power updating intervals of all links are the same, i.e., all links update their power in a round robin fashion. According to (4.7), the power updating process requires the local measurement of $I_i(k)$, or equivalently $\gamma_i(k)$, at the receiving nodes. The accuracy of these measurements depends on the time window that these parameters are observed, averaged and measured. In particular, the averaging process is necessary to overcome the randomness of the network parameters and measurements. Each link measures these values right before its power update for a certain period in which, ideally other links do not change their powers. The latter requirement imposes some limitations on all distributed power control algorithms such as the Bambos algorithm and the proposed algorithm.

Let t_{ij} denote the time interval between the power update of the link i and the next power update of the link j. Obviously, since the power updating periods for all links are equal, the values of t_{ij} are always fixed and do not change with time. Moreover, $\forall j \neq i : t_{ij} \leq T_o$ and let t_{min} be defined as $t_{min} = \min_{ij}(t_{ij})$. Therefore, each link has to be capable of monitoring, measuring and calculating the $I_i(k)$ values in t_{min} seconds. In the real world, t_{min} has to be greater than a certain threshold t_{th} determined by the processing speed and hardware specifications of the receiving nodes.

The t_{th} protection period insures a reliable estimation of the SIR used for power

updating. To provide such a t_{th} protection period the following steps are recommended; upon the arrival of a new link into the network, it monitors its interference level for a few iterations prior to any transmission. Since each change in the interference level corresponds to a power update of the existing links, this link can determine the exact moment of power updating of the links in each iteration (not necessarily the update moment of each link, since some links may update their powers at the same time). Finally, the new link starts transmitting in a window at least t_{th} seconds apart from the power-updating instances of other links.

It is important to note that the original Bambos power control algorithm can be considered as a special case of the proposed semi-asynchronous algorithm where all links are updated at the same time. In this case, $\forall j \neq i : t_{ij} = T_o$ and $\min(t_{ij}) = T_o$.

Furthermore, if no two links are allowed to update their powers at the same time, then each SIR change of the new link corresponds to the power update of only one link. As a result, the new link knows the total number of links in the network, by monitoring the number of changes in its received SIR in each iteration. Note that recalling from Chapter 2, the channel gain parameters are constant during the observation period due to the assumption that the convergence of the power control and admission control schemes is much faster than the channel variability. Considering this assumption, when the links update their powers at distinct instances and the aforementioned guard time is require, the total number of links has to be limited in order to ensure the fast convergence of the proposed method.

4.5 Simulation Results

In order to examine the concept of the proposed semi-asynchronous power control algorithm with active link protection an example ad hoc network with four radio links is considered. This example is similar to the one used by Bambos *et al.* in [36]. As mentioned earlier, since the proposed modifications do not change the main properties of the Bambos algorithm, the performance of the proposed algorithm mainly remains the same as that of the Bambos algorithm.

Consider a wireless network with 4 links according to the single-hop model described

in Section 2.1. The channel gain models large-scale propagation effects, i.e., the path loss and the shadowing effects [32]. Variations due to small-scale propagation effects are usually assumed to be averaged out in the context of SIR-based power control [33]. The channel gain between the transmitter of the link j and the receiver of the link i, is modeled as

$$G_{ij} = K_o \frac{a_{ij}}{r_{ij}^4} \tag{4.10}$$

where r_{ij} represents the distance between these two nodes, a_{ij} models the power attenuation due to the shadowing and K_o is a unitless constant depending on other parameters such as antenna characteristics, reference distance, etc. [32]. All a_{ij} variables are assumed to be independent and log-normally distributed with a mean of 0 dB and a standard deviation of 8 dB [38, 39]. For all links, the maximum transmitting power P^{max} is equal to 5 W, the thermal noise power η is set to 10^{-11} W and K_o is set to 0.0142 (corresponding to $f_c = 2$ GHz and a reference distance of 10 m). All links have the same active link protection step size of $\delta = 1.26$, i.e., 1 dB, and a QoS of 14 dB which results in each link aiming for an SIR of 15 dB. The link receivers are located on a square $X - Y$ plane [36] at (100,100), (100,-100), (-100,100) and (-100,-100) with their transmitters located at (131,173), (140,-81), (-140,151) and (-91,-140), respectively, all expressed in meters.

Figure 4.1 shows the evolution of the SIR of the example network using the Bambos power control algorithm. Figure 4.2 presents the evolution of the SIR of the same network using the proposed semi-asynchronous power control algorithm where the SIR of each radio link used in the power updating process is calculated *prior to each power update*. Figure 4.3 presents the SIR values of the same system used in Figure 4.3, with the difference that the SIR values are shown only at the end of each iteration so the evolution of those values can be compared to that of the Bambos algorithm in Figure 4.1. Since there are four links in the network and according to the proposed semi-asynchronous power control algorithm, each link is updated at a different moment, the curves in Figure 4.2 show four instances of the SIR change in each iteration. It is important to note for the sake of simplicity and clarity in Figure 4.2, it is assumed that all links update their powers with an equal time window of $\frac{T_o}{4}$ between each other's power updates, i.e., $t_{min} = \frac{T_o}{4}$.

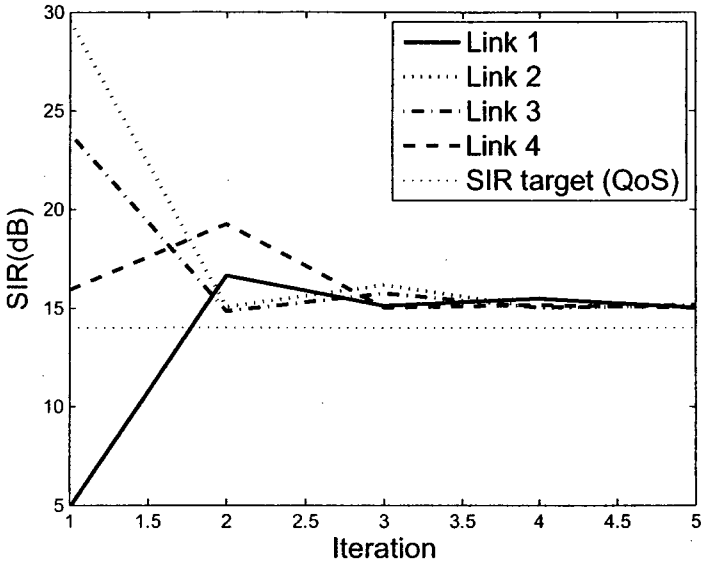

Figure 4.1: SIR evolutions of 4 radio links based on the Bambos power control algorithm.

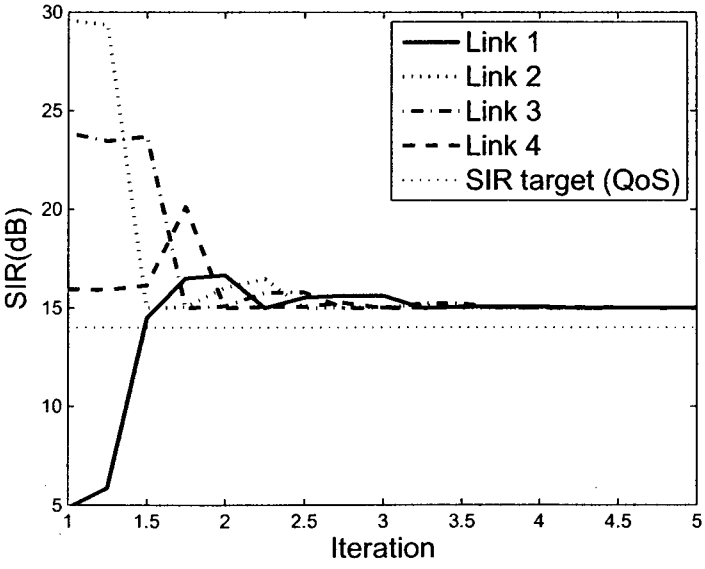

Figure 4.2: SIR evolutions of 4 radio links based on the proposed asynchronous power control algorithm with the SIR calculated prior to each power update.

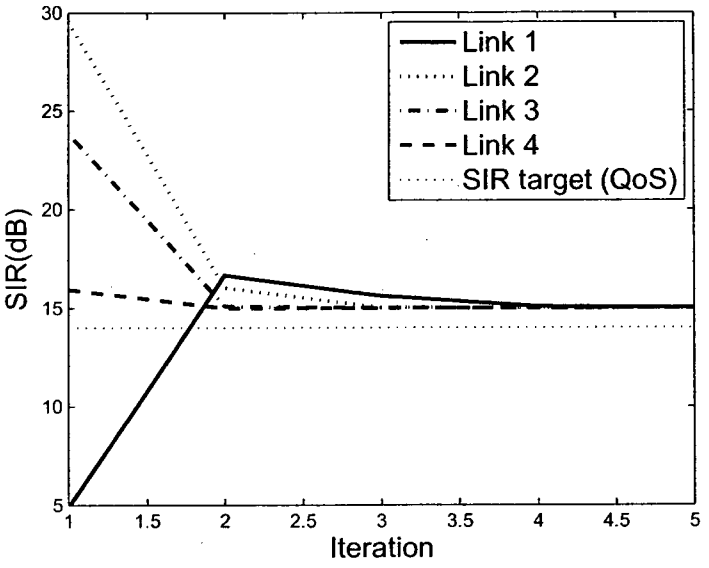

Figure 4.3: SIR evolutions of 4 radio links based on the proposed asynchronous power control algorithm with the SIR values calculated at the end of each complete iteration.

By comparing these three figures, it can be verified that, as expected, the proposed algorithm relaxes the synchronization requirement of the Bambos algorithm and at the same time, has a performance very close to that of the Bambos algorithm. For larger networks, it is possible to show that by assuming a fixed iteration period, the convergence of the proposed semi-asynchronous algorithm is better than that of the Bambos algorithm. This can be justified by the following rationale; using the proposed algorithm, the power of each link is updated based on the power elements of other links which on average, are updated in less than $\frac{T_o}{2}$ seconds prior to that time. However, using the Bambos algorithm the power elements used in the power updating equation of each link are updated in T_o seconds prior to that time. As a result, the response time of the proposed algorithm to the channel interference is almost twice as fast as that of the Bambos algorithm.

4.6 Conclusion

In this chapter, a new generalized semi-asynchronous power control algorithm with active link protection for wireless ad hoc networks was introduced. This algorithm is a modified version of the algorithm proposed by Bambos *et al.* where it preserves most of the properties of that algorithm. The synchronous power control with active link protection algorithm proposed by Bambos *et al.*, is considered as a special case of the proposed algorithm. This algorithm and its key parameters were discussed in detail. The power-updating timing issues of the proposed algorithm for real world applications were investigated. It was shown that the proposed algorithm can also provide the users with some information about the network structure such as the total number of the links in the network. The concept of the proposed algorithm was examined by using an example ad hoc network and evaluating the numerical results.

Chapter 5

Admission Control for Asynchronous Power-Controlled Ad Hoc Networks

A new distributed admission control algorithm for the asynchronous power-controlled wireless ad hoc networks is proposed in this chapter. Most of the existing distributed admission control algorithms are categorized either as the time-out or SIR-saturation based algorithms trading off the convergence speed against the performance, whereas the proposed admission control is based on the Perron-Frobenius theorem and has an ideal performance. The proposed algorithm determines the admissibility of a new link in a fixed number of power control iterations by using only the local measurements of that link. This algorithm is presented for the general case of the asynchronous Foschini-Miljanic power control algorithm and can be applied to a wide variety of the distributed power-controlled ad hoc networks with some modifications and restrictions.

5.1 Introduction

In wireless networks, the quality of transmission can be improved by using advanced transmission control algorithms such as power control techniques, admission control algorithms, etc. As discussed in the previous chapter, power control algorithms manage the power allocation process in a wireless network where the participating links share an interference channel. A power control mechanism not only helps the links to acquire their QoS but

also minimizes the power requirements. Such minimum power allocation decreases the overall interference of the network and consequently, results in a system with a higher capacity/throughput. However, when a new link enters the network the resource allocation, power elements and the SIR of the existing links may be widely affected and therefore, some links might experience power outage and/or service interruption. To avoid such scenarios, an admission control algorithm should be emplaced in order to grant network access to a new link while protecting the QoS of the existing links from any degradation. In fact, upon the arrival of a new link in the network, the admission control algorithm decides whether this link can achieve its target QoS while the network remains stable or not. If so, this link is admissible and eventually becomes active, i.e., achieves its QoS. Otherwise, the new link is inadmissible and has to drop out and become silent. Note that the accuracy of this admission decision can be affected by two types of error [14]; in error type I, an inadmissible link is erroneously accepted into the network resulting in an outage. In error type II, an admissible link is erroneously rejected. An ideal admission decision has to be free of both error types I and II.

Due to the layered architecture of wireless networks, the QoS has different definitions at different layers. At the physical layer, the QoS usually translates into the minimum required SIR, whereas at the network layer the QoS may refer to the end-to-end transmission delay, the required bandwidth, the call blocking and dropping probabilities, etc. [4, 5]. In the literature, there exists an extensive amount of research under the name of the admission control at the network layer [6, 45, 5, 46]. Because of these different definitions of QoS at the physical and the network layers, their admission control mechanisms refer to different concepts. It is important to note that, this work addresses the admission control only at the physical layer where the QoS parameters refer to the minimum SIR requirements in a shared wireless interference channel.

Admission control algorithms can roughly fall into three categories; the first category corresponds to the wireless networks where the admission decisions are made at a central unit, i.e., a base station, and then those decisions are communicated to all users. This category is referred to as the *fully centralized* admission control [26]. The second category includes the networks where each link receives some information about the network from

a central unit, however, it makes its own admissibility decision. This category is referred to as the *semi-distributed* admission control [14, 21]. In the third category, there is no central unit in the network and as a result, each user has to determine its admissibility solely based on its local measurements/information. This category is referred to as the *fully distributed* admission control [19].

Admission control algorithms are widely used in the wireless centralized networks where all users communicate through a central unit. They can be fairly simple such as the ones used in TDMA and FDMA multiple access networks, or more sophisticated such as those used in CDMA networks [39, 47, 48]. In both scenarios, they take advantage of the available centralized management/signaling and therefore, they are either fully centralized or semi-distributed schemes. Contrary to the centralized networks, wireless ad hoc networks do not have any centralized control unit and therefore, the power and admission control algorithms have to be distributed at the link level; that is each link not only adjusts its transmitter power, but also determines its admissibility exclusively based on its local measurements and no or very limited signaling provided at the network level. In this work, we consider wireless ad hoc networks and as a result, the admission control investigated here falls into the category of fully distributed admission control algorithms.

When the full knowledge of the network is available, the admissibility of the new link can be examined by the feasibility criteria developed based on the theory of non-negative matrices [24, 25]. In the literature, various admission control algorithms have been proposed based on aforementioned robust feasibility criteria. For example, in [26], Bambos and Pottie examine a preliminary version of this approach where the channel gain matrix is calculated by using pilot signals. A more distributed and comprehensive pilot-based method is investigated in [14] where Andersin *et al.* present an interactive method providing both the admission control and active link protection. Due to the use of pilot signals these algorithms are not distributed and therefore, not applicable to ad hoc networks. In [27], Xiao *et al.* propose an error free distributed admission control algorithm, however, this algorithm has a slow convergence and is not applicable to the power control algorithms with ALP. In [19], Bambos *et al.* propose two admission control algorithms based on the

SIR convergence of the new link. These two admission control algorithms are fully distributed, however, their performances are not ideal and they require periodic optimization which is not feasible in practice.

In this chapter, we propose a fully distributed admission control by taking full advantage of the power control scheme and the feasibility criteria. This algorithm is evaluated for two power control algorithms in the asynchronous mode; namely, the asynchronous ALP and the Foschini-Miljanic power control algorithms described in Chapter 4. The main challenge in this work is how to use the feasibility criteria to determine the admissibility without having the full knowledge of the network required for setting up such criteria. The proposed approach is presented in two steps; in the first step, the use of the feasibility criteria, in the context of the admission control, is investigated and it is shown that for this particular application, the full knowledge of the network parameters is not required. In fact, a normalization process is presented which normalizes some of the unknown parameters without affecting the admissibility property of the network. In the second step, it is shown that the rest of the required parameters can be extracted from the local measurements of the new link. As a result, the admissibility of that link is determined solely based on its local measurements. Due to the use of the feasibility criteria, the proposed method has an ideal admission control performance. In addition, it is applicable to the power control algorithms with the active link protection, its performance does not depend on the power/SIR convergence of the new link and finally, it does not require any parameter to be optimized.

The rest of this chapter is organized as follows. In Section 5.2 the modeling framework is defined. In Section 5.3, the existing admission control algorithms related to this work are briefly reviewed. The concept of the local measurements and the basis of the network normalization are presented in Section 5.4. Section 5.5 introduces the proposed admission control algorithm for the asynchronous Foschini-Miljanic power control algorithm. In Section 5.6, the proposed algorithm is extended to the asynchronous ALP power control algorithm. In Section 5.7, the performance of the proposed admission control algorithm is evaluated and compared to those of other algorithms through extensive computer simulations. Finally, Section 5.8 concludes this chapter.

5.2 System Model

The local measurements, to be exploited by the proposed admission control, highly depend on the power control algorithm used by the network. Therefore, as a part of the system model, it is vital to define the power control algorithms to be considered in this chapter. Recalling from Chapter 4, all distributed power control algorithms are variants of the Foschini-Miljanic power control algorithm. One of these algorithms is the asynchronous ALP power control, developed in the same chapter, which provides active link protection for practical applications, when all powers are updated in a round robin fashion and at distinct time instances. We refer to this non-simultaneous power updating arrangement as the *interference observable* property. In fact, this asynchronous algorithm and in general, any asynchronous variant of the Foschini-Miljanic power control algorithm with the interference observable property can be used in conjunction with the proposed admission control algorithm in this chapter. Therefore, the proposed admission control algorithm is investigated for the asynchronous ALP and the general Foschini-Miljanic power control algorithms with the interference observable property.

Assuming the aforementioned power control arrangement, in the following, the admission control problem is modeled for the single-hop ad hoc networks communicating over a single channel, as described in Section 2.1. Assume a wireless ad hoc network with $(N-1)$ active links, where each link operates at a SIR equal to or higher than its required QoS. A new link, labeled as the link 1, with a QoS of Q_1 enters the network and starts transmitting. In order to satisfy the interference observable property, no two links update their powers at the same time and the power elements are updated in a round robin fashion. This power updating arrangement is asynchronous in the sense that the links do not update their power elements *at the same moment*. The existing (active) links are labeled from 2 to N in their power updating order starting from the link 1. Moreover, each power iteration starts with the power updating of the link 1 and ends with the power updating of the link N. Let $P_i(k)$ denote the updated power value of the link i at the kth iteration. Therefore, according to (2.1), the SIR value of the link i at the kth iteration after its power update can

be expressed as

$$\frac{G_{ii}P_i(k)}{\eta_i + \sum_{j=1}^{i-1} G_{ij}P_j(k) + \sum_{j=i+1}^{N} G_{ij}P_j(k-1)} = \gamma_i(k). \tag{5.1}$$

Note that prior to joining the new link, all existing $(N-1)$ links are active, i.e., the original network is feasible. Therefore, the admissibility of the link 1 is equivalent to the feasibility of the new N-link network. Consequently, the *admissibility* of the link 1 and the *feasibility* of the whole network refer to the same concept and are used interchangeably in this chapter.

Finally, it is important to note that in a wireless ad hoc network, it is possible to have multiple links (users) seeking admissibility in a short period of time. The admission control in this case can be either based on a one-by-one or a multiple-oriented processing approach [14]. In [49], Andersin *et al.* consider these approaches for a fundamentally similar problem of mobile removal and show that the one-by-one processing outperforms the multiple-oriented one. Based on that result, in [14], they conclude that the same phenomenon can be expected in the admission control process as well. This deduction can be justified by noting that multiple arrivals increase the interference level, which consequently results in a higher admission error. Moreover, multiple arrivals to the same channel are rare events due to the facts that the link arrival has a Poisson distribution, multiple channels are usually available in a network and ad hoc networks have a fairly small to medium size. Therefore, we use the same assumption as that of [14, 27] and consider the single-arrival network model with one-by-one admission control algorithms. However, the proposed algorithm can be easily extended to multiple-arrival network models for the original Foschini-Miljanic power control algorithm.

5.3 Related Work

In this section, first, the related admission control algorithms in the literature are briefly reviewed. Then, the admission control process in the power-constrained networks is addressed, and finally, the admissibility definitions of the candidate power control schemes, i.e., the Foschini-Miljanic and asynchronous ALP power control algorithms, are discussed

and their impacts on the performance of the admission control process are addressed.

5.3.1 Review of Admission Control Algorithms

Most of the admission control algorithms in the literature are based on the robust feasibility criteria used in the Foschini-Miljanic power control algorithms mentioned in Chapter 4. Although in these algorithms the admission decision is ideal, they require the full knowledge of the network parameters, i.e., the channel gain matrix and the QoS requirements. In [26], Bambos and Pottie examine a preliminary version of this approach where the channel gain matrix is calculated by using pilot signals. A more distributed and comprehensive pilot-based method is investigated in [14] where Andersin *et al.* present an interactive method providing both the admission control and active link protection property based on the Foschini-Miljanic algorithm. We refer to both the power control and admission control techniques of this approach as the *Soft and Safe* or in short the *S&S* algorithms. In the interactive S&S admission control, the admissibility of a new link is evaluated based on the power convergence of the whole network. In fact, an inadmissible link is rejected when at least one of the stable power elements reaches its maximum value. Due to the use of pilot signals, the S&S algorithm is considered as a semi-distributed admission control. This algorithm is error types I and II free, however, it has a slow convergence. In [21], Kim examines a similar but faster approach by trading off a low admission error type II for the convergence speed. In [14], Andersin *et al.* also propose a distributed non-interactive admission control algorithm based on some maximum thresholds on the interference levels of the transmitter and the receiver of the new link. This method is simple to implement but has relatively high error types I and II.

In [27], Xiao *et al.* propose an interesting error free distributed admission control algorithm. In this method, first, the new link measures its interference level and then transmits with a constant power. After the convergence of all powers to some new values, it compares its new interference level with the first measurement and determines its admissibility. We refer to this admission control algorithm as the *Xiao* algorithm. Note that in this method, the power control mechanism of the new link is disabled during the first

phase where it transmits with a constant power and waits until all power elements converge. Therefore, the worst case admission processing delay is equal to the number of iterations required by all links' power elements to converge. Also, if the new link is admissible, it does not achieve its QoS until all powers converge again in the second phase where the power control of the new link is activated. As a result, an admissible link requires as twice the number of iterations as that of a plain power control algorithm to achieve its QoS. Moreover, this algorithm is not applicable to the power control algorithms with the active link protection such as the asynchronous ALP and the Bambos algorithms.

In [50], Bambos *et al.* introduce the concept of the channel probing for the multi-channel networks. In this method, the SIR of a new link is estimated based on its interference level by approximating the power control step size to 1. Because of using such an approximation, the admission decision is not very reliable. In fact, this method is proposed as a channel congestion measurement mechanism to switch the new link to a less congested channel rather than an admission control algorithm.

In [19], Bambos *et al.* propose two general admission control algorithms based on the SIR convergence of the new link; the SIR-saturation and the time-out based algorithms. These algorithms are applicable to both the Foschini-Miljanic and asynchronous ALP power control algorithms, and since they do not require any pilot signals, they are fully distributed as well. A brief description of these algorithms is provided in the following.

Time-out based admission control: The new link updates its power for a certain period of time referred to as the *time threshold.* At the end of this period, if it achieves its QoS, it is considered admissible. Otherwise, it is inadmissible and becomes silent. The rationale behind this algorithm is that if the QoS requirements are simultaneously feasible, then all links become active in finite time. In this method, it is indeed the power control algorithm which accepts or rejects the new link after a certain number of iterations.

SIR-saturation based admission control: The new link monitors its SIR improvement at each iteration. If this improvement is less than a certain threshold while the SIR value is less than its QoS, it resets its power to zero and becomes silent. The rationale behind this algorithm is that if a network is infeasible, then all power elements diverge to

infinity while the SIRs of all links converge to some finite values below their QoS, geometrically fast [19].

Both the time-out and SIR-saturation based algorithms are based on some thresholds and design parameters that might be different from one link to another and have to be optimized by either having the full knowledge of the network parameters or a trial-and-error process. Moreover, even by initially setting these thresholds with the optimized values, when the network configuration changes, e.g., a new link is admitted, those initial values are no longer the optimum ones and consequently, these algorithms may not operate with their best performance.

5.3.2 Admission Control in Power-Constrained Networks

In theory, each transmitter can infinitely increase its power, whereas in practical applications the transmitting powers cannot go beyond some maxima. Such limitations are due to the specifications of the hardware components or the use of a battery with limited power and/or lifetime. As stated in Section 2.1.1, in an unconstrained network if the Perron-Frobenius eigenvalue is less than one, then all links achieve their QoS, the new link is admitted and the power elements converge to the Pareto-optimal power vector ($\mathbf{P}^*$). In a power-constrained network, if one of the power elements of $\mathbf{P}^*$ is greater than its maximum limit, then that link does not achieve its QoS and consequently, the network is not feasible and the new link has to be considered inadmissible. Therefore, an ideal admission control algorithm should take into account the power limitation of each link in the network as well. The interactive S&S admission control algorithm in [14], has such an ideal admission decision at the expense of broadcasting the global network information to all links. Obviously, this algorithm is not fully distributed.

In [19], Bambos *et al.* study this problem and propose a forced drop-out (FDO) mechanism to avoid a power outage in a power limited network. That is, if an existing link reaches its maximum power level, it transmits a network-wide *distress signal* and any inactive link receiving this distress signal becomes silent. However, accommodating such a global signal in a distributed network might decrease the capacity of the network.

In order to reduce the effect of having the distress signal on the network resources, this signal is usually transmitted over a narrow time- or frequency-slot. The same mechanism is considered in [27] as well. To the best of our knowledge, there is no more effective solution to this problem which affects the error type I of any distributed admission control algorithm.

In terms of power constraints, this work follows the same approach as those of [19] and [27], i.e., the admission control algorithms are developed for power-unconstrained networks. However, the same algorithms equipped with the FDO mechanism can be applied to the power-constrained networks as well. In fact, in Section 5.7 the performance of the proposed algorithms are investigated for a power-constrained network.

5.3.3 Admissibility Definition and Reference Performance

The admissibility definition, i.e., the criteria to declare a new link admissible, differs from one power control to another. For example, in the original Foschini-Miljanic algorithm a new link is admitted if it achieves its QoS and its power converges to a finite value. However, in the more practical case of the asynchronous ALP power control, a link is admitted as soon as it achieves its QoS at the time of its power update regardless of its power convergence. Obviously, these different admissibility definitions affect the performance of the admission control algorithms as well.

In order to determine the admissibility of a new link, ideally we would like to have the power control algorithm update the power elements for an infinite number of iterations and then check whether that link is eventually admitted or not. Clearly, this is not possible due to a) a long processing delay, b) resulting in an unstable network if the new link is inadmissible. In reality, an admission control algorithm determines the admissibility of a new link by trying to predict the behavior of the network for such a scenario. Therefore, the admissibility performance of a power control algorithm performing infinite iterations can be considered as the reference performance for any of its admission control algorithms. We call an admission control *definite*, if it achieves such a reference admissibility performance.

It can be verified that the time-out and SIR-saturation based admission control algorithms, mentioned earlier, may not be definite depending on their total number of power iterations. For example, if an admissible link has a slow SIR convergence, it is considered inadmissible and forced to drop out by both algorithms. However, if the total number of iterations goes to infinity, they both become definite admission control algorithms.

5.4 Local Measurements

As mentioned earlier, the proposed distributed admission control algorithm determines the admissibility of a new link based on the only available information, i.e., the set of local measurements of that link. In this section, first a framework to define and model these local measurements is developed and then, the main network normalization theorem using the local measurements is presented. Note that in the following, a generic power control algorithm is considered that converges to the optimum power vector. As a result, the findings of this section are applicable to both the asynchronous ALP and Foschini-Miljanic power control algorithms, to be examined later in this chapter.

The local measurements are modeled as follows. Following any power update, i.e., power change, in the network, the interference (or SIR) of the new link changes as well. Moreover, each power iteration starts with the power updating of the link 1 and ends with the power updating of the link N, as described in Section 5.2. Therefore, the first SIR change of the link 1 in each iteration corresponds to its own power update, the second SIR change corresponds to that of the link 2 and so on. Considering (5.1), let $In(i,k)$ be the total interference at the receiver of the link 1 after the power update of the link i at the kth iteration

$$In(i,k) = \eta_1 + \sum_{j=2}^{i} G_{1j}P_j(k) + \sum_{j=i+1}^{N} G_{1j}P_j(k-1). \tag{5.2}$$

Since no two links update their powers at the same time, the ith increase (or decrease) of the interference of the link 1 at the kth iteration, denoted by $d_i(k)$, is resulted by only

the power update of the link i, i.e.,

$$d_i(k) = In(i,k) - In(i-1,k) = G_{1i} \times (P_i(k) - P_i(k-1)). \tag{5.3}$$

Note that $In(i,k)$ includes the noise power η_1 which is unknown to the receiver and because of that, the interference generated by other links, i.e., $\sum_{j=2}^{i} G_{1j}P_j(k) + \sum_{j=i+1}^{N} G_{1j}P_j(k-1)$, cannot be calculated from $In(i,k)$ values. However, $d_i(k)$ does not include the noise power and therefore, it directly represents the power changes of other links.

The absolute power value of each link can be expressed in terms of its initial power value and the local measurements of the link 1 as

$$P_i(k) = P_i(0) + \frac{\sum_{j=1}^{k} d_i(j)}{G_{1i}}. \tag{5.4}$$

The following lemma establishes the relationship between the feasibility of a network for a given set of QoS requirements and the set of local measurement values.

Lemma 5.1 *Network $\mathcal{A}$ with the QoS requirement of $\mathbf{Q} = [Q_i]$ is feasible, if and only if for any set of power vectors $\mathbf{P(k)} = [P_i(k)]$ generated by a generic power control, the local measurement $d_i(k)$ values eventually become zero, i.e.,*

$$\forall i \in \{1, ..., N\} : \lim_{k \to \infty} d_i(k) = 0. \tag{5.5}$$

Proof: The proof is presented in two parts;

a) *if* part: We show that if (5.5) exists, then the network $\mathcal{A}$ with $\mathbf{Q} = [Q_i]$ is feasible. Considering (5.3), the limit (5.5) implies that $P_i(k)$ elements converge to some fixed values P_i', i.e.,

$$\forall i : \lim_{k \to \infty} P_i(k) = P_i'.$$

This is not possible unless $\mathbf{P'} = [P_i']$ is the optimum power vector $\mathbf{P^*}$ and satisfies all QoS requirements at the same time. The existence of such a power vector proves that the

network $\mathcal{A}$ with $\mathbf{Q} = [Q_i]$ is feasible.

b) *only if* part: Assume the network $\mathcal{A}$ is feasible. Consequently, any set of power vectors $\mathbf{P(k)}$ eventually converges to the optimum solution and becomes constant, i.e.,

$$\forall i : \lim_{k \to \infty} P_i(k) = P_i^*.$$

Equivalently, $\forall i : \lim_{k\to\infty} P_i(k) = P_i(k-1)$ and as a result, $\forall i : \lim_{k\to\infty} d_i(k) = 0$ which completes the proof. □

Recalling from Section 2.1.1, the feasibility of a set of QoS requirements can be determined by calculating the Perron-Frobenius eigenvalue of the matrix $\mathbf{F}$ defined as

$$F_{ij=} \begin{cases} 0, & \text{if } i = j \\ \frac{Q_i G_{ij}}{G_{ii}} & \text{if } i \neq j \end{cases}.$$

For a network with N links the construction of matrix $\mathbf{F}$ requires the knowledge of $(N^2 + N)$ network parameters, i.e., all $\forall i : Q_i$ and $\forall i, j : G_{ij}$. However, in this work we show that given a set of local measurement $d_i(k)$ values, some of these parameters do not affect the feasibility criteria and consequently, they can be normalized.

A network normalization process can be considered as a transformation of the parameters of the network $\mathcal{A}$ into those of the network $\mathcal{A}'$, i.e., $\mathcal{A}' = T(\mathcal{A})$. The following powerful but yet simple theorem states the main requirement for a network transformation process which does not affect the admissibility property.

Theorem 5.2 *From the point of view of the link* 1, *the network $\mathcal{A}$ has the same feasibility (admissibility) property as that of the network $\mathcal{A}'$, where $\mathcal{A}' = T(\mathcal{A})$, if for any set of power vectors $\mathbf{P(k)} = [P_i(k)]$ of $\mathcal{A}$, there exists a valid set of power vectors $\mathbf{P'(k)} = [P_i'(k)]$ for $\mathcal{A}'$ where*

$$\forall i, k : d_i(k) = d_i'(k). \tag{5.6}$$

Proof: It is shown that if (5.6) holds and one of these networks is feasible, then the other one has to be feasible as well. Obviously, if both networks are infeasible, they already

have the same feasibility property.

Now assume that the network $\mathcal{A}$ is feasible. According to Lemma 5.1, for the set of power vectors $\mathbf{P(k)} = [P_{ij}(k)]$

$$\forall i : \lim_{k\to\infty} d_i(k) = 0.$$

By comparing the above equation and the assumption (5.6), it is clear that for the set of power vectors $\mathbf{P'(k)} = [P'_{ij}(k)]$

$$\forall i : \lim_{k\to\infty} d'_i(k) = 0$$

which according to Lemma 5.1 proves that the network $\mathcal{A}'$ is feasible as well. □

According to this theorem, in the admission control process, the link 1 can *assume* any transformation of the actual network parameters that complies with (5.6). In fact, this theorem is the basis of the normalization transformations developed in the next sections which eventually result in the proposed admission control algorithm.

It is important to note that the transformation process introduced in Theorem 5.2 only preserves the feasibility property. However, the power vectors of those networks might not be the same. In fact, not only it is impossible to calculate the actual power vectors of the whole network at the link 1, but also such information has no effect on the admissibility of the link 1.

5.5 Proposed Admission Control for Foschini-Miljanic Algorithm

In this section, an admission control algorithm is proposed for the asynchronous Foschini-Miljanic power control algorithm; first, a brief description of the Foschini-Miljanic power control algorithm is presented. Next, the network normalization process is discussed. Then, the concept of interference equation is introduced. After, the core idea of the proposed algorithm is described for an example network of 3 links, and finally, the proposed algorithm

for a general network with N links is presented.

5.5.1 Foschini-Miljanic Power Control

The Foschini-Miljanic power control algorithm [16, 19] is described by the following iterative equation

$$P_i(k+1) = \frac{Q_i}{\gamma_i(k)} P_i(k). \tag{5.7}$$

Under this scheme, if γ_i is less than Q_i, then P_i is increased and if γ_i is more than Q_i, then P_i is decreased. Note that (5.7) converges to the Pareto-optimal power solution ($\mathbf{P}^*$) if the set of QoS requirements is feasible, and diverges to infinity otherwise (see Section 2.1.1 and 4.2).

This is a distributed algorithm at the link level where each link i updates its power solely based on the measurements at its receiver and some information from its transmitter. In this work, the Foschini-Miljanic algorithm is considered in the asynchronous mode with the interference observable property described in the system model. Equation (5.1) can be considered as the asynchronous version of (5.7).

5.5.2 Network Normalization

In the following, a normalization process is developed for a given set of local measurements at the link 1 based on the network transformation principle provided in Theorem 5.2. This process reduces the number of unknown parameters required to determine the admissibility of the new link by normalizing some of them to one, and at the same time, it preserves the admissibility property of the network.

It is very important to note that the following normalized values are in fact the assumptions made at the link 1 during the process of determining its admissibility and there is no actual action performed on the network itself.

Theorem 5.3 *Given a set of local measurements $d_i(k)$ of the link 1 for the network $\mathcal{A}$, at*

the link 1, *the QoS of each link* $i \neq 1$ *can be normalized to* 1, *i.e.,*

$$\forall i \neq 1 : Q_i = 1 \tag{5.8}$$

without affecting the feasibility property of the network.

Proof: Let $\mathbf{P(k)} = [P_i(k)]$ be a valid set of power vectors of $\mathcal{A}$. Moreover, let $\mathcal{A}'$ be the normalized network defined as

$$\begin{aligned}
&\forall i: && \eta'_i = \eta_i \\
&\forall i \neq j: && G'_{ij} = G_{ij} \\
&\forall i \neq 1: && G'_{ii} = G_{ii}/Q_i \ , \ G'_{1,1} = G_{1,1} \\
&\forall i \neq 1: && Q'_i = 1 \ , \ Q'_1 = Q_1
\end{aligned}$$

By setting $\mathbf{P'(k)} = [P'_i(k)]$ equal to $\mathbf{P(k)} = [P_i(k)]$, it is shown that not only this set is a valid set of power vectors for $\mathcal{A}'$, but also it satisfies the condition (5.6) of Theorem 5.2.

Considering the fact that $\mathbf{P(k)}$ and the parameters of $\mathcal{A}$ satisfy (5.1), for $\forall i \neq 1$ the power equation corresponding to $\mathcal{A}'$ and $\mathbf{P'(k)}$ can be achieved by dividing both sides of (5.1) by Q_i and a proper substitution of $\mathcal{A}'$ parameters. For $i = 1$, the equation (5.1) would be the same for both networks. Therefore, $\mathbf{P'(k)}$ is indeed a valid set of power vectors of $\mathcal{A}'$. Furthermore, since G_{1i} values and power elements in both networks are the same, it is obvious that $\forall i : d_i(k) = d'_i(k)$ satisfying (5.6). Therefore, according to Theorem 5.2 the admissibility of $\mathcal{A}'$ and $\mathcal{A}$, given the same set of the local measurement values of the link 1, are the same and the proof is complete. □

Note that in Theorem 5.3, the QoS of the link 1 is not normalized and it is kept the same as the actual value known to this link. The rationale behind keeping Q_1 intact is that according to the proof of Theorem 5.3, if Q_1 is set to 1, then $G_{1,1}$ has to be scaled as well. Consequently, $d'_1(k) \neq d_1(k)$ which violates the condition of Theorem 5.2.

Theorem 5.4 *Given a set of local measurements* $d_i(k)$ *of the link* 1 *for the network* $\mathcal{A}$, *at the link* 1, *the gain parameters corresponding to the transmitter of each link* j *can be*

scaled with an arbitrary scaling factor of C_j (an element of scaling vector $\mathbf{C} = [C_j]$), i.e.,

$$\forall i, j : \; G'_{ij} = G_{ij}/C_j \tag{5.9}$$

without affecting the feasibility property of the network.

Proof: Let $\mathbf{P(k)} = [P_j(k)]$ be a valid set of power vectors of $\mathcal{A}$. Furthermore, let $\mathcal{A}'$ be the normalized network where its elements for $\mathbf{C} = [C_j]$ are defined as

$$\begin{aligned} \forall i : &\quad \eta'_i = \eta_i \\ \forall i, j : &\quad G'_{ij} = G_{ij}/C_j \\ \forall i : &\quad Q'_i = Q_i \end{aligned} .$$

By setting the elements of $\mathbf{P'(k)} = [P'_j(k)]$ as $\forall j, k : P'_j(k) = P_j(k) \times C_j$, it is shown that not only this set is a valid set of power vectors for $\mathcal{A}'$, but also it satisfies the condition (5.6) in Theorem 5.2.

It is straightforward to show that the interferences generated by each link j at the receivers of other links in $\mathcal{A}'$ are exactly the same as those in $\mathcal{A}$, i.e., $\forall i, j : P_j(k) \times G_{ij} = P'_j(k) \times G'_{ij}$. Since $\mathbf{P(k)}$ and the parameters of $\mathcal{A}$ satisfy (5.1), by a proper substitution of $\mathcal{A}'$ parameters, the power equation corresponding to $\mathcal{A}'$ and $\mathbf{P'(k)}$ is resulted. Therefore, $\mathbf{P'(k)}$ is a valid set of power vectors for $\mathcal{A}'$. Furthermore, considering the local measurement values as the interferences generated by other links at the link 1, it can be verified that $\forall i, k : d_i(k) = d'_i(k)$ providing (5.6). Therefore, according to Theorem 5.2 the admissibility of $\mathcal{A}'$ and $\mathcal{A}$, given the same set of the local measurement of the link 1, are the same and the proof is complete. □

Theorem 5.5 *Given a set of local measurements $d_i(k)$ of the link 1 for the network $\mathcal{A}$, at the link 1, all gain parameters and the noise power used in the power updating equation of each link $i \neq 1$ can be scaled with an arbitrary scaling factor of D_i (an element of scaling vector $\mathbf{D} = [D_i]$), i.e.,*

$$\forall i \neq 1, j : \; G'_{ij} = G_{ij}/D_i \;\; , \;\; \eta'_i = \eta_i/D_i \tag{5.10}$$

without affecting the feasibility property of the network.

Proof: Let $\mathbf{P(k)} = [P_i(k)]$ be a valid set of power vectors of $\mathcal{A}$. Furthermore, let $\mathcal{A}'$ be the normalized network of $\mathcal{A}$ where its elements for $\mathbf{D} = [D_i]$ are defined as

$$\begin{aligned} &\forall i \neq 1: \quad \eta'_i = \eta_i / D_i \ , \ \eta'_1 = \eta_1 \\ &\forall i \neq 1, j: \quad G'_{ij} = G_{ij}/D_i \ , \ G'_{1j} = G_{1j} \\ &\forall i: \quad Q'_i = Q_i \end{aligned}$$

By setting $\mathbf{P'(k)} = [P'_i(k)]$ equal to $\mathbf{P(k)} = [P_i(k)]$, it is shown that not only this set is a valid set of power vectors for $\mathcal{A}'$, but also it satisfies the condition (5.6) in Theorem 5.2.

Since $\mathbf{P(k)}$ and the parameters of $\mathcal{A}$ satisfy (5.1), by dividing both the numerator and denominator of the left-hand side of that equation by D_i and a proper substitution of $\mathcal{A}'$ parameters, the power equation corresponding to $\mathcal{A}'$ and $\mathbf{P'(k)}$ is resulted. Therefore, $\mathbf{P'(k)}$ is a valid set of power vectors for $\mathcal{A}'$. Furthermore, since G_{1i} values and power elements in both networks are the same, it can be verified that $\forall i : d_i(k) = d'_i(k)$ providing (5.6). Therefore, according to Theorem 5.2, the admissibility of $\mathcal{A}'$ and $\mathcal{A}$, given the same set of the local measurements of the link 1, is the same and the proof is complete. □

The normalization processes presented in Theorems 5.3, 5.4 and 5.5 can be applied simultaneously to a network for any arbitrary vectors of $\mathbf{C} = [C_j]$ and $\mathbf{D} = [D_i]$. For a network with the asynchronous Foschini-Miljanic power control algorithm, we select each C_j element of vector $\mathbf{C}$, in Theorem 5.4, to be equal to G_{1j} which results in $\forall j : G'_{1j} = 1$. Furthermore, we select each D_i element of vector $\mathbf{D}$, in Theorem 5.5, to be equal to G_{ii} resulting in $\forall i \neq 1 : G'_{ii} = 1$. As a result, the following normalized network model is used in the rest of this section;

$$\forall i \neq 1: \quad Q_i = 1, G_{1i} = 1, G_{ii} = 1, G_{1,1} = 1. \tag{5.11}$$

Consequently, (5.3) and (5.4) become

$$\forall i : d_i(k) = In(i,k) - In(i-1,k) = P_i(k) - P_i(k-1) \tag{5.12}$$

$$P_i(k) = P_i(0) + \sum_{j=1}^{k} d_i(j) \tag{5.13}$$

and the power updating equation of (5.1) can be rewritten for links $\forall i \neq 1$ as

$$\forall i \neq 1: \quad \frac{P_i(k)}{\eta_i + \sum_{j=1}^{i-1} G_{ij} P_j(k) + \sum_{j=i+1}^{N} G_{ij} P_j(k-1)} = 1 \tag{5.14}$$

and for the link 1 it becomes

$$\frac{P_1(k)}{\eta_1 + \sum_{j=2}^{N} P_j(k-1)} = Q_1. \tag{5.15}$$

Moreover, (5.14) and (5.15) can be rearranged as

$$\forall i \neq 1: \quad \eta_i + \sum_{j=1}^{i-1} G_{ij} P_j(k) + \sum_{j=i+1}^{N} G_{ij} P_j(k-1) = P_i(k) \tag{5.16}$$

$$\eta_1 + \sum_{j=2}^{N} P_j(k-1) = P_1(k)/Q_1. \tag{5.17}$$

5.5.3 Power Equation vs. Interference Equation

Since the power equation (5.16) consists of $P_i(k)$ and η_i parameters which are unknown to the link 1, that equation cannot be directly used at the link 1. Therefore, in this section we derive another characteristic equation that only consists of the available local measurements at the link 1, i.e., $d_i(k)$ values. To do so, we start with two consecutive iterations of (5.16)

$$\forall i \neq 1: \quad \eta_i + \sum_{j=1}^{i-1} G_{ij} P_j(k) + \sum_{j=i+1}^{N} G_{ij} P_j(k-1) = P_i(k) \tag{5.18}$$

$$\forall i \neq 1: \quad \eta_i + \sum_{j=1}^{i-1} G_{ij} P_j(k-1) + \sum_{j=i+1}^{N} G_{ij} P_j(k-2) = P_i(k-1). \tag{5.19}$$

Subtracting $P_i(k-1)$ from $P_i(k)$ results in

$$\forall i \neq 1: \sum_{j=1}^{i-1} G_{ij}(P_j(k)-P_j(k-1))+\sum_{j=i+1}^{N} G_{ij}(P_j(k-1)-P_j(k-2)) = P_i(k)-P_i(k-1). \tag{5.20}$$

Considering (5.12), the above equation can be rewritten as

$$\forall i \neq 1, k \geq 2: \sum_{j=1}^{i-1} G_{ij}d_j(k) + \sum_{j=i+1}^{N} G_{ij}d_j(k-1) = d_i(k). \tag{5.21}$$

Note that having $k \geq 2$ is due to the fact that the index of $d_i(k)$ has to be equal to or greater than 1.

Applying the same steps to the link 1, using (5.17), results in

$$\forall k \geq 2: Q_1 \times [\sum_{j=2}^{N} d_j(k-1)] = d_1(k). \tag{5.22}$$

We refer to (5.21) and (5.22) as the *interference equations*. Clearly, these equations do not depend on the initial power or noise power values (i.e., $P_i(0)$ and η_i). Note that according to the admissibility criteria stated in Section 2.1.1, the matrix $\mathbf{F}$ and consequently the admissibility of the link 1 do not depend on the noise power of the receivers. In fact, noise power values are only required to calculate the optimum power solution which is not of immediate interest for determining the admissibility of the link 1.

Although the interference equation (5.21) turns out to simplify the network model by eliminating $P_i(0)$ and η_i values, it remains to be proved that this equation is sufficient to determine the feasibility of the network. Such proof is the topic of the next sections of this chapter.

5.5.4 Example Network of 3 Links

Before stating and proving the proposed admission control algorithm for the general case of a wireless ad hoc network with N links, the core idea of this algorithm is examined for an example network of 3 links in this section.

In this example, the new link 1 with a QoS of Q_1 enters a network consisting of 2

stable links. This results in a network with a total of 3 links. Assuming the normalized parameters presented in Section 5.5.2, at the link 1, we show that this link can determine its admissibility in 3 iterations based on its local measurement values.

The interference equation (5.21) can be rewritten for the second and third iterations of the link 2 as

$$G_{2,1}d_1(2) + G_{2,3}d_3(1) = d_2(2) \tag{5.23}$$

$$G_{2,1}d_1(3) + G_{2,3}d_3(2) = d_2(3) \tag{5.24}$$

Let $\mathbf{A(2)}$ be the coefficient matrix of the left-hand sides of (5.23) and (5.24) with unknown parameters $G_{2,1}$ and $G_{2,3}$, i.e.,

$$\mathbf{A(2)} = \begin{bmatrix} d_1(2) & d_3(1) \\ d_1(3) & d_3(2) \end{bmatrix}.$$

The solution for the set of equations (5.23) and (5.24) depends on their linearly independence. The condition of (5.23) and (5.24) being linearly independent is expressed as

$$|\mathbf{A(2)}| \neq 0.$$

This is equivalent to $\mathbf{A(2)}$ being a full rank matrix.

In the following, both possibilities of $|\mathbf{A(2)}| \neq 0$ and $|\mathbf{A(2)}| = 0$ are considered separately and the proposed algorithm to determine the admissibility of the new link is investigated for each possibility.

A) Linearly dependent equations ($|\mathbf{A(2)}| = 0$): In this case, it is shown that the $d_i(k)$ values for any link and iteration can be calculated based on those of the first three iterations.

Since $|\mathbf{A(2)}| = 0$ and $\mathbf{A(2)}$ has only two rows, one row has to be a multiple of the other one; assume that the second row of $\mathbf{A(2)}$ is equal to R times of its first row, i.e.,

$$d_1(3) = R \times d_1(2) \ , \ d_3(2) = R \times d_3(1).$$

Considering (5.23) and (5.24), the same relation exists for the right-hand of those equations as well, i.e., $d_2(3) = R \times d_2(2)$. In summary

$$\frac{d_3(2)}{d_3(1)} = \frac{d_1(3)}{d_1(2)} = \frac{d_2(3)}{d_2(2)} = R.$$

Based on the fact that $d_3(k)$ in (5.21) depends on $d_2(k)$ and $d_1(k)$ and also the above equality, it is straightforward to show that

$$\frac{d_3(3)}{d_3(2)} = R.$$

Applying the above equalities to (5.22) for k equal to 3 and 4 results in $\frac{d_1(4)}{d_1(3)} = R$. In fact, by repeating the same procedure the local measurement $d_i(k)$ corresponding to any link i at any iteration k can be calculated based on those of the first 3 iterations by the recursive equation of

$$\forall i, k : \frac{d_i(k)}{d_i(k-1)} = R. \tag{5.25}$$

Therefore, by calculating the value of R from the first two iterations the local measurement values for the rest of the iterations can be predicted by the link 1 as well. According to Lemma 5.1, if these calculated (predicted) local measurement values $d_i(k)$ eventually go to zero, then the network is feasible and the link 1 is admissible. Otherwise, the link 1 is inadmissible. For this 3-link network, the feasibility condition can be simplified as $R < 1$.

Note that $\mathbf{A(3)}$ depends on $d_1(2)$, $d_1(3)$, $d_2(2)$ and $d_2(3)$, hence $|\mathbf{A(3)}| = 0$. Consequently, if the above steps were applied to $\mathbf{A(3)}$ the same results would be achieved.

B) Linearly independent equations ($|\mathbf{A(2)}| \neq 0$): The set of equations (5.23) and (5.24) can be solved by Cramer's rule method [51]. According to these equations the values of $G_{2,1}$ and $G_{2,3}$ only depend on the local measurements $d_i(k)$.

Recalling from the proof of part (A), if $|\mathbf{A(2)}| = 0$, then $|\mathbf{A(3)}| = 0$. Consequently, since $|\mathbf{A(2)}| \neq 0$, then $|\mathbf{A(3)}| \neq 0$. Therefore, the same steps can be applied to the link 3 and the gain parameters $G_{3,1}$ and $G_{3,2}$ can be similarly calculated.

Recalling from Section 2.1.1, the link 1 is admissible if the maximum modulus eigenvalue (ρ_f) of matrix $\mathbf{F}$ is less than 1. By substituting the normalized parameters in $\mathbf{F}$, the

eigenvalues (λ_i) of $\mathbf{F}$ are calculated as the roots of ($|\mathbf{F} - \lambda \mathbf{I}_3| = 0$), i.e.,

$$|\mathbf{F} - \lambda \mathbf{I}_3| = \begin{vmatrix} -\lambda & Q_1 \times \frac{1}{1} & Q_1 \times \frac{1}{1} \\ 1 \times \frac{G_{2,1}}{1} & -\lambda & 1 \times \frac{G_{2,3}}{1} \\ 1 \times \frac{G_{3,1}}{1} & 1 \times \frac{G_{3,2}}{1} & -\lambda \end{vmatrix} = 0 \tag{5.26}$$

where $G_{2,1}$, $G_{2,3}$, $G_{3,1}$ and $G_{3,2}$ are already calculated based on the local measurements of the link 1 and Q_1 is known to the link 1. Therefore, by constructing and solving (5.26), the link 1 can calculate λ_i values. If $\max(|\lambda_i|) < 1$, then the new link 1 is admissible and eventually all links achieve their designated QoS requirements. Otherwise, the link 1 is inadmissible and it becomes silent.

5.5.5 General Network of N Links

In the previous section, the core idea of the proposed algorithm was explained for an example network of 3 links. In this section, we investigate the proposed algorithm for a general network of N links, in which the new link enters the network of $N-1$ stable links. Using the normalized parameters presented in Section 5.5.2, we show that the link 1 can determine its admissibility in N iterations based on its local measurement values $d_i(k)$.

According to the interference equation (5.21), the local measurement $d_i(k)$ values of each link $i \neq 1$ in the first N iterations are expressed as

$$2 \leq k \leq N: \quad \sum_{j=1}^{i-1} G_{ij} d_j(k) + \sum_{j=i+1}^{N} G_{ij} d_j(k-1) = d_i(k). \tag{5.27}$$

The above set of $(N-1)$ linear equations corresponding to each link $i \neq 1$, can be represented in matrix form as

$$\mathbf{A(i)} \times \mathbf{X(i)} = \mathbf{B(i)} \tag{5.28}$$

where

$$\mathbf{A(i)} = \begin{bmatrix} d_1(2) & \cdots & d_{i-1}(2) & d_{i+1}(1) & \cdots & d_N(1) \\ \vdots & \vdots & \vdots & \vdots & \vdots & \vdots \\ d_1(N) & \cdots & d_{i-1}(N) & d_{i+1}(N-1) & \cdots & d_N(N-1) \end{bmatrix} \tag{5.29}$$

$$\mathbf{X(i)} = \begin{bmatrix} G_{i1} \\ \vdots \\ G_{i(i-1)} \\ G_{i(i+1)} \\ \vdots \\ G_{iN} \end{bmatrix}, \quad \mathbf{B(i)} = \begin{bmatrix} d_i(2) \\ \vdots \\ d_i(N) \end{bmatrix}. \tag{5.30}$$

Moreover, matrix $\tilde{\mathbf{A}}(\mathbf{i})$ is called the *augmented matrix* [51] of the equation set presented in (5.27)

$$\tilde{\mathbf{A}}(\mathbf{i}) = \left[\begin{array}{cccccc|c} d_1(2) & \cdots & d_{i-1}(2) & d_{i+1}(1) & \cdots & d_N(1) & d_i(2) \\ \vdots & \vdots & \vdots & \vdots & \vdots & \vdots & \vdots \\ d_1(N) & \cdots & d_{i-1}(N) & d_{i+1}(N-1) & \cdots & d_N(N-1) & d_i(N) \end{array}\right]. \tag{5.31}$$

The solution of (5.31) depends on the linearly independence of that set of equations. The condition of (5.31) being linearly independent can be expressed as

$$\forall i \neq 1 : |\mathbf{A(i)}| \neq 0. \tag{5.32}$$

This is equivalent to $\mathbf{A(i)}$ being a full rank matrix.

In the following, both possibilities of $|\mathbf{A(i)}| \neq 0$ and $|\mathbf{A(i)}| = 0$ are considered separately and the proposed algorithm is presented for each possibility.

A) Linearly dependent equations ($\exists r \neq 1 : |\mathbf{A(r)}| = 0$): We show that if there exists a linearly dependent $\mathbf{A(r)}$ or equivalently a rank deficient $\mathbf{A(r)}$, then all local measurement values $d_i(k)$ for any link and iteration can be calculated based on the local measurements in the first N iterations. The proof given in this section is provided for the case of

having 3 linearly dependent equations. However, it can be easily extended to other number of dependent equations as well.

Assume in $\mathbf{A(r)}$ rows k_1, k_2 and k_3 where $k_1 > k_2 > k_3$ are linearly dependent, i.e.,

$$\exists T, R : \begin{cases} \forall i < r : d_i(k_1+1) = R \times d_i(k_2+1) + T \times d_i(k_3+1) \\ \forall i > r : d_i(k_1) = R \times d_i(k_2) + T \times d_i(k_3) \end{cases} . \tag{5.33}$$

Note that each row k of $\mathbf{A(i)}$ corresponds to the interference equation for the iteration $k+1$. For link $(i = r)$ the left-hand side of (5.27) for iterations (k_1+1), (k_2+1) and (k_3+1) are linearly dependent with coefficients R and T of (5.33). Therefore, the same property also applies to the right-hand sides of those equations, i.e.,

$$d_r(k_1+1) = R \times d_r(k_2+1) + T \times d_r(k_3+1). \tag{5.34}$$

The next local measurement to be evaluated is $d_{r+1}(k_1+1)$. Again, for the link $(i = r+1)$ the left-hand side of (5.27) for iterations (k_1+1), (k_2+1) and (k_3+1) are linearly dependent according to (5.33) and (5.34). Consequently, the same property also applies to the right-hand sides of those equations, i.e.,

$$d_{r+1}(k_1+1) = R \times d_{r+1}(k_2+1) + T \times d_{r+1}(k_3+1). \tag{5.35}$$

Note that if $(r = N)$, then the next local measurement to be evaluated is $d_1(k_1+2)$. In that case instead of using (5.27), the same steps are applied to (5.22) resulting in

$$d_1(k_1+2) = R \times d_1(k_2+2) + T \times d_1(k_3+2). \tag{5.36}$$

The above procedure can be repeated for any link and iteration. In fact, by having the local measurements $d_i(k)$ between (k_3) and (k_1+1) iterations, the $d_i(k)$ values for any link i and iteration k can be calculated recursively as

$$\forall i, k > k_1 : d_i(k) = R \times d_i(k-(k_1-k_2)) + T \times d_i(k-(k_1-k_3)). \tag{5.37}$$

According to Lemma 5.1, if these calculated (predicted) local measurements eventually become zero, then the network is feasible and the link 1 is admissible. Otherwise, the link 1 is inadmissible and becomes silent.

B) Linearly independent equations ($\forall i \neq 1 : |\mathbf{A(i)}| \neq 0$): If all $\mathbf{A(i)}$ are linearly independent, or equivalently they are all full rank, then for each link i the set of linear equations (5.28) is solved by Cramer's rule method. Since for each link i matrices $\mathbf{A(i)}$ and $\mathbf{B(i)}$ only consist of the local measurement values, the elements of $\forall i \neq 1 : \mathbf{X(i)}$, i.e., the values of $\forall j \neq i, i \neq 1 : G_{ij}$, only depend on the local measurements as well.

Now, all the parameters required to construct the matrix $\mathbf{F}$ presented in Section 2.1.1 are either calculated, provided by the normalization process or known to the link 1 (e.g., Q_1). Recalling from the same section, the link 1 is admissible if the maximum modulus eigenvalue (ρ_f) of the matrix $\mathbf{F}$ is less than 1. Therefore, the link 1 first calculates $\forall j \neq i, i \neq 1 : G_{ij}$ based on the local measurements and constructs the matrix $\mathbf{F}$ by substituting the required parameters. Then, it calculates the eigenvalues (λ_i) of $\mathbf{F}$ as the roots of

$$|\mathbf{F} - \lambda \mathbf{I}_N| = 0.$$

If $\max(|\lambda_i|) < 1$, then the new link is admissible and eventually all links achieve their designated QoS requirements. Otherwise, the link 1 is inadmissible and becomes silent.

Note that the proposed algorithm can be considered as a measurement-based admission control scheme where the admissibility is determined based on collecting data in the network. The collected information has to reflect the status of the network as well as the activity level of each link regarding the admissibility criteria. In other words, in this approach like any other measurement-based algorithms, the network has to be observable through the collected data [6]. In fact, we show that the interference observable property required for the asynchronous ALP power control is indeed *the only* requirement in order to have an observable network for the proposed admission control algorithm. Moreover, the proposed method is a definite admission control algorithm (see Section 5.3.3) for the power-unconstrained asynchronous Foschini-Miljanic power control algorithm. In fact, for this power control algorithm the proposed admission control is both type I and II error free.

5.6 Proposed Admission Control for Asynchronous ALP Algorithm

In Section 5.5, the proposed admission control algorithm was presented for the asynchronous Foschini-Miljanic power control algorithm. In this section, the extension of that algorithm to the asynchronous ALP power control algorithm is investigated. In fact, the proposed admission control algorithm can be applied as an add-on feature to a wide variety of the distributed power-controlled ad hoc networks with the interference observable power updating property.

In the following, first, a brief description of the asynchronous ALP power control algorithm is presented. Next, the network normalization process is discussed. Then, the concept of interference equation for this power control is examined, and finally, the proposed algorithm for a general network with N links is presented.

5.6.1 Asynchronous ALP Power Control

The asynchronous active link protection power control, proposed in Chapter 4, is described by the following iterative equation

$$P_i(k+1) = \begin{cases} \frac{\delta Q_i}{\gamma_i(k)} P_i(k) & \text{if } i \in \mathcal{C}_k \\ \min(\delta P_i(k), \frac{\delta Q_i}{\gamma_i(k)} P_i(k)) & \text{if } i \in \mathcal{D}_k \end{cases} \tag{5.38}$$

where δ represents the power step-size (also referred to as the protection margin), and $\mathcal{C}_k$ and $\mathcal{D}_k$ denote the active and inactive sets of links, respectively. The link i becomes active, as soon as at the time of its power update $\gamma_i(k) = \delta Q_i$ or equivalently $P_i(k) = \frac{\delta Q_i}{\gamma_i(k)} P_i(k-1)$. Similarly, the link i is considered inactive as long as at the time of its power update $\gamma_i(k) < \delta Q_i$. In this technique, if the increased QoS requirement of $\delta\mathbf{Q}$ is feasible, then (5.38) converges to the optimal power corresponding to $\delta\mathbf{Q}$, and diverges to infinity otherwise. Note that once a link becomes active, it remains active for the rest of the process. Moreover, the active link protection property is achieved at the expense of operating at a higher SIR δQ_i than the required Q_i. The order of the power updating

corresponds to the asynchronous mode with the interference observable property described in the system model.

Considering the system model presented in Section 5.2, for the active links, i.e., links 2 to N, the power updating equation (5.38) can be rewritten as

$$\forall i \neq 1 : \frac{G_{ii}P_i(k)}{\eta_i + \sum_{j=1}^{i-1} G_{ij}P_j(k) + \sum_{j=i+1}^{N} G_{ij}P_j(k-1)} = \delta Q_i. \tag{5.39}$$

However, the power updating equation of the link 1 may be different depending on its status; if the link 1 is active its power updating equation is the same as (5.39) and if it is inactive, it updates its power according to

$$P_1(k) = \delta P_1(k-1). \tag{5.40}$$

Note that during the observation period, i.e., the first N iterations, if at any iteration the link 1 becomes active, then it is considered admissible by the power control and no further admission processing is required. Therefore, the proposed algorithm only considers the scenario in which the link 1 is inactive during the first N iterations, i.e., it updates its power based on (5.40).

5.6.2 Network Normalization

For the asynchronous ALP power control algorithm, Theorem 5.6 normalizes Q_i values. It is straightforward to verify that Theorems 5.4 and 5.5, presented in Section 5.5.2, are still valid for this power control.

Theorem 5.6 *Given a set of local measurements $d_i(k)$ of the link 1 for the network $\mathcal{A}$, at the link 1, the QoS of each link $i \neq 1$ can be normalized to $1/\delta$, i.e.,*

$$\forall i \neq 1 : Q_i = 1/\delta \tag{5.41}$$

without affecting the feasibility property of the network.

Proof: Considering the power updating equation of (5.39), the proof is similar to that of Theorem 5.3. □

By using Theorem 5.6, the right-hand side of (5.39) becomes 1. By applying Theorem 5.6 as well as Theorems 5.4 and 5.5 with the same vectors $\mathbf{C} = [C_i]$ and $\mathbf{D} = [D_i]$ as those in Section 5.5.2, the following normalized network model can be considered at the link 1

$$\forall i \neq 1: \quad Q_i = 1/\delta, G_{1i} = 1, G_{ii} = 1, G_{1,1} = 1. \tag{5.42}$$

Consequently, the power updating equation of (5.39) becomes

$$\forall i \neq 1: \quad \frac{P_i(k)}{\eta_i + \sum_{j=1}^{i-1} G_{ij} P_j(k) + \sum_{j=i+1}^{N} G_{ij} P_j(k-1)} = 1 \tag{5.43}$$

or equivalently

$$\forall i \neq 1: \quad \eta_i + \sum_{j=1}^{i-1} G_{ij} P_j(k) + \sum_{j=i+1}^{N} G_{ij} P_j(k-1) = P_i(k). \tag{5.44}$$

Note that the power updating equation of the link 1 remains the same as (5.40), i.e.,

$$\delta P_1(k-1) = P_1(k). \tag{5.45}$$

5.6.3 Interference Equation

Comparing (5.44) to its counterpart (5.16) in the Foschini-Miljanic algorithm shows that the power updating equations for links 2 to N in both normalized networks are exactly the same and therefore, the interference equations of links 2 to N for the asynchronous ALP power control remain the same as (5.21), i.e.,

$$\forall i \neq 1, k \geq 2: \quad \sum_{j=1}^{i-1} G_{ij} d_j(k) + \sum_{j=i+1}^{N} G_{ij} d_j(k-1) = d_i(k). \tag{5.46}$$

However, the interference equations of the link 1 are different and in this case it is derived by subtracting two consecutive iterations of (5.45), i.e.

$$d_1(k) = \delta d_1(k-1). \tag{5.47}$$

5.6.4 General Network of N Links

Recalling from Section 5.5.5, the proposed admission control algorithm constructs $\forall i \neq 1 : \mathbf{A(i)} \times \mathbf{X(i)} = \mathbf{B(i)}$ using the interference equations (5.21) of links 2 to N. Also, as mentioned in the previous section, the interference equations of the asynchronous ALP algorithm for links 2 to N are the same as those of (5.21). Therefore, the proposed admission control algorithm can construct $\forall i \neq 1 : \mathbf{A(i)} \times \mathbf{X(i)} = \mathbf{B(i)}$ following the same steps presented in Section 5.5.5 and depending on $|\mathbf{A(i)}|$ being zero or not, it can determine the admissibility of the new link.

A) Linearly dependent equations ($\exists r \neq 1 : |\mathbf{A(r)}| = 0$): Recalling from Section 5.5.5, based on the linear coefficients the original proposed admission control algorithm predicts $d_i(k)$ values for any link and iteration and then according to Lemma 5.1, if $d_i(k)$ values converge to zero, the new link is considered admissible. Note that in the Foschini-Miljanic power control, the link 1 always updates its power using the same equation, whereas in the asynchronous ALP algorithm as soon as the link 1 becomes active, it uses a different power updating equation. Because of this difference, the proposed admission control algorithm is slightly different for these power control algorithms.

For the asynchronous ALP algorithm, the linear coefficients used to predicted $d_i(k)$ values are valid as long as the link 1 updates its power based on (5.40). As a result, $d_i(k)$ values cannot be predicted after the activation of the link 1 and therefore, Lemma 5.1 is not applicable anymore.

However, by using the valid predicted local measurements $d_i(k)$ prior to the activation of the link 1 and some available local information, the SIR value of that link can be calculated at any iteration prior to its activation; during the observation period, for any iteration $k_0 : 1 \leq k_0 \leq N$ the link 1 has the knowledge of $G_{1,1}$, $P_1(k_0)$ and $In(1, k_0)$. Moreover, for any iteration k prior to the activation of that link, we have $P_1(k) = P_1(k_0)\delta^{k-k_0}$

according to (5.40). Therefore, by substituting this equation, (5.2) and (5.3) in (5.1), the SIR value of the link 1 at iteration k (right after its power update) is calculated as

$$\frac{G_{11}P_1(k_0)\delta^{k-k_0}}{In(1,k_0)+\sum_{j=2}^{N}\sum_{l=k_0}^{k-1}d_j(l)}=\gamma_1(k). \tag{5.48}$$

By comparing the calculated $\gamma_1(k)$ to the QoS, the exact iteration that the link 1 becomes active can be predicted. Obviously, if for any number of iterations, the calculated SIR does not achieve the QoS, the new link is considered inadmissible.

B) Linearly independent equations ($\forall i \neq 1 : |\mathbf{A(i)}| \neq 0$): In this case, the algorithm is exactly the same as the one presented for the asynchronous Foschini-Miljanic power control.

At the end, we would like to mention that for the case of linear dependent equations, i.e., case A), equation (5.48) predicts the exact same behavior as that of the asynchronous ALP power control algorithm and therefore, the proposed admission control admits the new link only if it predicts that the power control eventually activates that link as well. As a result, the accuracy of the admission decision is subjected to the same limitations as those of the power control algorithm itself. This confirms that the proposed algorithm is a definite admission control (see Section 5.3.3) for the power-unconstrained asynchronous ALP power control. In the simulation section, some limitations of the asynchronous power control algorithm are discussed and a variant of (5.48) is proposed.

5.7 Simulation Results

In this section, the performance of the proposed algorithm for the asynchronous ALP power control is evaluated through extensive computer simulations. For comparison, the performance of both the time-out and SIR-saturation based admission control algorithms are investigated as well.

In the following, first the network configuration parameters are described. Later, the comparison method is discussed and finally, the numerical results are presented and evaluated.

5.7.1 Network Configuration

Consider an N-link wireless network consisting of $(N-1)$ active links and a new link seeking admission according to the single-hop model described in Section 5.2. The transmitter of each link is placed at random with a uniform distribution in a square area of 200×200 m^2. The receiver of each link is placed at a random distance from its transmitter according to the Gaussian distribution with a mean of 10 m and a standard deviation of 2 m. Also, the angle of each receiver compared to its transmitter is distributed uniformly in the range of $[0, 2\pi)$ given a reference direction. Note that given this setup, an extremely rare event of having a negative distance between a transmitter and its receiver implies an additional π radian rotation of the original angle of those two nodes.

The channel gain models large-scale propagation effects, i.e., the path loss and the shadowing effects [32]. Variations due to small-scale propagation effects are usually assumed to be averaged out in the context of SIR-based power control [33]. The channel gain between the transmitter of the link j and the receiver of the link i, is modeled as

$$G_{ij} = K_o \frac{a_{ij}}{r_{ij}^4} \tag{5.49}$$

where r_{ij} represents the distance between these two nodes, a_{ij} models the power attenuation due to the shadowing and K_o is a unitless constant depending on other parameters such as antenna characteristics, reference distance, etc. [32]. All a_{ij} variables are assumed to be independent and log-normally distributed with a mean of 0 dB and a standard deviation of 8 dB [38, 39]. For all links, the maximum transmitting power P^{max} is equal to 1 W, the thermal noise power η is set to 10^{-12} W and K_o is set to 0.0142 (corresponding to $f_c = 2$ GHz and a reference distance of 10 m). The initial power of the new link is set to 10^{-11} W. All links have the same active link protection step size of $\delta = 1.58$, i.e., 2 dB, and a QoS of 10 dB including δ. Therefore, once a link becomes active any SIR above $Q - \delta = 8$ dB is acceptable.

In the rest of this section, the total number of links is set to 7, i.e., $N = 7$, since this value results in a balanced number of admissible and inadmissible network realizations for the described network.

Note that the simulation parameters are particularly chosen to have more reliable results and a better understanding of the admission control problem rather than matching a specific application.

5.7.2 Comparison Method

The comparison method used in this section is the same as that used in [14]. The performance of the time-out based, SIR-saturation based and proposed admission control algorithms are evaluated in terms of the error type I, error type II and number of iterations required to determine the admissibility of the new link.

The two error probabilities can be expressed as P(error type I)=Pr{to accept the new link$|H_0\}$ and P(error type II)=Pr{to reject the new link$|H_1\}$ where H_0 refers to the situation where the new link is inadmissible due to the network configuration parameters, e.g., the gain matrix, and the network limitations, e.g., the maximum power and QoS values, and H_1 represents the scenario where the new link is admissible [14]. The error type I results in a network power outage where some active links might become inactive and the error type II results in an erroneous blockage of the new link.

In order to have a high confidence interval for the probabilities of error types I and II, for every test case 10000 independent network realizations corresponding to each H_0 and H_1 event are simulated. The error type I is calculated as the percentage of new links being accepted under H_0 event and the error type II is calculated as the percentage of new links being rejected under H_1 event. Each network realization is generated as follows; first the network parameters such as the gain matrix are randomly generated according to the configuration presented in Section 5.7.1. Then assuming the link 1 being silent, the possibility of links 2 to 7 being active is evaluated by the feasibility criteria (see Section 2.1.1) and the links power constraints (note that a network realization might be feasible under the feasibility criteria, however, if its optimum power vector violates the maximum power limit, then it is considered infeasible). If the set of active links is not feasible, this network realization is discarded and another one is generated. If the set of active links is feasible, then the admissibility of the new link based on both the feasibility and maximum power

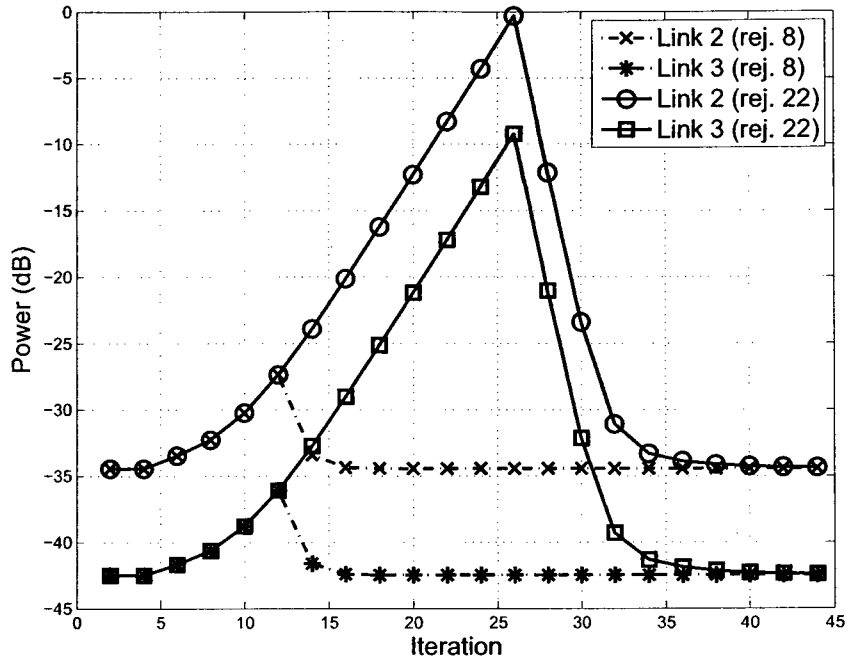

Figure 5.1: An example of power evolutions of two active links when an inadmissible link enters the network at 5th iteration and it is rejected after a) 22 iterations, and b) 8 iterations.

limit criteria is determined and this network realization is accordingly labeled corresponding to either of H_0 or H_1 event. Moreover, to ensure a reliable performance comparison all algorithms are evaluated based on the same set of network realizations.

The speed of each algorithm is evaluated based on the total number of iterations required to determine the admissibility of the new link where a faster algorithm requires less number of iterations. The advantages of having a faster algorithm over a slower one can be studied through an example; Figure 5.1 shows the power evolutions of two active links where the new link is inadmissible. The new link enters the network at the 5th iteration and forces the existing active links to increase their powers to maintain their QoS. Note that the new link has to be eventually rejected since it is not admissible. The power evolution of the active links, i.e., links 2 and 3, are presented for two different scenarios of a) the new link being rejected after 22 iterations (i.e., at the iteration 26), and b) the new link being rejected after 8 iterations (i.e., at the iteration 12). In the first scenario, the powers of both

active links are increased by almost 34 dB before the new link is rejected. Furthermore, after the rejection of the new link, these active links require another 12 iterations to become stable again and achieve their previous power levels. Therefore, during the whole admission control process, the powers of two active links are affected for a total of 34 iterations. In the second scenario, i.e., the rejection after 8 iterations, the power of these active links are increased by only 8 dB compared to 34 dB in the previous scenario. Moreover, because of this low power increase, the two active links only require 4 iterations to become stable again. Therefore, during the whole admission control process, the powers of two active links are only affected for a total of 12 iterations. In summary, when the new link is inadmissible, a faster admission control algorithm has the following advantages over a slower one:

1. Obviously, it determines the admissibility of the new link in a shorter time period.
2. It reduces the power fluctuation and consequently, the power consumption of the active links is reduced as well.
3. It affects the overall network interference for fewer iterations resulting in a more stable network.

For the proposed admission control algorithm, the total number of required iterations is always fixed and is equal to the total number of the links in the network, i.e., N. In the time-out based algorithm the total number of required iterations is also fixed and is equal to the time threshold. However, this parameter is not a fixed value for the SIR-saturation based algorithm; in this algorithm, the number of required iterations for a specific SIR threshold depends on the SIR convergence of the link 1 which differs from one network realization to another. As a result, for the SIR-saturation based algorithm the number of required iterations is calculated as the average of those values for all network realizations corresponding to a specific SIR threshold.

5.7.3 Numerical Results

In the following, the performance results for the time-out based, SIR-saturation based and proposed admission control algorithms are presented and evaluated.

5.7.3.1 Time-Out Based Algorithm

The error probabilities for this algorithm with different values of the time threshold (expressed in total number of iterations) are presented in Figure 5.2. As shown, the probability of the error type II decreases as the time threshold increases. This is due to the fact that by increasing the number of iterations the power of an admissible new link becomes higher and consequently, the probability of that link achieving its QoS goes up, resulting in a lower probability of error type II.

As illustrated in Figure 5.2, by increasing the number of iterations the probability of the error type I increases. This increase is indeed an artifact of the ALP power control algorithm rather than a result of the admission control process; according to the admissibility definition of the ALP power control (see Section 5.3.3), the link 1 is considered active as soon as it achieves its QoS. Note that for an active link i any SIR value above $(Q_i - \delta)$ is acceptable, however, it updates its power targeting Q_i. If the QoS of all links are feasible, then all power elements converge to some finite values. Nevertheless, when the QoS of all links are not simultaneously feasible, i.e., the new link is inadmissible, in some rare scenarios the new link might achieve its QoS at a moment that some active links operate at SIR values lower than their QoS. Therefore, the link 1 becomes active, whereas it should have been rejected. In Figure 5.2, by increasing the number of iterations, the SIR value of the new link in such scenarios gets closer to its QoS and therefore, the probability of achieving that target increases, resulting in a higher probability of the error type I. This limitation of the active link protection power control algorithm has been also mentioned in [19].

According to Figure 5.2, in order to have a balanced rate of error types I and II the value of the time threshold has to be set to 37 resulting in an equal rate of error types I and II of 5% (see Table 5.1). However, as mentioned in Section 5.3, this optimum time threshold highly depends on the network dynamics and parameters, and cannot be optimized

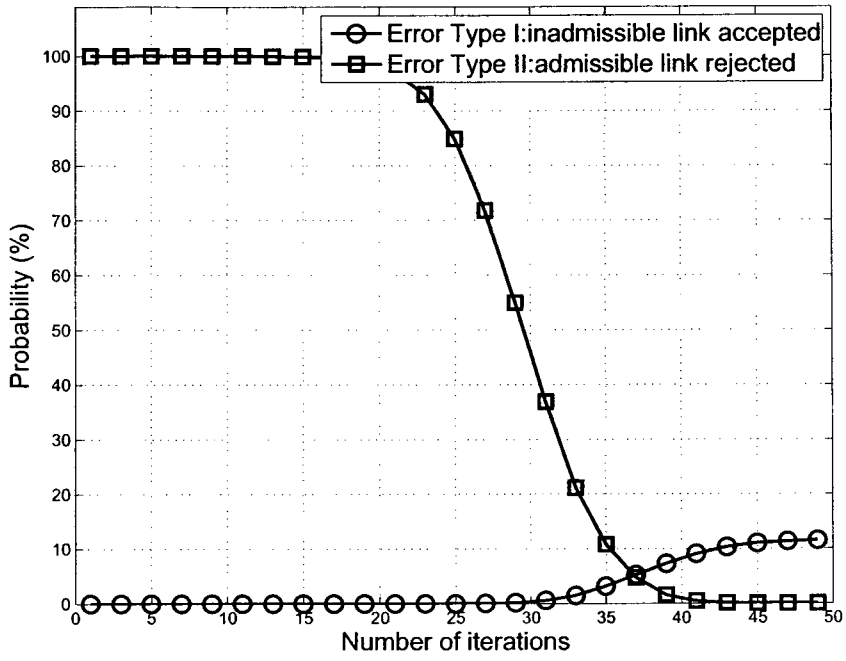

Figure 5.2: Error probabilities of the time-out based admission control algorithm for different time threshold values (expressed in total number of iterations).

independently. Also note that due to requiring such a high value of the time threshold this algorithm is considered as a slow admission control algorithm.

5.7.3.2 SIR-Saturation Based Algorithm

The error probabilities under SIR-saturation based admission control algorithm for different values of the SIR threshold (expressed in dB) are demonstrated in Figure 5.3.a. Also, the average number of required iterations for achieving those SIR thresholds is presented in Figure 5.3.b. Note that the maximum SIR threshold value cannot be higher than δ, i.e., 2 dB in this case. The rationale behind this rule is that due to the nature of the ALP power control the SIR improvement of the new link is always less than δ. As a result, if the SIR threshold is equal to or greater than δ, the new link is rejected at the first iteration.

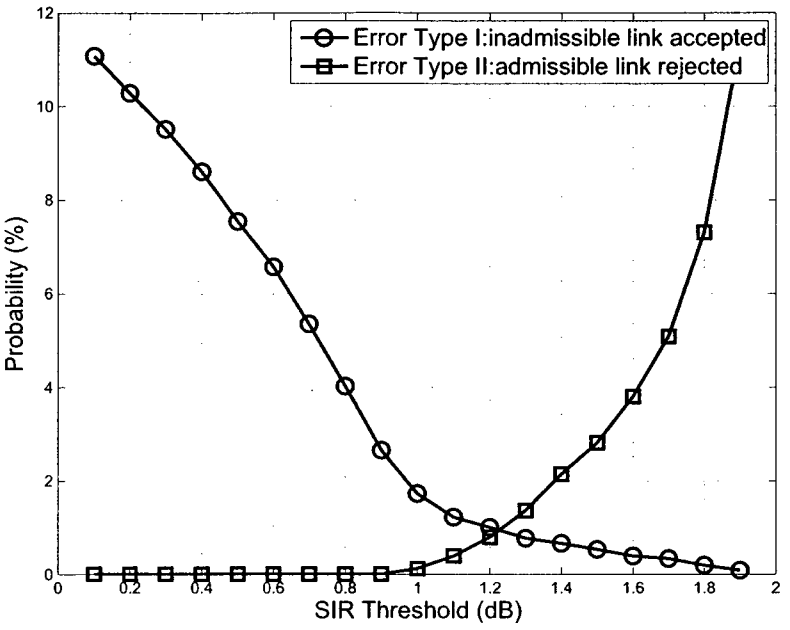

a)

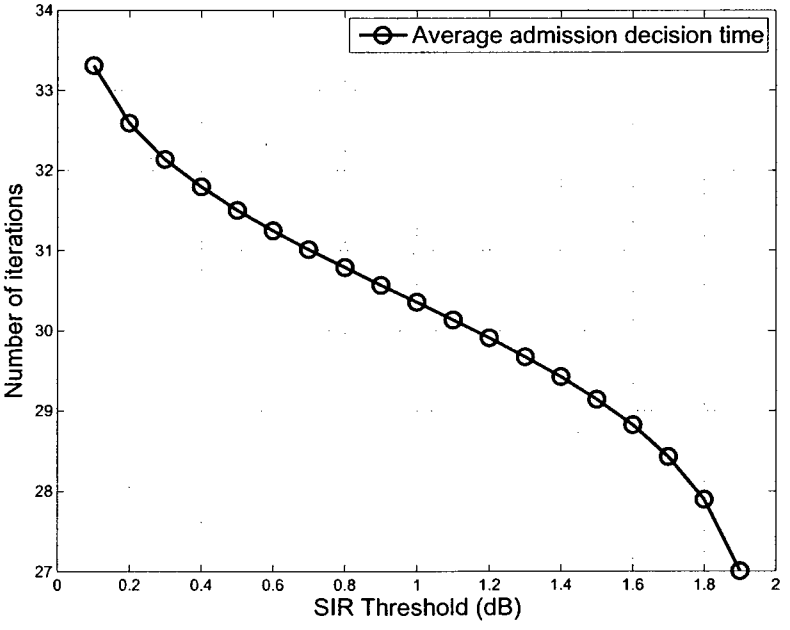

b)

Figure 5.3: SIR-saturation based algorithm: a) error probabilities for different SIR thresholds, b) the average of the required number of iterations for different SIR thresholds.

As shown in Figure 5.3.a, the increase of the SIR threshold results in a higher probability of the error type II. This observation can be justified as follows; the SIR of an admissible link improves at each iteration compared to that of the previous one until it achieves its QoS. However, if the improvement at some iteration is less than the SIR threshold, then the new link is rejected. Obviously, by increasing the SIR threshold value more admissible links fall into this category and consequently, the error type II increases.

By decreasing the SIR threshold the number of iterations required to have the SIR improvement of the new link less than that threshold increases. This is also confirmed in Figure 5.3.b which illustrates that a lower SIR threshold requires a higher number of iterations to determine the admissibility. Furthermore, Figure 5.3.a shows that in contrast to the error type II, by decreasing the SIR threshold the error type I goes up. Considering the fact that a lower SIR threshold requires a higher number of iterations, this increase in the error type I can be justified by the same argument presented for the error type I of the time-out based admission control algorithm.

According to Figures 5.3.a-b, in order to have a balanced rate of error types I and II the SIR threshold has to be set to 1.2 dB resulting in an equal rate of error types I and II of 1% and the average number of iterations of 30 (see Table 5.1). Note that, although the average number of the iterations is 30, the actual number of required iterations fluctuates between 15 and 45. As mentioned in Section 5.3, this optimum threshold highly depends on the network dynamics and parameters and cannot be optimized independently. Furthermore, because of requiring such a large number of iterations this algorithm is considered as a slow admission control process.

5.7.3.3 Proposed Admission Control Algorithm

The error probabilities of the original proposed admission control algorithm for the asynchronous ALP power control, discussed in Section 5.6, are presented in Table 5.1. As shown, the required number of iterations to determine the admissibility of the new link is equal to 7, i.e., the number of links. The probability of the error type II is equal to 0.01% which is considerably lower than those of the SIR-saturation and time-out based algorithms. That is, there is only 1 admissible link being rejected in 10000 trials.

Table 5.1: Performance comparison of different admission control algorithms.

	Error Type I	Error Type II	Number of Iterations
Optimized Time-Out	5.0%	5.0%	37
Optimized SIR-Saturation	1.0%	1.0%	30 average (between 15 and 45)
Original Proposed Algorithm	11.4%	0.01%	7
Modified Proposed Algorithm	1.68%	0.01%	7

The probability of the error type I is equal to 11.4%, which is mainly caused by the network realizations that have linearly dependent interference equations. Recalling from Section 5.6, for these network realizations the proposed admission control algorithm predicts the exact behavior of the power control algorithm. In fact, it can be verified that the proposed algorithm has almost the same probability of the error type I as that of the time-out based admission control discussed in Section 5.7.3.1, where the asynchronous ALP power control algorithm simply performs 50 iterations, i.e., a time threshold equal to 50. As explained in Section 5.7.3.1, this high value of the error type I is an artifact of the power control and its admissibility definition rather than a result of the admission process. Moreover, it is observed that most of these events of the error type I correspond to the scenarios where an inadmissible new link achieves a SIR value slightly higher than its QoS and becomes active at a moment that some of the active links operate below their QoS values.

Considering the above observation, we propose a slight modification to improve the performance of the proposed algorithm. In this approach, the requirement to admit a new link is tightened in order to filter out some of those momentary SIR spikes of the inadmissible links that make them admitted. More specifically, a new link is admitted if its SIR value achieves $(Q_1 + \delta)$. Since in the asynchronous ALP power control the SIR change of each link in each iteration is always equal to or less than δ, this tighter requirement results into having the SIR of the new link higher than Q_1 for the whole iteration prior to admitting that link. It is important to note that the tighter admission requirement of the new link is only applied to the network realizations with linearly dependent equations.

The performance of the modified proposed admission control with a tighter admission requirement of $(Q_1 + \delta)$ is presented in Table 5.1. Comparing the performance of this modified version with that of the original proposed algorithm in the Table 5.1, shows that both approaches have the same probability of the error type II of 0.01%, whereas the probability of the error type I of the modified one is dramatically reduced to 1.68% from 11.4%.

Considering such a significant performance improvement by increasing the new link QoS requirement from Q_1 to $(Q_1 + \delta)$, one may argue that the same modification can be applied to the original asynchronous ALP power control algorithm as well. This is not possible, since increasing the new link QoS requirement violates the active link protection property of the power control algorithm, and also such a modification results in higher than required power elements of other active links. Note that none of these issues are problematic for the proposed admission control algorithm because in the admission process all values are being calculated (predicted) and no actual power element is affected.

Note that since the proposed algorithm relies on the local measurements, the process of measuring the SIR values at the new link has to be as precise as possible in order to capture the network dynamics and predict the admissibility correctly.

As the conclusion, the proposed admission control algorithm with a tighter admission requirement has the following advantages over the time-out and SIR-saturation based algorithms

1. The proposed algorithm has much lower rates of the error types I and II in most cases.

2. The proposed algorithm determines the admissibility of the new link only in 7 iterations, i.e., the number equal to the total number of the links. Therefore, it is at least 4 times faster than the time-out and SIR-saturation based algorithms with their optimized thresholds (see Section 5.7.2 for the benefits of a faster algorithm).

3. Both the time-out and SIR-saturation based algorithms require some parameter optimization which is not possible in a dynamic ad hoc network. On the contrary, the proposed admission control algorithm does not require any optimization and it always operates with its best performance.

5.8 Conclusion

In this chapter, a new distributed admission control algorithm for the asynchronous power-controlled wireless ad hoc networks was introduced. This admission control was developed based on the Perron-Frobenius theorem and the local measurements of the new link. A normalization process was also presented normalizing some of the network parameters without affecting the admissibility of the new link. The proposed algorithm was presented for the general case of the asynchronous Foschini-Miljanic power control algorithm and then, it was extended to the asynchronous ALP power control. The performance of this algorithm was evaluated and compared to those of other distributed algorithms through some computer simulations. It was shown that the proposed algorithm is faster and also has a lower probability of error types I and II compared to other algorithms.

Chapter 6

Feasible SIR Region

This chapter studies the feasible SIR region for both the single-hop and multi-hop wireless ad hoc networks where a single channel or multiple channels are available. The feasible SIR region of ad hoc networks provides a valuable insight into the general capacity region and also helps us to design better transmission control algorithms. In fact, the border of the feasible SIR region can be considered as an upper limit for the achievable rates of any power and admission control schemes.

6.1 Introduction

In order to design better transmission control algorithms, such as power control and admission control algorithms, it is of a great importance to identify the upper bounds for the achievable rates of these algorithms. In theory, this upper limit is described by the general capacity region of wireless ad hoc networks. The general capacity region of ad hoc networks is yet unknown and remains as an open problem. However, there are several researches addressing capacity-related regions in wireless networks for some special cases and scenarios.

In [28], Gupta and Kumar evaluate the lower and upper bounds of the capacity of the wireless networks by allowing the number of nodes to go to infinity and using statistical averaging techniques. Since the number of nodes goes to infinity and in this limit all networks are the same, these bounds hold for all networks. In [52], Grossglauser and Tse

employ the same approach with the assumption of the node mobility and show that large gains on capacity can be achieved. In [29], Toumpis and Goldsmith define the capacity of a network, under a given transmission protocol, as the convex hull (time sharing) of all basic rate matrices. Their technique requires producing *all* rate matrices, which is not feasible. As a result, in order to have a finite number of possible transmission schemes, the network parameters have to be quantized and limited, e.g., the power elements are either zero or maximum.

The capacity-related properties of wireless networks are also studied in the context of the power allocation [17, 16]. In [53], Elbatt and Ephremides focus on the next neighbor transmission performed in two phases of scheduling and power control. In the scheduling phase, a subset of the transmitters is selected to reduce the interference and in the power control phase, the feasibility of having simultaneous transmissions in the selected subset is examined. This process is repeated until a feasible subset is found. In [16] and other similar works such as [17, 7], the authors present an iterative algorithm to calculate the power elements in order to achieve a predefined set of rates. Note that almost all aforementioned works have one thing in common; that is, in almost all of them, the interference from other links is modeled as the additive noise, due to the complex nature of finding the capacity region of ad hoc networks. As a result, the calculated regions are considered as the collection of the feasible rates rather than the capacity region itself.

In this chapter, we focus on the common ground of all transmission control schemes and emphasize on the important fact that no matter which transmission control algorithms the network uses, at any given instant the network is dealing with only one power vector (multiple power vectors correspond to multiple time slots). In this case, the boundary of the feasible SIR region represents an upper bound for the rates achievable by all single power vectors at any given instant (snapshot). It is important to note that, in this definition of the feasible SIR region, no time domain scheduling (time sharing) is considered. This feasible SIR region not only is one step closer to the general capacity region, but also helps us to design better transmission schemes for wireless networks. For example, an ideal power control can only achieve a rate vector within the feasible SIR region and an ideal admission control should reject any new link which results in a rate vector outside of this region.

The rest of this chapter is organized as follows. In Section 6.2, we study the feasible SIR region for single-hop wireless ad hoc networks where both scenarios of having a single channel and multiple channels are considered. In Section 6.3, the findings and algorithm of single-hop networks are extended to multi-hop networks. Finally, in Section 6.4, the convexity of the feasible SIR region of single-channel single-hop networks for both scenarios of power-constrained and power-unconstrained systems is investigated.

Note that, as explained in Chapter 2, the concept of the feasible SIR region for single-hop networks refers to the feasible link SIR region, whereas for multi-hop networks it refers to the feasible path SIR region. The notion of the link or path in these definitions is omitted when they can be easily deduced from the context.

6.2 Single-Hop Ad Hoc Networks

In this section, we consider the single-hop network model, as described in Section 2.1. In the following, the feasible SIR region is initially studied for the ad hoc networks communicating over only one shared channel; first, the theoretical conditions of the power vectors producing the link SIR vectors on the border of the feasible SIR region are investigated in Section 6.2.1. Next, in Section 6.2.2, based on those aforementioned conditions, a simple algorithm is presented to generate that region and some numerical results are provided. Finally, in Section 6.2.3, the findings and proposed algorithm are extended to the case of having multiple channels available to the network.

6.2.1 Conditions of the Border of Feasible SIR Region

The feasible SIR region of a wireless network is completely described by its border, which is defined as follows;

Definition 6.1 *The border of the feasible SIR region is defined as the collection of all achievable Pareto-optimal SIR vectors, i.e., for each SIR vector* $\boldsymbol{\gamma} = [\gamma_i]$ *belonging to the border, there is no other achievable SIR vector* $\hat{\boldsymbol{\gamma}} = [\hat{\gamma}_i]$ *for which* $\forall i : \gamma_i \leq \hat{\gamma}_i$.

The following theorem provides the basic condition for a link SIR vector to be on the border of the feasible SIR region of a power-constrained single-hop ad hoc network;

Theorem 6.2 *(*Maximum power for at least one link) *The link SIR vector* $\boldsymbol{\gamma} = [\gamma_i]$ *is on the border of the feasible SIR region, if and only if its power vector* $\mathbf{P} = [P_i]$ *has at least one link transmitting with its maximum power* $P^{\max}$.

Proof: The proof is presented in two parts:

a) *if* part: We show that if there is at least one power element with the maximum value, i.e., $\exists l : P_l = P^{\max}$, then the link SIR vector $\boldsymbol{\gamma} = [\gamma_i]$ is on the border of the feasible SIR region. As a counter example, assume that $\boldsymbol{\gamma} = [\gamma_i]$ is not on the border of feasible SIR region. Therefore, there exists another power vector $\hat{\mathbf{P}} = [\hat{P}_i]$ with the link SIR vector $\hat{\boldsymbol{\gamma}} = [\hat{\gamma}_i]$, for which $\forall i : \gamma_i \leq \hat{\gamma}_i$ and $\exists r : \gamma_r < \hat{\gamma}_r$. According to Lemma 3.3, we have $\forall i : P_i < \hat{P}_i$ which is impossible for the link l, since $P_l = P^{\max}$ and $\hat{P}_l$ cannot be greater than the maximum value.

b) *only if* part: We show that if a link SIR vector is on the border of the feasible SIR region, then at least one power element of its corresponding power vector has to have the maximum value. The proof is similar to the proof of part (b) of Theorem 3.6; if there is no power element equal to the maximum value, by scaling all power elements, a new power vector is resulted whose link SIR vector is component-wise greater than $\boldsymbol{\gamma} = [\gamma_i]$, which is in contradiction with the definition of the link SIR vectors to be on the border of feasible SIR region. □

6.2.2 Generating the Border of Feasible SIR Region

According to Theorem 6.2, any power vector with at least one power element equal to the maximum value generates a SIR vector on the border of the feasible SIR region. Using this simple condition, the following algorithm is proposed to generate the complete border of the feasible SIR region in N steps for an N-link network. At each step, the power of one link is set to its maximum value and the powers of other links span from zero to maximum. Each of these power vectors corresponds to a link SIR vector on the border and

the collection of all these link SIR vectors represents the complete border of the feasible SIR region.

In the following, the numerical results for an example network are presented; first, the simulation setup is described and then, the performance of the proposed algorithm for a randomly generated example network is investigated.

Consider an N-link wireless network according to the single-hop model described in Section 2.1. The transmitter of each link is placed at random with a uniform distribution in a square area of 200×200 m^2. The receiver of each link is placed at a random distance from its transmitter according to the Gaussian distribution with a mean of 10 m and a standard deviation of 2 m. Also, the angle of each receiver compared to its transmitter is distributed uniformly in the range of $[0, 2\pi)$ given a reference direction. Note that given this setup, an extremely rare event of having a negative distance between a transmitter and its receiver implies an additional π radian rotation of the original angle of those two nodes. The channel gain models large-scale propagation effects, i.e., the path loss and the shadowing effects [32]. Variations due to small-scale propagation effects are usually assumed to be averaged out in the context of SIR-based power control [33]. The channel gain between the transmitter of the link j and the receiver of the link i, is modeled as

$$G_{ij} = K_o \frac{a_{ij}}{r_{ij}^4} \tag{6.1}$$

where r_{ij} represents the distance between these two nodes, a_{ij} models the power attenuation due to the shadowing and K_o is a unitless constant depending on other parameters such as antenna characteristics, reference distance, etc. [32]. All a_{ij} variables are assumed to be independent and log-normally distributed with a mean of 0 dB and a standard deviation of 8 dB [38, 39]. For all links, the maximum transmitting power P^{max} is equal to 1 W, the thermal noise power η is set to 10^{-12} W and K_o is set to 0.0142 (corresponding to $f_c = 2$ GHz and a reference distance of 10 m). The initial powers of all links are set to 0.1 W.

We consider a network realization randomly generated according to the aforementioned network configuration. In this example, in order to be able to graphically depict the complete feasible SIR region in two dimensions, only two active links, i.e., $N = 2$, are

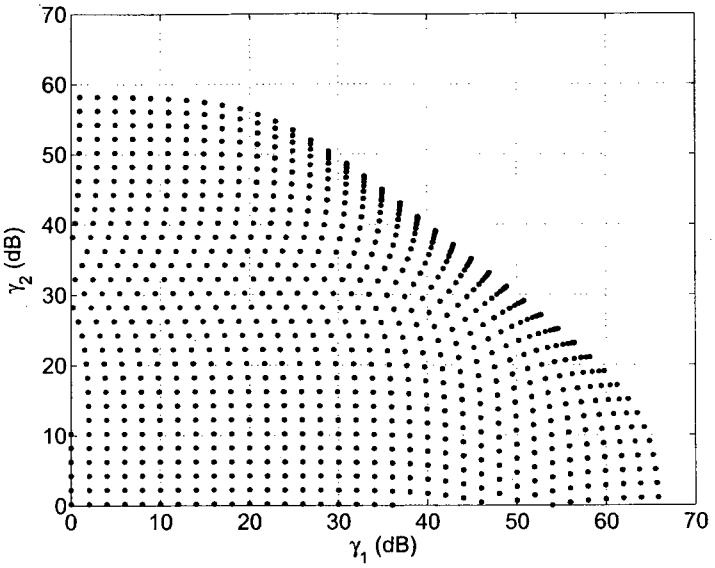

Figure 6.1: A Mont-Carlo simulation of the feasible SIR region for an example network with two active links.

considered. In order to show the feasible SIR region of the example network, the result of a Mont-Carlo simulation is presented in Figure 6.1 in which the power of each link varies within 50 levels with a step-size of 2 dB and for each possible power vector the corresponding link SIR vector is plotted. This Mont-Carlo simulation generates almost all areas of the feasible SIR region. In Figure 6.2, the proposed algorithm is used to produce the border of the feasible SIR region where sections $B1$ and $B2$ correspond to the areas in which the powers of the link 2 and link 1 are set to $P^{\max}$, respectively.

By comparing Figure 6.1 and Figure 6.2, it is clear that the graph generated based on the proposed simple algorithm is exactly on the border of the feasible SIR region illustrated in Figure 6.1.

6.2.3 Multi-Channel Communications

In the previous sections, it was assumed that there is only one wireless channel shared among the links. In this section, we show that all the results and the algorithms can be extended to the multi-channel communications scenario where there is more than one channel

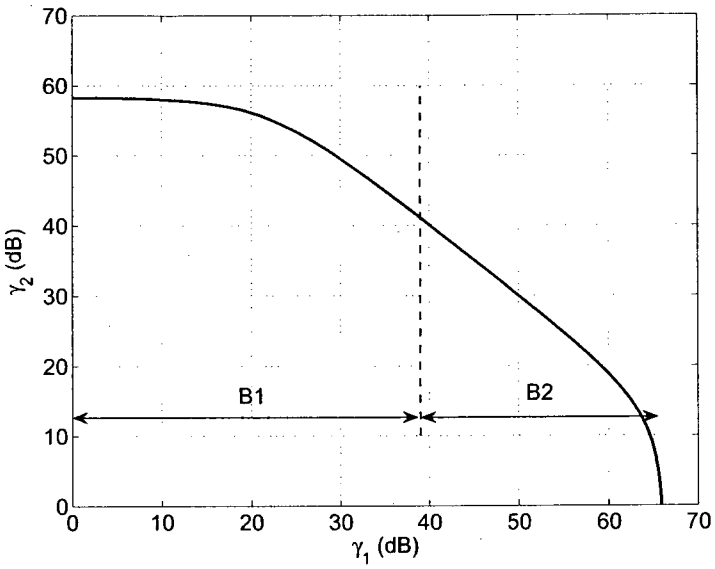

Figure 6.2: The border of the feasible SIR region of the example network in Figure 6.1 generated by using the proposed algorithm.

available to the network and each link is pre-assigned to communicate over one of these channels. Clearly, each channel contains at least one link.

In the following, Theorem 6.2, presented for the single-channel communications, is extended to the multi-channel communications.

Theorem 6.3 *In a multi-channel network, the link SIR vector* $\gamma = [\gamma_i]$ *is on the border of the feasible SIR region, if and only if its power vector* $\mathbf{P} = [P_i]$ *has at least one link in each subchannel transmitting with its maximum power* $P^{\max}$.

Proof: The link SIR vector on the border of the feasible SIR region can be viewed as a collection of the SIR sets each corresponding to a subchannel. Clearly, the Pareto optimality condition of the link SIR vector $\gamma = [\gamma_i]$ is equivalent to the Pareto optimality of each of those SIR subsets in their corresponding subchannels. By applying Theorem 6.2 to each of these subchannels, it can be verified that at least one of the power elements in each subchannel has to be equal to the maximum value in order to produce a Pareto-optimal SIR set. □

Theorem 6.3 provides the basic condition for a link SIR vector to be on the border of the feasible SIR region of a multi-channel power-constrained single-hop ad hoc network. The algorithm to generate this border is in principle similar to the one presented for the single-channel networks. Consequently, for a network with N links, the complete border of the feasible SIR region can be generated in $(\frac{N}{M})^M$ steps where M denotes the number of the subchannels (assuming equal number of links per subchannel). At each step, the power of one link in each subchannel is set to its maximum and the powers of other links span from zero to the maximum value in a fixed step-size. Each of these power vectors corresponds to a link SIR vector on the border and the collection of all these link SIR vectors represents the complete border of the feasible SIR region.

6.3 Multi-Hop Ad Hoc Networks

In the previous section, we studied the feasible SIR region for single-hop ad hoc networks. In particular, the basic conditions of the power control vectors producing the link SIR vectors on the border of the feasible SIR region were investigated and a simple algorithm was proposed to generate the border of that region. In this section, those concepts are investigated for multi-hop wireless ad hoc networks and the proposed algorithms are extended to the networks based on the multi-hop network model presented in Section 2.2.

In multi-hop ad hoc networks, each pair of the original source and final destination nodes is communicating via a routing path. As discussed in Chapter 3, we assume proactive (predefined) routing path scenarios where the information about the routing path selection and the link allocation is already provided by other layers/sub-layers of the network [40].

In this section, we initially consider the single-channel networks; first, the basic conditions of the minimal power vectors producing the link SIR vectors on the border of the feasible SIR region are studied, in Section 6.3.1. Next, in Section 6.3.2, based on those aforementioned conditions a simple algorithm is presented to generate that region and some numerical results are provided. Finally, in Section 6.3.3, the findings and proposed algorithm are extended to the case of having multiple channels available to the network.

6.3.1 Conditions of the Border of Feasible SIR Region

In this section, we consider a multi-hop ad hoc network communicating over only one shared channel. In the following, based on the findings of Section 3.4, the necessary and sufficient conditions for the path SIR vectors to be on the border of the feasible SIR region are investigated. Recalling from Section 3.4.1, the path SIR vectors are identified and analyzed by their minimal power vectors.

Moreover, we show that such a path SIR vector can be generated by only a unique power vector.

Theorem 6.4 (Maximum power for at least one link of the minimal power vector) *The path SIR vector* $\mathbf{\Gamma} = [\Gamma_j]$ *is on the border of the feasible SIR region, if and only if its minimal power vector* $\mathbf{P}^L = [P_{ij}^L]$ *has at least one link transmitting with its maximum power, i.e.,* $P^{\max}$.

Proof: Let $\boldsymbol{\gamma^L} = [\gamma_{ij}^L]$ be the link SIR vector of $\mathbf{P}^L = [P_{ij}^L]$ with $P_{rt} = P^{\max}$. The proof is presented in two parts:

a) *if* part: The proof is similar to the proof of part (a) of Theorem 3.21.

b) *only if* part: The proof is similar to that of Theorem 3.20. □

As explained in Section 3.4.1, each path SIR vector might be generated by more than one power vector, i.e., $|\mathcal{X}(\mathbf{\Gamma})| \geq 1$. However, we show that each path SIR vector $\mathbf{\Gamma} = [\Gamma_j]$ on the border of the feasible SIR region is produced by only one power vector which in fact is its minimal power vector $\mathbf{P}^L = [P_{ij}^L]$.

Theorem 6.5 *Any path SIR vector* $\mathbf{\Gamma} = [\Gamma_j]$ *on the border of the feasible SIR region can be generated by only its corresponding minimal power vector* $\mathbf{P}^L = [P_{ij}^L]$, *i.e.,*

$$|\mathcal{X}(\mathbf{\Gamma})| = 1.$$

Proof: According to Theorem 6.4, $\mathbf{P}^L = [P_{ij}^L]$ has at least one maximum power element, i.e., $\exists r, t : P_{rt}^L = P^{\max}$. By a counter example, we assume that there is another power vector $\hat{\mathbf{P}} = [\hat{P}_{ij}]$ with the link SIR vector $\hat{\boldsymbol{\gamma}} = [\hat{\gamma}_{ij}]$ where $\hat{\mathbf{P}} \in \mathcal{X}(\mathbf{\Gamma})$. By the definition of

the minimal power vector, we have $\forall i,j : \gamma_{ij}^{L} \leq \hat{\gamma}_{ij}$ and also

$$\forall i,j : P_{ij}^{L} \leq \hat{P}_{ij}. \tag{6.2}$$

The above inequality implies that $\hat{P}_{rt}^{L} = P^{\max}$. Therefore, satisfying $\gamma_{rt}^{L} \leq \hat{\gamma}_{rt}$ requires to have

$$\sum_{ij \neq rt} G_{rt,ij} \hat{P}_{ij} \leq \sum_{ij \neq rt} G_{rt,ij} P_{ij}^{L}.$$

which is in contradiction to (6.2), unless $\forall i,j : P_{ij}^{L} = \hat{P}_{ij}$. Consequently, $\hat{\mathbf{P}}$ is the same as $\mathbf{P^L}$ and $\mathcal{X}(\mathbf{\Gamma})$ has only one element. □

6.3.2 Generating the Border of Feasible SIR Region

According to Theorem 6.4, a path SIR vector is on the border of the feasible path SIR region if its minimal power vector has at least one maximum power element. This condition can be used to generate the border of the feasible SIR region. In this simple method, the minimal power vector of each possible path SIR vector is calculated by using the feasibility criteria described in Section 2.1.1 and then the resulted minimal power vector is verified against the maximum power limit. For a network with L paths, the complete border of the feasible path SIR region can be generated as follows. First, the SIR values of $(L-1)$ paths span from zero to the maximum possible value generating different sets of SIR values. Secondly, for each set of these SIR values, the SIR of the remaining path, i.e., the one that is not included for generating the possible SIR sets, is calculated iteratively by using the feasibility criteria until at least one element of its minimal power vector becomes equal to the maximum limit. Note that each generated power vector corresponds to a path SIR vector on the border and the collection of all these path SIR vectors represents the complete border of the feasible path SIR region.

In the following, the numerical results for an example network are presented; first, the simulation setup is described and then, the performance of the proposed algorithm for a randomly generated example network is investigated.

Consider an N-link wireless network with L routing paths according to the multi-hop model described in Section 2.2. The original transmitter of each routing path is placed at random with a uniform distribution in a square area of 200×200 m^2. The receiver of each link is placed at a random distance from its transmitter according to the Gaussian distribution with a mean of 10 m and a standard deviation of 2 m. Also, the angle of each receiver compared to its transmitter is distributed uniformly in the range of $[0, 2\pi)$ given a reference direction where an extremely rare event of having a negative distance between a transmitter and its receiver implies an additional π radian rotation of the original angle of those two nodes. Note that each intermediate node, i.e., the node which is neither the original source nor the final destination of a routing path, consists of one receiver and one transmitter where the channel gain between these two modules is set to zero. The channel gains, maximum transmitting powers, thermal noise and other parameters are the same as those of the simulation configuration considered in Section 6.2.2.

In the following, we consider a network realization randomly generated according to the aforementioned network configuration. In order to be able to graphically depict the complete feasible SIR region in two dimensions, only two routing paths, i.e., $L = 2$, and four active links, i.e., $N = 4$, are considered. In order to show the feasible SIR region for this example, the result of a Mont-Carlo simulation is presented in Figure 6.3 in which the SIR of each path varies within 40 levels with a step-size of 1 dB, and the feasibility of each SIR vector is verified according the feasibility criteria described in Section 2.1.1 and the maximum power limit. The feasible path SIR vectors are plotted in Figure 6.3. This Mont-Carlo simulation generates almost all areas of the feasible SIR region. In Figure 6.4, the proposed algorithm is used to produce the border of the feasible SIR region.

By comparing Figure 6.3 and Figure 6.4, it is clear that the graph generated based on the proposed simple algorithm is exactly on the border of the feasible SIR region illustrated in Figure 6.3.

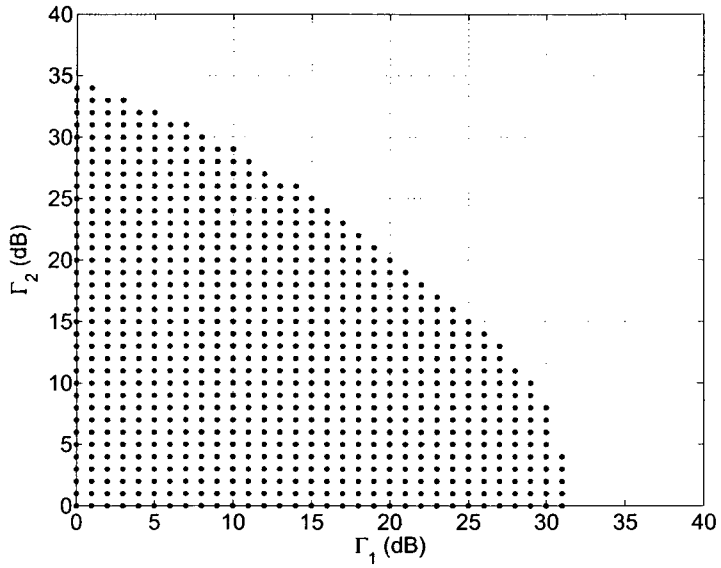

Figure 6.3: A Mont-Carlo simulation of the feasible path SIR region for an example network with two routing paths and four active links.

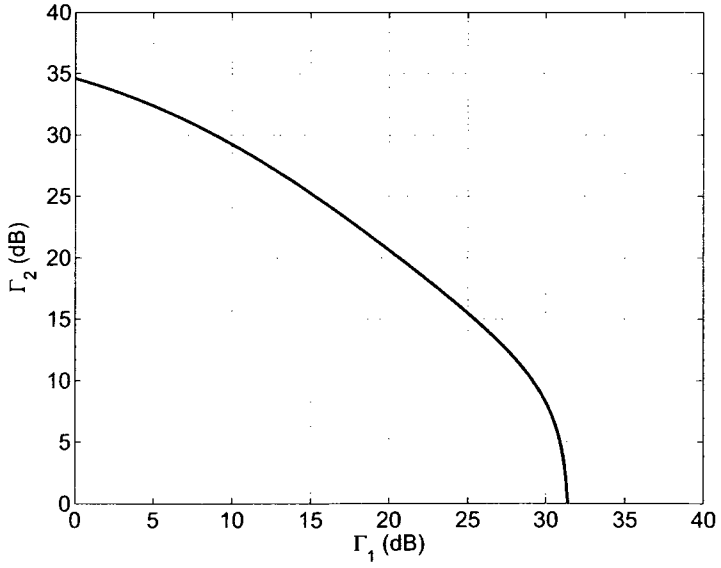

Figure 6.4: The border of the feasible path SIR region of the example network depicted in Figure 6.3.

6.3.3 Multi-Channel Communications

In the previous section, the feasible SIR region for the single-channel multi-hop ad hoc networks was studied. However, as mentioned in Section 3.4.4, in practice the intermediate links in the routing paths cannot transmit and receive simultaneously on the same channel and therefore, it is recommended to use two separate channels for the reception and transmission. As a result, to complete this multi-hop communications section, in the following, we study the feasible SIR region for multi-channel multi-hop networks where more than one channel is available to the network. In this section, first the necessary and sufficient conditions for the path SIR vectors to be on the border of the feasible SIR region of a single-channel multi-hop network, described by Theorem 6.4, are extended to the multi-channel case and then, based on these conditions, an algorithm is proposed to generate the border of the SIR region.

Considering the fact that each link of a routing path is operating in a specific subchannel, the following theorem states that a path SIR vector is on the border of the SIR region if in its minimal power vector every path has at lease one link communicating over a channel which contains a maximum power element. It is important to note that the maximum power link of this channel is not necessary in the same routing path; it can be a part of any routing path using the minimal power vector.

Theorem 6.6 *In a multi-hop network, the minimal power vector* $\mathbf{P}^L = [P_{ij}^L]$ *corresponds to a path SIR vector* $\mathbf{\Gamma} = [\Gamma_j]$ *on the border of the SIR region, if and only if each routing path uses at least one channel containing a maximum power element* $P^{\max}$.

Proof: The proof is presented in two parts:

a) *if* part: We show that if $\mathbf{P}^L = [P_{ij}^L]$ has a maximum power element in at least one channel of each routing path, then it has to be on the border of the SIR region.
As a counter example, assume that there exists another minimal power vector $\hat{\mathbf{P}}^L = [\hat{P}_{ij}^L]$ with the path SIR vector $\hat{\mathbf{\Gamma}} = [\hat{\Gamma}_j]$ for which $\forall j : \Gamma_j \leq \hat{\Gamma}_j$ and $\exists k : \Gamma_k < \hat{\Gamma}_k$. By the assumption, let C_y be the subchannel involved in the path k containing the maximum power element, i.e., $\exists (rt) \in C_y : P_{rt} = P^{\max}$. According to Lemma 3.3, we have $\forall (ij) \in$

$C_y : P_{ij} < \hat{P}_{rt}$ which is impossible, since $P_{rt} = P^{\max}$ and $\hat{P}_{rt}$ cannot be higher than the maximum power.

b) *only if* part: As a counter example, assume that there exists a routing path k for which none of its assigned channels have a maximum power element. We show that in this case, the corresponding path SIR vector $\mathbf{\Gamma} = [\Gamma_j]$ is not a Pareto-optimal vector and cannot be on the border.

If there is no maximum power elements in all channels involving in path k, then by applying a similar power scaling as that of presented in Theorem 3.20, a new power vector $\hat{\mathbf{P}} = [\hat{P}_{ij}]$ with the path SIR vector $\hat{\mathbf{\Gamma}} = [\hat{\Gamma}_j]$ is resulted for which the link SIR of the links communicating over those power-scaled channels are increased and the rest of the power elements in other subchannels remain the same. Consequently, the SIRs of all links in the path k are increased. Therefore $\forall j \neq k : \Gamma_j \leq \hat{\Gamma}_j$ and $\Gamma_k < \hat{\Gamma}_k$ which is in contradiction with Pareto optimality of the path SIR vector $\mathbf{\Gamma} = [\Gamma_j]$. □

Based on the necessary and sufficient conditions presented in Theorem 6.6, the following simple algorithm to generate a path SIR vector on the border of the SIR region is presented. Start with any arbitrary feasible path SIR vector $\mathbf{\Gamma} = [\Gamma_j]$ for which $\forall ij : P_{ij}^L \leq P^{\max}$. As explained for the single-channel multi-hop case in Section 6.3.2, the minimal power vector is calculated using the feasibility criteria presented in Section 2.1.1. If all routing paths have at least one channel with a maximum power element, the resulted path SIR vector is on the border. Otherwise, let the routing path k be the routing path for which none of its assigned channels have a maximum power. By using the feasibility criteria and considering the maximum power limit, the value of Γ_k is gradually increased and the power elements are consequently calculated until one of the channels in that routing path has a maximum power element. Note that in this process the SIR of other routing paths remain the same. This procedure is repeated and the path SIR values are updated until there is no routing path left without at least one of its assigned channels containing a maximum power element. As a result, the conditions of Theorem 6.6 are met and the resulted path SIR vector is on the border of the feasible path SIR region.

The proposed algorithm generates only one path SIR vector on the border of the SIR region. However, as mentioned in Section 6.3.2, the border of the SIR region is identified as

the set of all Pareto-optimal path SIR vectors. In order to produce this collection, a different path SIR vector has to be generated at each run of the algorithm. To accomplish this objective, this algorithm can be run with different seed parameters such as different initial path SIR vectors, different order of routing path selection to update the power elements and increase the path SIR value, etc.

6.4 Convexity of the Feasible SIR Region

If the feasible SIR region is not a convex set, then methods, such as coupling power control algorithms with scheduling techniques, should be emplaced to improve the average SIR values over a time period [54]. On the other hand, if this region is a convex set, then no scheduling is required for improving the average SIR values. As mentioned earlier, in the definition of the feasible SIR region, no time domain scheduling (time sharing) is involved. As a result, the convexity of the feasible SIR region is not automatically guaranteed. Therefore, in this section, the convexity of the feasible SIR region, for single-channel single hop networks, is investigated.

As mentioned earlier, in the definition of the feasible SIR region, no time domain scheduling (time sharing) is involved. As a result, the convexity of the feasible SIR region is not automatically guaranteed. Note that if this region is not a convex set, then other methods, such as coupling power control algorithms with scheduling techniques, should be emplaced to improve the average SIR values over a time period [54]. On the other hand, if this region is a convex set, then no scheduling is required for improving the average SIR values. This section investigates the convexity of the feasible SIR region, for single-channel single hop networks.

In general, the feasible SIR region is not a convex set [55, 56]. This can be verified for a general network with two active links [57], where its $\mathbf{F}$ matrix is expressed as

$$\mathbf{F} = \begin{bmatrix} 0 & \gamma_1 \frac{G_{12}}{G_{11}} \\ \gamma_2 \frac{G_{21}}{G_{22}} & 0 \end{bmatrix}.$$

The Perron-Frobenius eigenvalue ρ_f of $\mathbf{F}$ is

$$\sqrt{\frac{\gamma_1\gamma_2 G_{12}G_{21}}{G_{11}G_{22}}}.$$

According to the Perron-Frobenius theorem there exists a non-negative power vector achieving the link SIR vector $[\gamma_1 \ \ \gamma_2]$, if and only if $\rho_f < 1$, or equivalently

$$\gamma_1\gamma_2 < \frac{G_{11}G_{22}}{G_{12}G_{21}}. \tag{6.3}$$

It can be easily verified that the feasible SIR region provided by (6.3) under both the unconstrained and constrained power assumptions is not a convex set [54].

Besides the convexity, the log-convexity of the feasible SIR region is also studied in the literature [55, 57]. The log-convexity can be considered as the convexity of the feasible SIR region where SIR values are expressed in dB, i.e., in logarithmic format. Fortunately, it can be verified that the feasible SIR region is indeed a log-convex set. In the following, the log-convexity of feasible SIR region is investigated for both the power-unconstrained and power-constrained networks. The results for the power-unconstrained networks section are mainly from [57] and are reported here for the completeness of the discussion.

6.4.1 Power-Unconstrained Networks

The log-convexity of the general 2-link network, considered in the previous section, can be investigated by calculating the logarithm of (6.3) as

$$\log\gamma_1 + \log\gamma_2 < c$$

where $c = \log G_{11} + \log G_{22} - \log G_{12} - \log G_{21}$. Now, consider two achievable log link SIR vectors $[\log\gamma_1 \ \ \log\gamma_2]$ and $[\log\hat{\gamma}_1 \ \ \log\hat{\gamma}_2]$, i.e.,

$$\log\gamma_1 + \log\gamma_2 < c \ , \ \log\hat{\gamma}_1 + \log\hat{\gamma}_2 < c.$$

Due to the fact that

$$\alpha(\log\gamma_1 + \log\gamma_2) + (1-\alpha)(\log\hat{\gamma}_1 + \log\hat{\gamma}_2) < c$$

we can conclude that any linear combination of these two link SIR vectors, denoted by $\alpha[\log\gamma_1 \ \log\gamma_2]+(1-\alpha)[\log\hat{\gamma}_1 \ \log\hat{\gamma}_2]$, is also achievable. This confirms the log-convexity of any networks with two active links.

In order to provide the log-convexity for a general network with N links, the following well-known inequality is required [58, 57].

Theorem 6.7 *(Holder's inequality): If* $x_i, y_i \geq 0, p > 1$, *and* $1/p + 1/q = 1$, *then*

$$\left(\sum x_i^p\right)^{1/p}\left(\sum y_i^q\right)^{1/q} \geq \sum x_i y_i.$$

Proof: See [58]. □

In the following, the main theorem providing the log-convexity property is stated [57];

Theorem 6.8 *If the link SIR vectors* $\boldsymbol{\gamma} = [\gamma_i]$ *and* $\hat{\boldsymbol{\gamma}} = [\hat{\gamma}_i]$ *are both feasible, then the link SIR vector* $\boldsymbol{\gamma}^{(\alpha)} = [\gamma_1^\alpha \hat{\gamma}_1^{1-\alpha} \cdots \gamma_N^\alpha \hat{\gamma}_N^{1-\alpha}]$ *where* $0 \leq \alpha \leq 1$, *is also feasible.*

Proof: Let $\mathbf{P} = [P_i]$ and $\hat{\mathbf{P}} = [\hat{P}_i]$ be the power vectors corresponding to the link SIR vectors $\boldsymbol{\gamma}$ and $\hat{\boldsymbol{\gamma}}$, respectively. We construct a power vector $\mathbf{P}' = [P_i']$ where $P_i' = P_i^\alpha \hat{P}_i^{(1-\alpha)}$. The corresponding link SIR vector is denoted by $\boldsymbol{\gamma}' = [\gamma_i']$.

It is straightforward to show that for all i

$$\frac{\gamma_i'}{\gamma_i^\alpha \hat{\gamma}_i^{1-\alpha}} = \frac{\left(\sum_{j\neq i} G_{ij}P_j + \eta_i\right)^\alpha \left(\sum_{j\neq i} G_{ij}\hat{P}_j + \eta_i\right)^{1-\alpha}}{\sum_{j\neq i} G_{ij}P_j^\alpha \hat{P}_j^{1-\alpha} + \eta_i}.$$

By Holder's inequality, the right-hand side of the above equation is not less than 1, which implies that

$$\forall i: \quad \gamma_i' \geq \gamma_i^\alpha \hat{\gamma}_i^{1-\alpha}.$$

Therefore, $\gamma' \geq \gamma^{(\alpha)}$. By construction we know that γ' is feasible and consequently, $\gamma^{(\alpha)}$ is also feasible. □

As a result, $\log(\gamma^{(\alpha)})$ is a convex combination of $\log\gamma$ and $\log\hat{\gamma}$ and the feasible SIR region is log-convex. In other words, the feasible SIR region expressed in decibels is a log-convex set.

6.4.2 Power-Constrained Networks

Although Theorem 6.8 is presented for the power-unconstrained networks, it is straightforward to show that it also satisfies the maximum power criterion and therefore, the feasible SIR region of a power-constrained single-hop ad hoc network is a log-convex set as well.

Lemma 6.9 *If the power vector* $\mathbf{P} = [P_i]$ *and* $\hat{\mathbf{P}} = [\hat{P}_i]$ *in Theorem 6.8 are constrained by the maximum power value* $P^{\max}$, *i.e.,* $\forall i : P_i \leq P^{\max}$ *and* $\forall i : \hat{P}_i \leq P^{\max}$, *the constructed power vector* $\mathbf{P}' = [P_i']$ *is also limited to* $P^{\max}$, *i.e.,* $\forall i : P_i' \leq P^{\max}$.

Proof: Since $P_i' = P_i^{\alpha}\hat{P}_i^{(1-\alpha)}$, the maximum value of P_i' is obtained by maximizing P_i and $\hat{P}_i$, that is

$$P_i^{\alpha}\hat{P}_i^{(1-\alpha)} \leq \left[(P^{\max})^{\alpha}(P^{\max})^{(1-\alpha)} = P^{\max}\right].$$

Therefore $\forall i : P_i' \leq P^{\max}$. □

Since $\gamma' \geq \gamma^{(\alpha)}$, according to Lemma 3.2 $\boldsymbol{P}' \geq \boldsymbol{P}^{(\alpha)}$. Consequently, $\forall i : P_i^{(\alpha)} \leq P^{\max}$.

6.5 Conclusion

The feasible SIR region refers to the collection of all achievable SIR vectors by a single power vector. The border of this feasible SIR region can be considered as the instantaneous upper bound for achievable rates of any transmission control algorithms. In this chapter, the feasible SIR region for both the single-hop and multi-hop power-constrained ad hoc networks was studied. In particular, the properties of the power vectors producing the SIR vectors on the border of the feasible SIR region were investigated for both scenarios where

either a single channel or multiple channels are available. Moreover, simple algorithms were proposed to generate the border of the feasible SIR region. The convexity of the feasible SIR region was also investigated for the single-channel single-hop ad hoc networks.

Chapter 7

Conclusion

We conclude this thesis by first summarizing the results and contributions and then, presenting some ideas for the future work.

7.1 Summary of the Work

Wireless networks have become an indispensable component of almost any communication systems. In particular, there has been a growing interest in wireless ad hoc networks, where no centralized management is required and therefore, they can be setup and become operational in almost no time. Due to the absence of a central control unit, no channelization of resources, such as TDMA and FDMA, can be used. As a result, one or more wireless channels are shared among all links where the transmission power of one link is considered as the interference at the receivers of other links. Because of this shared nature of the wireless channels and the existence of high co-channel interference in wireless ad hoc networks, the role of the transmission control algorithms, such as power control and admission control algorithms, becomes extremely important. Power control algorithms manage the power allocation process in the network and admission control algorithms grant network access to a new link while protecting the transmission quality of other links. One of the main challenges to design transmission control algorithms for ad hoc networks is that due to the distributed nature of ad hoc networks, the transmission control algorithms have to be also distributed and should not rely on any information to be provided at the network level.

In this work, new transmission control algorithms for power-controlled ad hoc networks were investigated. Each of these algorithms was designed to achieve a particular performance objective, which was further evaluated through comprehensive examples and computer simulations.

First, a new power control algorithm was proposed to achieve the maximum uniform rate of a power-constrained ad hoc network. This algorithm requires only one phase of power convergence and less information to be broadcast from the links in comparison to the existing algorithms. But, most importantly it is autonomous in the sense that it does not require a central unit to perform any state-machine process. The design and the performance of this algorithm were investigated for both the single-hop and multi-hop communications ad hoc networks and for each case, the possibility of having either a single channel or multiple channels available to the network was investigated.

Moreover, a semi-asynchronous power control algorithm was developed which allows the links to update their powers asynchronously in a round-robin fashion and at the same time, protects the transmission quality of the existing links in the network. This algorithm fills the gap between the existing fully asynchronous power control algorithm, which does not provide the active link protection, and the power control algorithm with active link protection, which requires the power of all links to be updated synchronously.

Furthermore, a new distributed admission control algorithm for the asynchronous power-controlled wireless ad hoc networks was introduced. This admission control was developed based on the Perron-Frobenius theorem and the local measurements of the new link. A normalization process was presented normalizing some of the network parameters without affecting the admissibility of the new link. The proposed algorithm was investigated for the general case of the asynchronous Foschini-Miljanic power control algorithm and later, it was extended to the asynchronous power control algorithm with active link protection. It was shown that the proposed algorithm is faster and has a lower probability of error compared to other algorithms.

Finally, the feasible SIR region was studied for both the single-hop and multi-hop ad hoc networks and for each case, the possibility of having either a single channel or multiple channels available to the network was investigated. In addition, for each case a simple

algorithm was proposed to generate the border of the feasible SIR region. It is important to note that no matter which transmission control algorithms the network uses, at any given instant the network is dealing with only one power vector. Therefore, the border of the feasible SIR region can be considered as the instantaneous upper bound for the achievable rates of any transmission control algorithms.

7.2 Future Work

Promising avenues of research are identified during the development of this thesis and they are highlighted in the following.

As mentioned in the Chapter 2, in this work the transmitted power of each link is considered as the interfering signal at the receivers of other links. However, it is interesting to investigate the possibility of performing some form of successive interference cancellation techniques to improve the transmission quality of the links. Particularly, in the multi-hop networks where there are more than one link involved in the transmission of the information, the intermediate links already have the knowledge of the transmitted data by the next links in the path. As a result, with such perfect knowledge, those links are able to cancel the interference generated by the next links in that routing path which consequently, improves their links' SIR values.

The asynchronous ALP power control algorithm proposed in Chapter 4 allows only one power update of any link in the power updating interval of other links. Therefore, the power updating intervals of all links are the same. It is interesting to expand this concept and allow more power updates for some links within the power updating intervals of other links. Although in this case the power updating intervals are different, new methods should be investigated to protect the QoS of the active links.

The admission control algorithm proposed in Chapter 5 requires that all links update their powers at distinct time instances. Although the performance of this algorithm is ideal, it is useful to see whether there is a possibility to use some approximation of this algorithm and measure the SIR values at end of each iteration rather than each power update.

Bibliography

[1] R. W. Nettleton and H. Alavi, "Power control for a spread spectrum cellular mobile radio system," in *Proc. IEEE Veh. Tech. Conf. (VTC)*, Toronto, Canada, May 1983, pp. 242–244.

[2] S. Ariyavisitakul, "Sir based power control in a cdma system," in *Proc. IEEE GLOBECOM*, Dec. 1992, pp. 868–873.

[3] N. Bambos and S. Kandukuri, "Power-controlled multiple access scheme for next-generation wireless packet networks," *IEEE Wireless Commun. Mag.*, vol. 9, no. 3, pp. 58–64, Jun. 2002.

[4] C. Comaniciu and H. V. Poor, "Jointly optimal power and admission control for delay sensitive traffic in cdma networks with lmmse receivers," *IEEE Trans. Signal Process.*, vol. 51, no. 8, pp. 2031–42, Aug. 2003.

[5] M. Ghaderi and R. Boutaba, "Call admission control in mobile cellular networks: a comprehensive survey," *Wireless Communications and Mobile Computing*, vol. 6, pp. 69–93, Feb. 2006.

[6] S. Valaee and B. Li, "Distributed call admission control in. wireless ad hoc networks," in *Proc. IEEE Veh. Tech. Conf. (VTC)*, vol. 2, Vancouver, Canada, Sep. 2002, pp. 1244–1248.

[7] S. A. Grandhi, R. Vijayan, D. J. Goodman, and J. Zander, "Centralized power control in cellular radio systems," *IEEE Trans. on Veh. Technol.*, vol. 42, no. 4, pp. 466–468, Nov. 1993.

[8] H. Boche and M. Schubert, "A general theory for sir balancing," *EURASIP Journal on Wireless Communications and Networking*, vol. 2006, 2006.

[9] M. Ebrahimi, M. A. Maddah-Ali, and A. K. Khandani, "On the achievable rates of wireless networks," in *Proc. 39th CISS 2005*, Baltimore, Mar. 2005.

[10] S. Kandukuri and S. Boyd, "Optimal power control in interference limited fading wireless channels with outage probability specifications," *IEEE Trans. Wireless Commun.*, vol. 1, pp. 48–55, Jan. 2002.

[11] S. A. Grandhi and J. Zander, "Constrained power control in cellular radio system," in *Proc. IEEE Veh. Tech. Conf.VTC-94*, 1994, pp. 824–828.

[12] L. Faybusovich, "Power control under fnite power constraints," *Communications in Information and Systems*, vol. 1, no. 4, pp. 395–406, 2001.

[13] N. Bambos, "Toward power-sensitive network architectures in wireless communication: concepts, issues and design aspects," *IEEE Personal Communications Magazine*, vol. 5, pp. 50–59, Mar. 1998.

[14] M. Andersin, Z. Rosberg, and J. Zander, "Soft and safe admission control in cellular networks," *IEEE/ACM Trans. on Networking*, vol. 5, no. 2, pp. 255–265, 1997.

[15] A. Goldsmith, L. J. Greenstein, and G. L. Foschini, "Error statistics of real-time power measurements in cellular channels with multipath and shadowing," *IEEE Trans. on Veh. Technol.*, vol. 43, no. 3, pp. 439–446, Aug. 1994.

[16] G. J. Foschini and Z. Miljanic, "A simple distributed autonomous power control algorithm and its convergence," *IEEE Trans. on Veh. Technol.*, vol. 42, no. 4, pp. 641–646, Nov. 1993.

[17] D. Mitra, "An asynchronous distributed algorithm for power control in cellular radio systems," in *Proc. 5th WINLAB Workshop*, vol. 1, Rutgers University, New Branswick, NJ, Oct. 1993, pp. 249–257.

[18] R. Yates and C. Huang, "A framework for uplink power control in cellular radio systems," *IEEE J. Sel. Areas Commun.*, vol. 13, pp. 1341–1347, Jul. 1995.

[19] N. Bambos, S. C. Chen, and G. J. Pottie, "Channel access algorithms with active link protection for wireless communication networks with power control," *IEEE/ACM Trans. on Networking*, vol. 46, no. 2, pp. 388–404, Mar. 2000.

[20] T. Holliday, A. Goldsmith, N. Bambos, and P. Glynn, "Distributed power and admission control for time-varying wireless networks," in *Proc. IEEE GLOBECOM*, Dallas, Texas, Nov. 2004, pp. 768–774.

[21] D. Kim, "Efficient interactive call admission control in power-controlled mobile systems," *IEEE Trans. on Veh. Technol.*, vol. 49, pp. 1017–1028, May 2000.

[22] S. V. Hanly, "Capacity and power control in spread spectrum macro diversity radio networks," *IEEE Trans. Commun.*, vol. 44, pp. 247–256, Feb. 1996.

[23] R. Yates and C. Y. Huang, "Integrated power control and base station. assignment," *IEEE Trans. on Veh. Technol.*, vol. 44, pp. 638–644, Mar. 1995.

[24] E. Seneta, *Nonnegative Matrices and Markov Chains*. New York: Springer, 1981.

[25] F. R. Gantmacher, *The Theory of Matrices*, New York, NY: Chelsea, 1971.

[26] N. Bambos and G. Pottie, "Power control based admission policies in cellular radio networks," in *Proc. IEEE GLOBECOM*, Orlando, Florida, Dec. 1992, pp. 7–9.

[27] M. Xiao, N. B. Shroff, and E. K. P. Chong, "Distributed admission control for power-controlled cellular wireless systems," *IEEE/ACM Trans. on Networking*, vol. 9, no. 6, pp. 790–800, Dec. 2001.

[28] P. Gupta and P. R. Kumar, "The capacity of wireless networks," *IEEE Trans. Inf. Theory*, vol. 46, no. 2, pp. 388–404, Mar. 2000.

[29] S. Toumpis and A. J. Goldsmith, "Capacity regions for wireless ad hoc networks," *IEEE Trans. Wireless Commun.*, vol. 2, no. 4, pp. 735–748, Jul. 2003.

[30] R. Diestel, *Graph Theory*, 2nd ed. New York: Springer Verlag, Jan. 2000.

[31] C. W. Sung and W. S. Wong, "A distributed fixedstep power control algorithm with quantization and active link quality protection," *IEEE Trans. on Veh. Technol.*, vol. 48, no. 2, pp. 553–562, Mar. 1999.

[32] A. Goldsmith, *Wireless Communications*, 1st ed. New York: Cambridge University Press, Aug. 2005.

[33] C.-Y. Huang, "Radio resource management in power controlled cdma systems," Ph.D. dissertation, Rutgers Univ., New Brunswick, NJ, 1996.

[34] R. W. Nettleton and H. Alavi, "Power control for a spread spectrum cellular mobile radio system," vol. Proc. IEEE Veh. Tech. Conf. (VTC), Toronto, Canada, May 1983, pp. 242–244.

[35] R. Yates and C. Y. Huang, "A framework for uplink power control in cellular radio systems," *IEEE J. Sel. Areas Commun.*, vol. 13, pp. 1341–1347, Jul. 1995.

[36] N. Bambos, S. C. Chen, and G. J. Pottie, "Channel access algorithms with active link protection for wireless communication networks with power control," *IEEE/ACM Trans. on Networking*, vol. 46, no. 2, pp. 388–404, Mar. 2000.

[37] S. A. Grandhi, J. Zander, and R. Yates, "Constrained power control," *Internal Report TRITA-IT-R 94:06, ISSN 1103-534X, ISRN KTH/IT/R-94/06-SE, Royal Institiute of Technology, Stockholm, Sweden*, Mar. 1994.

[38] S. C. Chen, N. Bambos, and G. J. Pottie, "Admission control schemes for wireless communication networks with adjustable transmitter powers," in *Proc. IEEE INFOCOM*, Toronto, ON, Jun. 1994, pp. 21–28.

[39] C. Y. Huang and R. D. Yates, "Call admission in power controlled cdma systems," in *Proc. IEEE Veh. Tech. Conf. (VTC)*, vol. 3, Atlanta, GA, Apr. 1996, pp. 1665–69.

[40] E. M. Royer and C.-K. Toh, "A review of current routing protocols for ad-hoc mobile wireless networks," *IEEE Personal Communications Magazine*, vol. 6, no. 2, pp. 46–55, Apr. 1999.

[41] P. D. L. Beasley, A. G. Stove, B. J. Reits, and B. As, "Solving the problems of a single antenna frequency modulated cw radar," in *Proc. IEEE Radar Conf.*, 1990, pp. 391–395.

[42] Q. Jiming, Q. Xinjian, and R. Zhijiu, "Development of a 3 cm band reflected power canceller," in *Proc. IEEE Radar Conf.*, 2001, pp. 1098–1102.

[43] S. Chen, M. A. Beach, and J. P. McGeehan, "Division-free duplex for wireless application," *Electron. Lett.*, vol. 34, no. 2, pp. 147–148, Jan. 1998.

[44] R. P. Grimaldi, *Discrete and Combinatorial Mathematics: An Applied Introduction*, 4th ed. Reading, MA: Addison-Wesley Longman, 1998.

[45] S. Bhatnagar and B. Badrinath, "Distributed admission control to support guaranteed services in core-stateless networks," in *Proc. IEEE INFOCOM*, vol. 3, San Fransisco, CA, Apr. 2003, pp. 1659–1669.

[46] D. Gao, J. Cai, and K. N. Ngan, "Admission control in ieee 802.11e wireless lans," *IEEE Netw.*, vol. 19, no. 4, pp. 6–13, Aug. 2005.

[47] D. Ayyagari and A. Ephremides, "Optimal admission control in cellular ds-cdma systems with multimedia traffic," *IEEE Trans. Wireless Commun.*, vol. 2, no. 1, pp. 195–202, Jan. 2003.

[48] H. Jia, Z. Zhang, G. Yu, and S. Li, "A distributed call admission control and network selection scheme for hybrid cdma-ofdma networks," in *Proc. IEEE WCNC*, Hong Kong, Mar. 2007, pp. 3774–3779.

[49] M. Andersin, Z. Rosberg, and J. Zander, "Gradual removals in cellular pcs with constrained power control and noise," *IEEE/ACM Trans. on Networking*, vol. 2, pp. 27–43, 1996.

[50] N. Bambos, S. Chen, and D. Mitra, "Channel probing for distributed access control in wireless communication networks," in *Proc. IEEE GLOBECOM*, Singapore, Nov. 1995, pp. 322–326.

[51] E. Kreyszig, *Advanced Engineering Mathematics*, 8th ed. New York: Wiley, Oct. 1998.

[52] M. Grossglauser and D. Tse, "Mobility increases the capacity of ad-hoc wireless networks," in *Proc. IEEE INFOCOM*, vol. 3, Anchorage, AL, Apr. 2001, pp. 1360–1369.

[53] T. Elbatt and A. Ephremides, "Joint scheduling and power control for wireless ad-oc networks," in *Proc. IEEE INFOCOM*, Jun. 2002, pp. 976–984.

[54] S. Stanczak and H. Boche, "The infeasible sir region is not a convex set," *IEEE Trans. Commun.*, vol. 54, no. 11, pp. 1905–1907, Nov. 2006.

[55] H. Boche and S. Stanczak, "Log-concavity of sir and characterization of the feasible sir region for cdma channels," in *Proc. 37th Asilomar Conference on Signals, Systems, and Computers*, vol. 1, Monterey, USA, Nov. 2003, pp. 413–417.

[56] ——, "Log-convexity of the minimum total power in cdma systems with certain quality-of-service guaranteed," *IEEE Trans. Inf. Theory*, vol. 51, no. 1, pp. 374–381, Jan. 2005.

[57] C. W. Sung, "Log-convexity property of the feasible sir region in power-controlled cellular systems," *IEEE Commun. Lett.*, vol. 6, no. 2, pp. 248–249, Jun. 2002.

[58] M. R. Spiegel, *Mathematical Handbook of Formulas and Tables*. New York: McGraw-Hill, 1968.